

ΠΑΝΕΠΙΣΤΗΜΙΟ ΚΡΗΤΗΣ
ΤΜΗΜΑ ΧΗΜΕΙΑΣ

ΓΕΝΙΚΟ ΜΕΤΑΠΤΥΧΙΑΚΟ ΠΡΟΓΡΑΜΜΑ

**ΕΡΓΑΣΤΗΡΙΟ ΦΑΣΜΑΤΟΣΚΟΠΙΑΣ ΠΥΡΗΝΙΚΟΥ
ΜΑΓΝΗΤΙΚΟΥ ΣΥΝΤΟΝΙΣΜΟΥ (NMR)**



ΜΕΤΑΠΤΥΧΙΑΚΟ ΔΙΠΛΩΜΑ ΕΙΔΙΚΕΥΣΗΣ

**ΕΠΙΔΡΑΣΗ ΤΗΣ ΘΕΙΩΣΗΣ ΣΤΗ ΔΕΣΜΕΥΣΗ
ΕΛΕΥΘΕΡΩΝ ΡΙΖΩΝ ΚΑΙ ΣΤΙΣ
ΑΝΤΙΟΞΕΙΔΩΤΙΚΕΣ ΙΔΙΟΤΗΤΕΣ ΤΟΥ ΟΙΝΟΥ**

ΣΟΦΙΑ ΤΑΧΤΑΛΙΔΟΥ

Υπεύθυνος καθηγητής: Απόστολος Σπύρος

ΗΡΑΚΛΕΙΟ 2018

**UNIVERSITY OF CRETE
DEPARTMENT OF CHEMISTRY**

GENERAL POSTGRADUATE PROGRAM

NMR LABORATORY



M.Sc. Thesis

**IMPACT OF SULFONATION ON THE
ANTIOXIDANT AND RADICAL SCAVENGING
PROPERTIES OF WINE**

SOFIA TACHTALIDOU

Thesis Supervisor: Apostolos Spyros

HERAKLION 2018

Στη μαμά μου, στον παππού μου Ηρακλή
και στη γιαγιά μου Σοφία

Examination Committee

Apostolos Spyros

Associate Professor in Analytical Chemistry, UoC

Maria Nikolantonaki

Assistant Professor, IUUVV, University of Burgundy

Spyros Pergantis

Professor in Analytical Chemistry, UoC

ΕΥΧΑΡΙΣΤΙΕΣ

Αρχικά θα ήθελα να ευχαριστήσω θερμά τον επιβλέποντα καθηγητή μου κ. Απόστολο Σπύρο και την καθηγήτριά μου κ. Μαρία Νικολαντωνάκη για τις γνώσεις που μου μετέδωσαν, την εμπιστοσύνη που μου έδειξαν, τις συμβουλές που μου παρείχαν, καθώς και για τη στήριξή τους καθ' όλη τη διάρκεια της μεταπτυχιακής μου διατριβής αλλά και κατά τη διαμονή μου στη Γαλλία.

Θα ήθελα να ευχαριστήσω και τον καθηγητή κ. Σπύρο Περγαντή που δέχτηκε να αξιολογήσει την μεταπτυχιακή μου εργασία. Ευχαριστώ επίσης και τους καθηγητές Christian Coelho και Regis Gougeon για την βοήθειά τους στην ολοκλήρωση της μεταπτυχιακής μου μελέτης.

Ευχαριστώ θερμά το Πανεπιστήμιο Βουργουνδίας, το IUVV “Jules Guyot” και το UMP-PAM για την αποδοχή, συνεργασία και χρηματοδότησή μου ώστε να διεξαχθεί επιτυχώς η μεταπτυχιακή μου διατριβή.

Ευχαριστώ ιδιαίτερα τα μέλη του εργαστηρίου μου στο Τμήμα Χημείας του Πανεπιστημίου Κρήτης, την Δρ. Έφη Μανωλοπούλου, την Ευαγγελία Ράλλη, την Ειρήνη-Σιμονέλα Τσάνα, την Μαρία Καλιτσουνάκη και την Ελένη Στειακάκη για την βοήθειά τους αλλά και την όμορφη παρέα τους, εντός και εκτός εργαστηρίου. Ευχαριστώ, επίσης, τα μέλη του εργαστηρίου μου στο IUVV “Jules Guyot” του Πανεπιστημίου Βουργουνδίας στη Ντιζόν, τον Δρ. Remy Romanet και τον Δρ. Florian Bahut για την πολύτιμη βοήθειά τους, καθώς και τις Zina, Nezha, Claire, Audrey, Jessica, Manon και Miriam για το υπέροχο κλίμα που υπήρχε και για την βοήθειά τους στην προσαρμογή μου στη Γαλλία.

Τέλος, θέλω να πω ένα μεγάλο ευχαριστώ στην οικογένειά μου για την στήριξη που είχα τόσο σε οικονομικό όσο και σε ψυχολογικό επίπεδο, καθώς και για την ενθάρρυνση και την υπομονή τους στις δύσκολες στιγμές μου.

ΒΙΟΓΡΑΦΙΚΟ ΣΗΜΕΙΩΜΑ

ΠΡΟΣΩΠΙΚΑ ΣΤΟΙΧΕΙΑ

Όνοματεπώνυμο	Σοφία Ταχταλίδου
Όνομα πατέρα	Λεωνίδα
Ημερομηνία γέννησης	3 Σεπτεμβρίου 1994
Τόπος γέννησης	Ωραιόκαστρο Θεσσαλονίκης
Διεύθυνση κατοικίας	25 ^{ης} Μαρτίου 72
Τηλέφωνο κατοικίας	2310-696441
Κινητό Τηλέφωνο	+306949662605,+330665906217
E-mail διεύθυνση	sofia_tachtalidou@yahoo.gr

ΕΚΠΑΙΔΕΥΣΗ

Φεβρουάριος 2017-Δεκέμβριος 2018: Γενικό Μεταπτυχιακό Πρόγραμμα Σπουδών του Τμήματος Χημείας της Σχολής Θετικών και Τεχνολογικών Επιστημών, Πανεπιστήμιο Κρήτης, με κατεύθυνση Αναλυτική Χημεία

Φεβρουάριος 2018 – Ιούλιος 2018: Συνεργασία με το Institut Universitaire de la Vigne et du Vin “Jules Guyot” – IUVV, Πανεπιστήμιο Βουργουνδίας, Ντιζόν, Γαλλία

Νοέμβριος 2016: Πτυχιούχος του Τμήματος Χημείας της Σχολής Θετικών και Τεχνολογικών Επιστημών του Πανεπιστημίου Κρήτης με βαθμό 7.28

Ιούνιος 2012: Απόφοιτος 1^{ου} Γενικού Λυκείου Ωραιοκάστρου Θεσ/νίκης με γενικό μέσο όρο 18.7

ΞΕΝΕΣ ΓΛΩΣΣΕΣ

Αγγλικά Επίπεδο: Lower

ΕΡΕΥΝΗΤΙΚΗ ΑΠΑΣΧΟΛΗΣΗ

- **Δεκέμβριος 2017-Δεκέμβριος 2018:** Γενικό Μεταπτυχιακό πρόγραμμα Χημείας με θέμα “Επίδραση της θείωσης στη δέσμευση ελευθέρων ριζών και στις αντιοξειδωτικές ιδιότητες του οίνου”, Πανεπιστήμιο Κρήτης, Τμήμα Χημείας, σε συνεργασία με το IUVV “Jules Guyot”, Πανεπιστήμιο της Βουργουνδίας, Ντιζόν, Γαλλία
- **Φεβρουάριος 2017-Νοέμβριος 2017:** Ερευνητική εργασία στο εργαστήριο NMR του Τμήματος Χημείας του Πανεπιστημίου Κρήτης με θέμα «Ανάλυση των πολυφαινολών του ελαιολάδου με φασματοσκοπία NMR»
- **Ιούλιος 2016-Οκτώβριος 2016:** Διπλωματική Εργασία με τίτλο «Προσδιορισμός της σύστασης του ελληνικού καφέ με φασματοσκοπία NMR», Επιβλέπων: Επ. Καθηγητής Απόστολος Σπύρος

ΙΚΑΝΟΤΗΤΕΣ ΚΑΙ ΤΕΧΝΙΚΕΣ

Εργαστηριακή εμπειρία:

- Στη λήψη φασμάτων NMR μίας και δύο διαστάσεων (1D και 2D NMR) σε φασματόμετρα Bruker DPX-300 MHz, Avance-500 MHz και Avance-600 MHz καθώς και στη λήψη φασμάτων EPR σε φασματόμετρο 300 MHz.
- Στην απομόνωση οργανικών ενώσεων από τρόφιμα (υγρή-υγρή εκχύλιση, απόσταξη, φυγοκέντριση, χρήση περιστροφικού εξατμιστή και λυοφιλιωτή).
- Στην ταυτοποίηση και ανάλυση οργανικών ενώσεων με φασματοσκοπικές μεθόδους NMR στην υγρή φάση.
- Στην αξιολόγηση της αντιοξειδωτικής ικανότητας χρησιμοποιώντας τη μέθοδο DPPH
- Στην τεχνική GC-FID

ΔΗΜΟΣΙΕΥΣΕΙΣ

- “NMR spectroscopy protocols for food metabolomics applications” E. Ralli, M. Amargianitaki, E. Manolopoulou, M. Misiak, G. Markakis, S. Tachtalidou, A. Kolesnikova, P. Dais and A. Spyros, in Metabolic profiling: Methods and protocols, Theodoridis G. Gika, H. G. Wilson, I. (Eds.), Springer, 2018

ΠΑΡΟΥΣΙΑΣΕΙΣ ΣΕ ΣΥΝΕΔΡΙΑ

- E. Manolopoulou, S. Tachtalidou, E. Beleli, A.M. Gómez-Caravaca, A. Segura-Carretero and A. Spyros “*Phenolics profiling in extra-virgin olive oil, olive leaves, and olive mill waste water by NMR spectroscopy*”. 10th International Conference on Instrumental Methods of Analysis, Ηράκλειο Κρήτης, Σεπτέμβριος 2017, Poster presentation
- S. Tachtalidou and A. Spyros “*Determination of the composition of Greek coffee by NMR spectroscopy*”. 19th Chemistry Postgraduates Conference, Ηράκλειο Κρήτης, Μάιος 2017, Poster presentation
- E. Beleli, N. Fragoulis, S. Tachtalidou, E. Manolopoulou and A. Spyros “*Total phenolics determination and profiling in olive oil by NMR spectroscopy*”. 19th Chemistry Postgraduates Conference, Ηράκλειο Κρήτης, Μάιος 2017, Poster presentation

ΠΑΡΑΚΟΛΟΥΘΗΣΗ ΣΥΝΕΔΡΙΩΝ

- 19th Chemistry Postgraduates Conference, Ηράκλειο Κρήτης, Μάιος 2017
- 22^o Πανελλήνιο Συνέδριο Χημείας, Δεκέμβριος 2016, Θεσσαλονίκη

ΣΥΜΜΕΤΟΧΕΣ ΣΕ ΣΕΜΙΝΑΡΙΑ

- ISO 22000:2005 Βασικές αρχές συστημάτων διαχείρισης ασφάλειας τροφίμων, Απρίλιος 2017, Ηράκλειο Κρήτης

ΔΙΔΑΚΤΙΚΗ ΕΜΠΕΙΡΙΑ

Σεπτέμβριος 2017 – Δεκέμβριος 2017: Βοηθός εργαστηρίου στο εργαστήριο Αναλυτικής Χημείας II (προπτυχιακό εργαστήριο)

ΧΡΗΣΗ ΥΠΟΛΟΓΙΣΤΙΚΩΝ ΣΥΣΤΗΜΑΤΩΝ

- Microsoft Office
- Origin
- NMR Processing Software, TOPSPIN, WINNMR
- EPR Processing Software

CURRICULUM VITAE

PERSONAL INFORMATION

First name: Sofia

Last name: Tachtalidou

Date of birth: 03/09/1994

Residence address: 25th Martiou 72, Oreokastro, Thessaloniki, Greece

Telephone number: 2310-696441

Mobile phone: +30 6949662605, +33 0665906217

e-mail address: sofia_tachtalidou@yahoo.gr

EDUCATION

1. **February 2017 – December 2018:** M.Sc. in Chemistry, Chemistry Dept., University of Crete, Heraklion Crete, Greece
2. **February 2018 – July 2018:** Internship, Institut Universitaire de la Vigne et du Vin “Jules Guyot” – IUVV, Dijon, France
3. **September 2012 – November 2016:** Chemistry degree with grade 7.28, Chemistry Dept., University of Crete, Heraklion Crete, Greece. Degree: 7.28

LANGUAGES

English: Certificate of Competency in English, Lower

RESEARCH EXPERIENCE

- **December 2017-December 2018:** M.Sc Thesis “Impact of sulfonation on the antioxidant and radical scavenging properties of wines”, University of Crete, Heraklion, Greece in collaboration with IUVV “Jules Guyot”, University of Burgundy, Dijon, France
- **March 2017-November 2017:** Research in “Analysis of olive oil polyphenols using NMR spectroscopy”, Chemistry Dept., University of Crete, Heraklion, Greece

- **July 2016-October 2016:** Undergraduate Thesis “Compositional analysis of Greek coffee using NMR spectroscopy”, Chemistry Dept., University of Crete, Heraklion, Greece

SKILLS AND TECHNIQUES

Laboratory experience in:

- Acquisition and processing of 1-D and 2-D NMR spectra (Bruker TopSpin 3.1, 3.5)
- Using Bruker DPX-300 MHz, Avance-500 MHz, Avance-600 MHz NMR spectrometers and 300 MHz EPR spectrometer
- Isolation of organic compounds from food (liquid extraction, distillation, centrifugation, use of rotary evaporator and freeze-dryer).
- Identification and quantification of organic compounds using liquid state NMR spectroscopy.
- Evaluation of the antioxidant capacity in wines using the DPPH assay
- Using the GC-FID technique

PUBLICATIONS

1. “NMR spectroscopy protocols for food metabolomics applications” E. Ralli, M. Amargianitaki, E. Manolopoulou, M. Misiak, G. Markakis, S. Tachtalidou, A. Kolesnikova, P. Dais and A. Spyros, in *Metabolic Profiling: Methods and Protocols, Methods in Molecular Biology, vol. 1738*, G. A. Theodoridis, H. Gika, I. Wilson (Eds), Humana Press, New York, NY, **2018**, Ch. 14, 203.

PARTICIPATION IN CONFERENCES

1. E. Manolopoulou, **S. Tachtalidou**, E. Beleli, A.M. Gómez-Caravaca, A. Segura-Carretero and A. Spyros “Phenolics profiling in extra-virgin olive oil, olive leaves, and olive mill waste water by NMR spectroscopy”, 10th International Conference on Instrumental Methods of Analysis, Heraklion, Crete, Greece, September 2017, Poster presentation
2. **S. Tachtalidou** and A. Spyros “Determination of the composition of Greek coffee by NMR spectroscopy”, 19th Chemistry Postgraduates Conference, Heraklion, Crete, Greece, May 2017, Poster presentation
3. E. Beleli, N. Fragoulis, **S. Tachtalidou**, E. Manolopoulou and A. Spyros “Total phenolics determination and profiling in olive oil by NMR

spectroscopy”.19th Chemistry Postgraduates Conference, Heraklion, Crete, Greece, May 2017, Poster presentation

CONFERENCES ATTENDED

- 19th Chemistry Postgraduates Conference, Heraklion, Crete, May 2017
- 22^o Panhellenic Conference in Chemistry , Thessaloniki, December 2016

PARTICIPATION IN SEMINARS

1. ISO 22000:2005 Food Safety Management Systems

TEACHING EXPERIENCE

September 2017 – December 2017: Lab assistant in the Analytical Chemistry II Laboratory (undergraduate)

DIGITAL SKILLS

- Microsoft Office
- Origin
- NMR Processing Software, TOPSPIN, WINNMR
- EPR Processing Software

ΠΕΡΙΛΗΨΗ

Στο πλαίσιο της παρούσας μεταπτυχιακής εργασίας μελετήθηκε η επίδραση της διαδικασίας της θείωσης στην δέσμευση ελεύθερων ριζών και στις αντιοξειδωτικές ιδιότητες του οίνου. Όπως είναι γνωστό, τα θειώδη χρησιμοποιούνται κατά την παραγωγή του οίνου για τη συντήρηση και κατ' επέκταση την παλαιώσή του. Το διοξείδιο του θείου (SO₂) έχει αντιμικροβιακές και αντιοξειδωτικές ιδιότητες αλλά κατά την παλαιώση του κρασιού, η συγκέντρωσή του ελαττώνεται. Η κυριότερη μορφή θειώδους στο pH του οίνου (pH=3,5) είναι το όξινο θειώδες ανιόν (HSO₃⁻), το οποίο όμως αντιδρά με διάφορες κατηγορίες ενώσεων που υπάρχουν στο κρασί όπως κετονικά οξέα, σάκχαρα, κινόνες, καρβονυλικές ενώσεις κλπ. και παράγει σουλφονιωμένα παράγωγα τα οποία πιθανώς επηρεάζουν τις αντιοξειδωτικές ιδιότητες του οίνου.

Στην παρούσα διατριβή, αρχικά πραγματοποιήθηκε στοχευμένη σύνθεση σουλφονιωμένων ενώσεων που πιθανώς σχηματίζονται στον οίνο με την αντίδραση του όξινου θειώδους ανιόντος με τις ενώσεις ακεταλδεΐδη, πυρουβικό οξύ, κυστεΐνη, γλουταθειόνη και γλυκόζη, ενώ το σουλφονιωμένο προϊόν του ασκορβικού οξέος ήταν εμπορικά διαθέσιμο. Οι συγκεκριμένες ενώσεις επιλέχθηκαν ώστε να καλύπτουν όλες τις κατηγορίες ενώσεων του οίνου που πιθανώς να αντιδρούν με το όξινο θειώδες ανιόν (HSO₃⁻). Για την ταυτοποίηση των ενώσεων που συντέθηκαν χρησιμοποιήθηκε τόσο η φασματοσκοπία πυρηνικού μαγνητικού συντονισμού (1D και 2D NMR) υγρής κατάστασης όσο και η υγρή χρωματογραφία συζευγμένη με φασματόμετρο μάζας (LC-MS-QToF).

Κάποιες από τις ενώσεις που συντέθηκαν (σουλφονιωμένα προϊόντα της ακεταλδεΐδης, του πυρουβικού οξέος και του ασκορβικού οξέος), μελετήθηκαν ως προς την ικανότητά τους στη δέσμευση ελεύθερων ριζών και τις αντιοξειδωτικές τους ιδιότητες. Για τη μελέτη αυτή χρησιμοποιήθηκαν δύο διαφορετικές αναλυτικές μεθοδολογίες, η μέθοδος DPPH και η φασματοσκοπία ηλεκτρονικού παραμαγνητικού συντονισμού (EPR). Τα πειραματικά αποτελέσματα που προέκυψαν από την παρούσα διατριβή παρουσιάζουν ιδιαίτερο ενδιαφέρον, καθώς αποδείχθηκε ότι τα σουλφονιωμένα προϊόντα ενώσεων όπως η ακεταλδεΐδη και το πυρουβικό οξύ, οι οποίες ως ελεύθερες μορφές δεν παρουσιάζουν αντιοξειδωτικές ιδιότητες, εμφανίζουν ικανότητα δέσμευσης ελευθέρων ριζών. Αξίζει επίσης να σημειωθεί ότι βρέθηκε ότι το ασκορβικό οξύ παράγει διάφορες ρίζες κατά την αντίδρασή του με ρίζες υδροξυλίου, καθώς και με το υπεροξείδιο του υδρογόνου. Αυτές οι νέες ρίζες, ανταγωνίζονται την υδροξυ-αιθυλ-ρίζα (ρίζα αιθανόλης) ως προς το ποια θα αντιδράσει με το POBN (spin trap). Αυτό έχει ως αποτέλεσμα το ασκορβικό οξύ με τη μέθοδο του DPPH να εμφανίζεται ως αντιοξειδωτικό ενώ με το EPR ως προοξειδωτικό. Τέλος, το σουλφονιωμένο ασκορβικό οξύ δρα για τον ίδιο λόγο ως προοξειδωτικό, ενώ φαίνεται πως σταθεροποιεί το ασκορβικό οξύ καθώς μειώνει την ικανότητα του ασκορβικού οξέος να παράγει και να αντιδρά με ελεύθερες ρίζες.

Στο τελευταίο μέρος αυτής της εργασίας μελετήθηκε αναλυτικά μια σειρά από δείγματα λευκών κρασιών τα οποία προέρχονταν από διάφορες περιοχές της Γαλλίας.

Στα δείγματα αυτά ταυτοποιήθηκαν με τη φασματομετρία LC-MS κάποιες από τις σουλφονιωμένες ενώσεις που μελετώνται στην παρούσα εργασία αλλά και κάποιες οι οποίες έχουν αναφερθεί στη βιβλιογραφία. Διαθέτοντας τα αποτελέσματα των μετρήσεων της αντιοξειδωτικής ικανότητας με τις μεθοδολογίες DPPH και EPR για τα συγκεκριμένα δείγματα κρασιών, στη συνέχεια αναπτύχθηκαν στατιστικά μοντέλα OPLS τα οποία έδειξαν ότι υπάρχει ισχυρή συσχέτιση μεταξύ των σουλφονιωμένων παραγώγων του οίνου, όπως η σουλφονιωμένη ακεταλδεΐδη και το σουλφονιωμένο πυρουβικό οξύ, και της αντιοξειδωτικής ικανότητας των οίνων όπως μετράται με τη μέθοδο DPPH και τη φασματοσκοπία EPR.

Λέξεις κλειδιά: NMR,EPR, DPPH, LC-MS-QToF, αντιοξειδωτική ικανότητα, λευκά κρασιά, σουλφονιωμένες ενώσεις

ABSTRACT

In the context of the present graduate thesis, the impact of sulfonation on the antioxidant and radical scavenging properties of wines, was studied. As it is well known, sulfites are used in the production of wine for the preservation and the successful aging of wine. Sulfur dioxide (SO_2) has antimicrobial and antioxidant properties but during the wine aging, its concentration is reduced. The predominant form of sulfites at the wine pH (pH = 3.5) is the bisulfite form (HSO_3^-), which reacts with various types of compounds present in wines, such as ketonic acids, sugars, quinones, carbonyl compounds etc. The sulfonated adducts in this way are considered to have an impact on the antioxidant properties of wine.

In the present study, the synthesis of several sulfonated compounds that are possibly formed in the wine by the reaction of the bisulfite with acetaldehyde, pyruvic acid, cysteine, glutathione and glucose was initially carried out, while the sulfonated ascorbic acid product was commercially available. These compounds were selected to cover all categories of wine compounds that are likely to react with the bisulfite (HSO_3^-). Both nuclear magnetic resonance (1D and 2D NMR) spectroscopy and liquid chromatography- conjugated with a mass spectrometer (LC-MS-QToF), were used to identify and characterize the synthesized compounds.

The antioxidant and radical scavenging properties of some of the synthesized compounds, namely acetaldehyde sulfonate, pyruvic sulfonate and ascorbic sulfonate were studied by two different analytical methodologies, the DPPH method and electron paramagnetic resonance (EPR) spectroscopy.. The experimental results obtained during this thesis are of particular interest, as it was shown that the sulfonated adducts of some compounds, such as acetaldehyde and pyruvic acid, possess radical scavenging properties although their parent compounds have no antioxidant properties., their It is also worth noting that in the EPR protocol ascorbic acid produces many radicals by its reaction with hydroxyl radical as well as with hydrogen peroxide. These new radicals compete with the hydroxyl-ethyl-radical (ethanol radical) in the reaction with the spin will trap POBN. Thus, in the DPPH method ascorbic acid is reported to be an antioxidant, while in the EPR assay it behaves as a prooxidant. Finally, it was found that ascorbic sulfonate contributes to

the stability of ascorbic acid, since after the reaction with the bisulfite, the production of the ascorbic radicals decreases.

In the last part of this work, a series of white wine samples from different regions of France, were analyzed in detail by using DPPH and EPR to study their antioxidant capacity and LC-MS spectrometry to determine their sulfonated compounds content. By combining the results of LC-MS sulfonate speciation with the antioxidant measurements by DPPH and EPR, multivariate statistical analysis OPLS models were developed. These models showed that there is a strong correlation between sulfonated products such as acetaldehyde sulfonate, and the antioxidant capacity of wines as measured by the DPPH method and EPR spectroscopy.

Keywords: NMR, EPR, DPPH, LC-MS-QToF, antioxidant properties, radical scavenging properties, white wines, sulfonated compounds

CONTENTS

Chapter 1. Introduction	1
1.1. Wine oxidation.....	1
1.2. Sulfonation in wines.....	3
1.3. Analytical methods.....	7
1.4. NMR spectroscopy.....	10
1.5. LC-MS-QToF.....	12
1.6. Important SO ₂ binders in wine.....	14
Aim of the project	17
Chapter 2. Experimental	18
2.1. Chemicals.....	18
2.2. Synthesis of sulfones.....	18
2.3. NMR characterization.....	19
2.4. DPPH assay.....	20
2.5. EPR spin trapping methodology.....	21
2.6. LC-MS-QToF.....	21
Chapter 3. Results-Discussion	23
3.1. NMR and LC-MS-QToF characterization of the sulfonated compounds.....	23
3.2. Evaluation of the antioxidant capacity of acetaldehyde sulfonate, pyruvic sulfonate and ascorbic sulfonate.....	56
3.2.1. DPPH assay.....	56
3.2.2. EPR method.....	58
3.3. Analysis of the sulfonated compounds in white wine samples by LC-MS-QToF.....	62
Chapter 4. Conclusions	68
Bibliography	70
Appendix	73

LIST OF FIGURES

	Page
Fig. 1: Wine oxidation reactions	2
Fig. 2: Examples of 1,2 and 1,4 addition of bisulfite to the carboxyl group of saturated and unsaturated carbonyl compounds	6
Fig. 3: The chemical structure of 2,2-diphenyl-1-picrylhydrazyl (DPPH)	8
Fig. 4: Schematic representation of an LC-MS system	13
Fig. 5: Schematic representation of a mass spectrometer with a QToF mass analyzer	13
Fig. 6: The biosynthesis of cysteine	15
Fig. 7: Aliphatic region of the ¹ H NMR spectra of acetaldehyde (a) and acetaldehyde sulfonate (b) in model wine solution (12% ethanol, 5g/L tartaric acid, pH=3.5, RT) and D ₂ O-TSP (1: acetaldehyde, 1a: acetaldehyde hydrated, 1b: acetaldehyde ethyl hemiacetal, 2: acetaldehyde sulfonate)	24
Fig. 8: ¹ H NMR spectra of acetaldehyde (a) and acetaldehyde sulfonate (b) in model wine solution (12% ethanol, 5g/L tartaric acid, pH=3.5, RT) and D ₂ O-TSP (1: acetaldehyde, 1a: acetaldehyde hydrated, 1b: acetaldehyde ethyl hemiacetal, 2: acetaldehyde sulfonate)	24
Fig. 9: MS [M-H] ⁻ spectrum of the acetaldehyde sulfonate (10 ⁻³ M, model wine: 12% ethanol, 5g/L tartaric acid, pH=3.5, RT)	26
Fig. 10: ¹ H NMR spectra of pyruvic acid (a) and pyruvic sulfonate (b) in model wine solution (12% ethanol, 5g/L tartaric acid, pH=3.5, RT) and D ₂ O-TSP. (3: pyruvic acid, 3a: pyruvic acid hydrated, 4: pyruvic sulfonate)	27
Fig. 11: MS [M-H] ⁻ spectrum of the pyruvic sulfonate (10 ⁻³ M, model wine: 12% ethanol, 5g/L tartaric acid, pH=3.5, RT)	28
Fig. 12: ¹ H NMR spectra of ascorbic acid (H1, H2, H3) (a) and ascorbic sulfonate (H1*, H2*, H3*) (b) in model wine solution (12% ethanol, 5g/L tartaric acid, pH=3.5, RT) and D ₂ O-TSP	29
Fig. 13: Homonuclear correlation ¹ H- ¹ H gCOSY 2D NMR spectrum of ascorbic sulfonate	30
Fig. 14: ¹ H- ¹³ C gHSQC 2D NMR spectra of ascorbic sulfonate	30
Fig. 15: ¹ H- ¹³ C gHMBC 2D NMR spectra of ascorbic sulfonate	31

Fig. 16: MS $[M+H]^+$ spectrum of ascorbic acid (10^{-4} M, model wine: 12% ethanol, 5g/L tartaric acid, pH=3.5, RT)	32
Fig. 17: MS $[M-H]^-$ spectrum of ascorbic sulfonate (10^{-3} M, model wine: 12% ethanol, 5g/L tartaric acid, pH=3.5, RT)	32
Fig. 18: ^1H NMR spectra of glucose (a) and glucose sulfonate (b) in model wine solution (12% ethanol, 5g/L tartaric acid, pH=3.5, RT) and D_2O -TSP. (α -g: α -glucose, β -g: β -glucose, 10a, 10b: 2 different forms of the glucose sulfonate)	33
Fig. 19: Homonuclear correlation ^1H - ^1H gCOSY 2D NMR spectrum of glucose sulfonate	35
Fig. 20: ^1H - ^{13}C gHSQC 2D NMR spectra of glucose sulfonate	36
Fig. 21: ^1H - ^{13}C gHMBC 2D NMR spectra of glucose sulfonate	36
Fig. 22: MS $[M-H]^-$ spectrum of glucose (10^{-4} M, model wine: 12% ethanol, 5g/L tartaric acid, pH=3.5, RT)	38
Fig. 23: MS $[M+H]^+$ spectrum of glucose sulfonate (10^{-3} M, model wine: 12% ethanol, 5g/L tartaric acid, pH=3.5, RT)	38
Fig. 24: ^1H NMR spectra of cysteine (a) and cysteine sulfonate (b) in model wine solution (12% ethanol, 5g/L tartaric acid, pH=3.5, RT) and D_2O -TSP. (11: cysteine, 12: cysteine sulfonate)	39
Fig. 25: Homonuclear correlation ^1H - ^1H gCOSY 2D NMR spectrum of cysteine sulfonate	40
Fig. 26: ^1H - ^{13}C gHSQC 2D NMR spectra of cysteine sulfonate	41
Fig. 27: ^1H - ^{13}C gHMBC 2D NMR spectra of cysteine sulfonate	42
Fig. 28: MS $[M+H]^+$ spectrum of cysteine (10^{-4} M, model wine: 12% ethanol, 5g/L tartaric acid, pH=3.5, RT)	43
Fig. 29: MS $[M-H]^-$ spectrum of cysteine sulfonate (10^{-3} M, model wine: 12% ethanol, 5g/L tartaric acid, pH=3.5, RT)	44
Fig. 30: ^1H NMR spectra of glutathione 7 (a) and glutathione sulfonate 8 (b) in model wine solution (12% ethanol, 5g/L tartaric acid, pH=3.5, RT) and D_2O -TSP	45
Fig. 31: Homonuclear correlation ^1H - ^1H gCOSY 2D NMR spectrum of glutathione sulfonate	46
Fig. 32: ^1H - ^{13}C gHSQC 2D NMR spectra of glutathione sulfonate	47
Fig. 33: ^1H - ^{13}C gHMBC 2D NMR spectra of glutathione sulfonate	48
Fig. 34: MS $[M+H]^+$ spectrum of glutathione (10^{-4} M, model wine: 12% ethanol, 5g/L tartaric acid, pH=3.5, RT)	50
Fig. 35: MS $[M-H]^-$ spectrum of glutathione (10^{-4} M, model wine: 12% ethanol, 5g/L tartaric acid, pH=3.5, RT)	51

acid, pH=3.5, RT)

Fig. 36: MS [M-H]⁻ spectrum of glutathione sulfonate (10⁻³ M, model wine: 12% ethanol, 5g/L tartaric acid, pH=3.5, RT) 51

Fig. 37: MS [M-H]⁻ spectrum of C₅H₁₀O₆N₂S₂ (**8a**) (10⁻³ M, model wine: 12% ethanol, 5g/L tartaric acid, pH=3.5, RT) 53

Fig. 38: Example of a graph that is created to measure the EC₂₀ of SO₂ (10⁻³ M) 56

Fig. 39: Antioxidant capacity of specific compounds using the DPPH method (*:No Reaction) 57

Fig. 40: Curves of the kinetics of the reaction of hydroxyl-ethyl radical with POBN when a compound is an antioxidant. (C1<C2<C3) 59

Fig. 41: Curves of the kinetics of the reaction of hydroxyl-ethyl radical with POBN when a compound is a prooxidant. (C1>C2>C3) 59

Fig. 42: Plot of the slope vs the % normalized I_{max} from the EPR kinetics diagrams for the sulfonated compounds. (Pyr-SO₃Na: pyruvic sulfonate, Acet-SO₃Na: acetaldehyde sulfonate, Asc: ascorbic acid, Asc-SO₃Na: ascorbic sulfonate, MW: model wine) 60

Fig. 43: Mechanism of radical scavenging activity of ascorbic acid 61

Fig. 44: Intensity of four sulfonated compounds in a wine sample from 2008 63

Fig. 45: Intensity of five sulfonated compounds in a wine sample from 2009 64

Fig. 46: Variable contribution plot of an OPLS model using LC-MS and EPR data (X variables) to predict the antioxidant capacity of wines based on DPPH (Y variable). The size of the points is a measure of the importance (VIP parameter) of the X variables 64

Fig. 47: Comparison of actual (y axis) and predicted (x axis) EC₂₀ values of wines based on an OPLS model that used LC-MS-QToF and EPR data 66

Fig. 48: Comparison of actual (y axis) and predicted (x axis) EC₂₀ values of wines based on an OPLS model that uses only LC-MS-QToF data 67

LIST OF TABLES

	Page
Table 1: Dissociation constants (k_d) for important SO ₂ binding electrophiles	5
Table 2: Theoretical and experimental m/z values of the sulfonation product of acetaldehyde (2) in 0.63 min	26
Table 3: Theoretical and experimental m/z values of the sulfonation product of pyruvic acid (4) in 0.63 min	28
Table 4: Assignment of ascorbic acid (5) and ascorbic sulfonate (6)	31
Table 5: Theoretical and experimental m/z values of ascorbic acid (5) at 0.70 min	32
Table 6: Theoretical and experimental m/z values of ascorbic sulfonate (6) at 0.63 min	33
Table 7: Assignment of glucose and glucose sulfonate 10a and 10b (as they are presented in Fig. 18 in spectrum b)	37
Table 8: Theoretical and experimental m/z values of glucose (9) at 0.57 min	38
Table 9: Theoretical and experimental m/z values of glucose sulfonate (10a & 10b) at 4.65 min	39
Table 10: Theoretical and experimental m/z values of cysteine (11) at 0.63 min	44
Table 11: Theoretical and experimental m/z values of cysteine sulfonate (12) at 0.63 min	44
Table 12: Assignment of glutathione and glutathione sulfonate	48
Table 13: Assignment of glutamate (8b) and dipeptide C ₅ H ₁₀ O ₆ N ₂ S ₂ (8a)	50
Table 14: Theoretical and experimental m/z values of glutathione (7) (positive form) at 0.70 min	52
Table 15: Theoretical and experimental m/z values of glutathione (7) (negative form) at 0.68 min	52
Table 16: Theoretical and experimental m/z values of glutathione sulfonate (8) at 0.64 min	52
Table 17: Theoretical and experimental m/z values of C ₅ H ₁₀ O ₃ N ₂ S (8a) at 0.64 min	53
Table 18: Assignment of free and sulfonated compounds	54
Table 19: Results of LC-MS-QToF of all the analyzed compounds (theoretical m/z , experimental m/z and the retention time)	55
Table 20: EC ₂₀ values of tested model compounds that were analyzed and the concentration that	57

was used

Table 21: First and maximum point of the curves of the kinetics for different concentrations of ascorbic acid	61
Table 22: List of the white wine samples	62
Table 23: Theoretical and experimental m/z values of α -ketoglutaric acid bisulfite (13) at 0.15 min	63
Table 24: Theoretical and experimental m/z values of indole lactic acid hexoside sulfonate (14) at 7.41 min	63
Table 25: Intensity of each compound ($\times 10^4$) in 26 white wine samples and the available results of DPPH and EPR	73

CHAPTER 1: INTRODUCTION

Several studies have shown that many diseases, such as cardiovascular diseases, cancer, diabetes, autoimmune diseases, neurodegenerative disorders, aging, hypertension, Parkinson, Alzheimer etc. can be associated to a nutritionally unbalanced diet. ^[1-4] In the early stages of such diseases, reactive oxygen species (ROS) are produced that can cause damage to biological structures such as proteins, lipids or DNA, even though human metabolism is armed with an antioxidant defense system that includes different enzymes to prevent these effects. ^[1, 5]

Wine is a widely consumed alcoholic beverage that has been produced for thousands of years (traced back to ~6000 BC) and is a product of the fermentation of grapes or must. Over the last decade, the health effects of wine consumption and its ability to prevent diseases such as those mentioned above, has been investigated. Antioxidants that occur in wine can be phenolic compounds (e.g. ferulic acid), sulfur and nitrogen compounds (e.g. glutathione, cysteine), vitamins (e.g. ascorbic acid, tocopherols) and flavonoids (e.g. anthocyanins, flavones). ^[2]

1.1. Wine oxidation

Wine oxidation can be distinguished into enzymatic oxidation and non-enzymatic oxidation. Enzymatic oxidation occurs in grape must and is correlated with the hydroxycinnamates and flavan-3-ols content of wines. Non-enzymatic oxidation, also known as chemical oxidation of wine, is initiated by the oxidation of polyphenols containing a catechol or a galloyl group. The phenolic hydroxyl groups attached to ring structures can act as reducing agents, hydrogen donors, singlet oxygen quenchers, superoxide radical scavengers and even as metal chelators. Reactive

oxygen species (ROS) are oxygen radicals, such as superoxide anion ($O_2^{\cdot-}$) and its conjugate acid hydroperoxyl (HOO^{\cdot}), hydroxyl (HO^{\cdot}), peroxy (ROO^{\cdot}), alkoxy (RO^{\cdot}) radicals. ROS also include other non-radical compounds that are either potential oxidizing agents or are easily converted to radicals, such as hydrogen peroxide (H_2O_2), ozone (O_3), hypochlorous acid ($HOCl$), singlet oxygen (1O_2), and lipid peroxide ($LOOH$). In wine, ROS can be produced by reduced transition metals ions [e.g. $Fe(II)$] in the stepwise addition of a single electron to triplet oxygen. More specifically, an electron is transferred to the oxygen forming a superoxide radical anion ($O_2^{\cdot-}$), which at wine pH exists as a hydroperoxyl radical (HOO^{\cdot}). In a second step, one more electron is transferred to produce a peroxide anion (O_2^{2-}), which at wine pH exists as a hydrogen peroxide (H_2O_2). The next reduction step will produce an even more reactive oxidant, the hydroxyl radical (HO^{\cdot}), which is able to oxidize almost any organic molecule present in wine. [2, 6]

Enzymatic and non-enzymatic oxidation reactions of phenolic compounds lead to the formation of quinones, which can spontaneously combine with nucleophilic compounds (phenols, thiols and amines) due to their high electrophilic character.

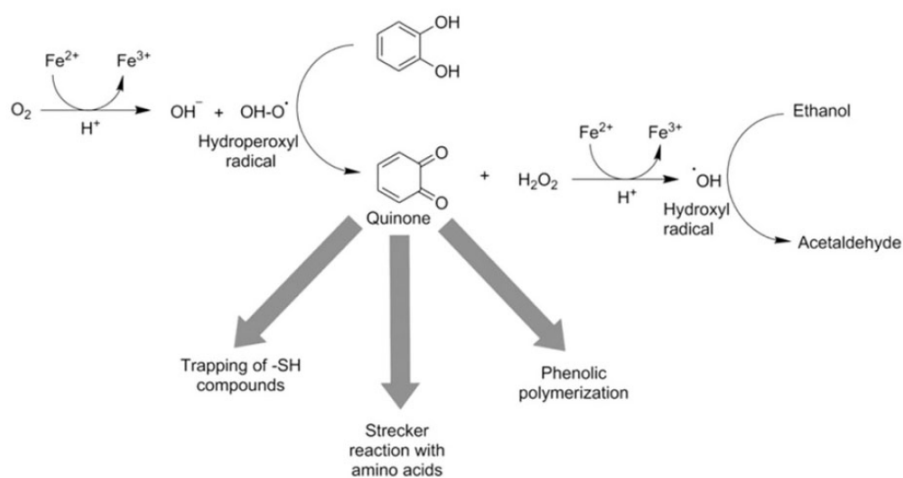


Fig. 1: Wine oxidation reactions [7]

For example, ascorbic acid and sulfur dioxide present in wine are able to reduce quinones. Ascorbic acid is present in grapes naturally but is usually rapidly consumed after crushing. Thus, it is present in white wines basically due to exogenous additions by producers, often just before bottling, but it can also be added at various stages during the wine production process. The levels of ascorbic acid added range from 50 to 150 mg/L. Addition of ascorbic acid in white wine takes place because it has the ability to scavenge molecular oxygen efficiently. Initially, ascorbic acid can be reduced easily and converted to dehydroascorbic acid and hydrogen peroxide. Dehydroascorbic acid then undergoes rapid degradation producing a variety of species including carboxylic acids, ketones, and aldehydes. When ascorbic acid is added to wine, it is important to also have adequate quantities of SO₂ present also, in order to efficiently remove hydrogen peroxide and also react with all the different carbonyl compounds created due to ascorbic acid oxidation. ^[6, 8] Furthermore, it has been shown that addition of ascorbic acid to Riesling and Chardonnay wines at bottling has an effect on wine color, and more specifically it was demonstrated that wines without any addition of ascorbic acid were browner and had a large overall color intensity. ^[9] Unfortunately, ascorbic acid has no antimicrobial activity and thus it can not replace sulfur dioxide in wine. ^[9]

1.2. Sulfonation in wines

Sulfur dioxide has been used for many purposes in wine production. First of all, it is an efficient antiseptic that provides protection against detrimental microorganisms, particularly bacteria. SO₂ also has high antioxidant activity as it inhibits or delays the deteriorating effects of oxidation by inhibiting the action of

enzymes that are oxidases. Finally, sulfur dioxide binds fermentation by-products that are responsible for off-flavors, maintaining the desired aroma profile. ^[10, 11]

It is necessary to control the SO₂ levels in wine for two main reasons. The first one is that high levels of SO₂ produce an unpleasant aroma and taste. The second and most important is that it might be related to some health risks, such as breathing difficulties, sneezing, hives, migraine etc. ^[12] SO₂ levels should be checked before bottling and at the end-product stage to conform with legal limits (between 160 and 350 mg/L depending on country legislation and the type of wine). ^[10, 13] The most common analytical method for determining sulfur dioxide in wines is the aeration-oxidation or modified Monier-Williams method, recommended by the Association of Official Analytical Chemists (AOAC) and by the International Organization of Vine and Wine (OIV). ^[10]

In aqueous solutions, molecular sulfur dioxide (SO₂), bisulfite (HSO₃⁻) and sulfite (SO₃²⁻) ions exist in equilibrium:



SO₂ is present in wine in two different forms: free and bound. Free SO₂ is the active form which provides protection to the wine and is calculated as the sum of SO₂, HSO₃⁻ and SO₃²⁻ concentrations. At wine pH (usually between 3 and 4), HSO₃⁻ is the predominant form representing about 94–99% of the total free form, the rest being SO₂, since SO₃²⁻ is usually negligible. ^[13-15] It is important to be able to measure free SO₂ accurately, since this will determine the redox chemistry and microbial stability of wine. The total levels of SO₂ must also be measured for safety and legal reasons. Molecular SO₂, which is a minor component at wine pH, has antimicrobial activity due to its ability to pass through the cellular membrane, but its antioxidant properties are limited. ^[7] Contrary to molecular SO₂, bisulfite (HSO₃⁻) has strong antioxidant

properties, but its antimicrobial properties are reduced compared to those of molecular SO₂.^[10] In addition, molecular SO₂ decreases over time as it is lost to the atmosphere via tank or barrel headspace and during processing activities. On the other hand, HSO₃⁻ is oxidized to sulfates (SO₄²⁻) by oxygen radicals, such as hydrogen peroxide (H₂O₂) but most importantly it can also bind to different types of compounds, such as carbonyl compounds, ketonic acids, sugars, quinones, anthocyanins and others forming α-hydroxysulfonate adducts.^[15-17] Bisulfite (HSO₃⁻) is a “soft” nucleophile and forms covalent adducts with soft electrophiles. The equilibrium in these reactions is often represented as a dissociation rather than a formation. The dissociation constant (K_d) has been calculated for the major binders of SO₂ mentioned above:



$$K_d = [\text{E}][\text{HSO}_3^-] / [\text{Adduct}]$$

Table 1: Dissociation constants (K_d) for important SO₂ binding electrophiles^[18]

Major SO ₂ binders		Other odor-active SO ₂ binders	
<i>E</i>	K _d (M ⁻¹)	<i>E</i>	K _d (M ⁻¹)
Glucose	2.2 × 10 ⁻¹		
Fructose	1.5		
Acetoin	8.0 × 10 ⁻²	Diacetyl	1.4 × 10 ⁻⁴
Galacturonic acid	1.6 × 10 ⁻²	β-Damascenone	Unknown
α-Ketoglutarate	4.9 × 10 ⁻⁴	β-Ionone	2.1 × 10 ⁻⁴
Pyruvate	1.4 × 10 ⁻⁴	Hexanal	3.5 × 10 ⁻⁶
Acetaldehyde	1.5 × 10 ⁻⁶	(<i>E</i>)-2-Pentenal	8.3 × 10 ⁻³
Anthocyanin ^a	1 × 10 ⁻⁵	(<i>E</i>)-2-Nonenal	Unknown

^aFor flavylium form of cyanidin-3-glucoside [5].

As shown in Table 1, the most important SO₂ binders in wine (those with the smallest K_d values) are acetaldehyde and several carbonyl compounds. There are two reaction pathways for the addition of bisulfite to carbonyls, as depicted in Fig. 2. The first one is observed for saturated carbonyl groups such as in acetaldehyde, and

involves nucleophilic addition directly on the carbonyl group (1,2 addition). The second pathway involves a Michael addition, and it is observed for unsaturated conjugated carbonyls (1,4 addition).^[18]

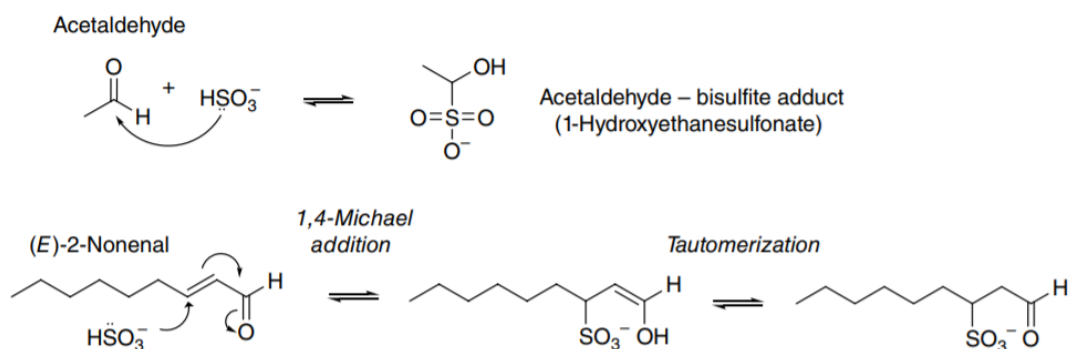


Fig. 2: Examples of 1,2 and 1,4 addition of bisulfite to the carbonyl group of saturated and unsaturated carbonyl compounds.^[18]

SO_2 binders with K_d values smaller than 1×10^{-5} are referred to as strong binders. In white wines, the only strong SO_2 binder is acetaldehyde, while other compounds like pyruvic acid are considered weak binders. HSO_3^- binding reactions may differ based on changes in wine chemistry but usually, the major SO_2 binder in most wines is acetaldehyde. Acetaldehyde is the product formed by the conversion of ethanol during wine oxidation and as already mentioned it has a strong SO_2 -binding ability. The only exception to the dominant binding ability of acetaldehyde is observed in some sweet wines (or musts), where 50% of the total SO_2 is bound to glucose, since in these wines glucose concentrations can reach up to 50 g/L.^[18, 19] On the other hand, some carbonyl compounds and ketonic acids may be observed to react reversibly with bisulfite to produce adducts from which, free SO_2 can be released.^[10, 13, 18]

During the last decades, the interest of the researchers has turned to the impact of sulfonation in wines and its correlation with wine aging. A recent study

demonstrated the impact of SO₂ addition to the must and metabolites like amino acids, carbohydrates or phenolic compounds, not only in a particular step of the wine-making process, but also during aging.^[11] There have been also studies that correlate wine aging with the amount of sulfonated flavanols and indoles present.^[20, 21] A basic question that arises from these studies is whether the sulfonated adducts produced possess any antioxidant capacity. By definition, an antioxidant is any substance that directly scavenges ROS by donating an electron, or acts indirectly to increase antioxidant defenses or inhibit ROS production. More specifically, indirect antioxidants are not always redox active but they activate the Keap1/Nrf2/ARE pathway and finally the phase II detoxifying enzymes and they participate to the synthesis or the generation of direct antioxidants.^[22, 23]

Another property that a compound should have in order to be considered as an antioxidant is the ability, after scavenging radical, to form a new radical that is stable on further oxidation through intramolecular hydrogen bonding.^[2, 24] Unfortunately, there is only one reported study regarding the formation of acetaldehyde-bisulfite adduct in beer where it was shown that carbonyl-bisulfite adducts possess radical scavenging activity and can trap active oxygen produced during the process of beer oxidation.^[25]

1.3. Analytical methods

There have been many studies aiming to establish and validate methods for the measurement of the antioxidant capacity of the different categories of compounds are present in wine, such as polyphenols, sugars, carbonyl compounds, organic acids, flavonoids etc. There are several methods that have been used to evaluate antioxidant activity in wine, including spectrophotometric and chromatographic assays. The

Folin–Ciocalteu (FC) assay has been adopted by the European Commission for the analysis of total polyphenols in wine but it is also used to measure the total reducing capacity of a wine sample. ^[1, 26] The ferric thiocyanate assay (FTC) measures antioxidant activity by the inhibition of lipid oxidation (peroxide compounds formed during lipid oxidation). ^[26] In the oxygen radical absorbing capacity (ORAC) assay, phycoerythrin is used to react with free radicals and the antioxidant capacity of polyphenols is quantified by using fluorescence spectroscopy. ^[5, 27] The 2,2'-azinobis(3-ethylbenzothiazoline-6-sulfonic acid) (ABTS) radical cation assay is a methodology where a light emitting-radical adduct is generated from ABTS and antioxidant capacity is measured by the absorption of the solution at 414 nm. ^[5, 28, 29] Another frequently used methodology involves N,N-dimethyl-p-phenylenediamine (DMPD). In this assay, and in the presence of an antioxidant compound which is able to transfer a hydrogen atom to the radical, the colored DMPD radical cation is discolored and the absorption intensity is measured spectrometrically at 505 nm. ^[29]

In the present dissertation, 2,2-diphenyl-1-picrylhydrazyl (DPPH) radical scavenging assay was used to assess antioxidant activity in wines.

This methodology uses DPPH which is one of the few stable organic nitrogen radicals, has a purple colour and can be measured spectrophotometrically.

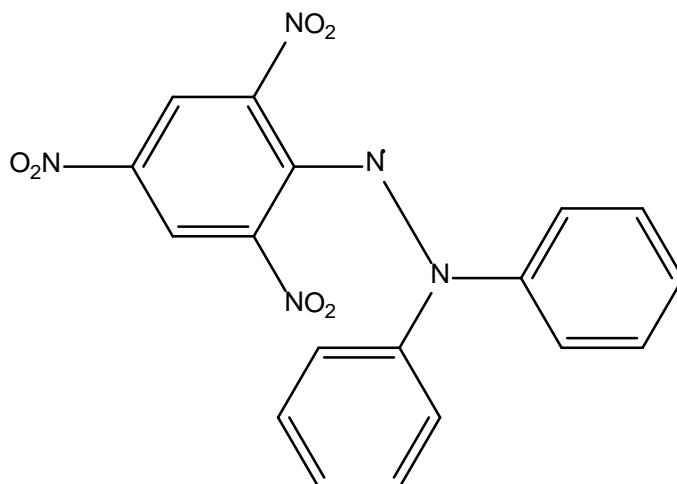


Fig. 3: The chemical structure of 2,2-diphenyl-1-picrylhydrazyl (DPPH)

In the presence of compounds that have the ability to transfer an electron or to donate hydrogen, the DPPH molecule becomes discolored and the colour change of the DPPH solution is used to quantify the antioxidant capacity of the compound that is present in the solution. DPPH is selective in its reaction with hydrogen-donors, as for example, it doesn't react with phenolic acids containing only one OH-group. Although the DPPH method is widely used, it does have some limitations. As can be seen in Fig. 3, the radical is located on a nitrogen atom at the center of the chemical structure of DPPH. Although this location is accessible to small molecules, it may provide limited access to larger molecules due to steric hindrance. Another problematic aspect of this assay was the difficulty in measuring the EC_{50} due to linearity changes over 40% of the absorbance. Recently, a new parameter has been proposed to express the assay results, the EC_{20} , representing the concentration of the substance needed to react with 20% of the DPPH radicals. [4, 5, 26, 30, 31]

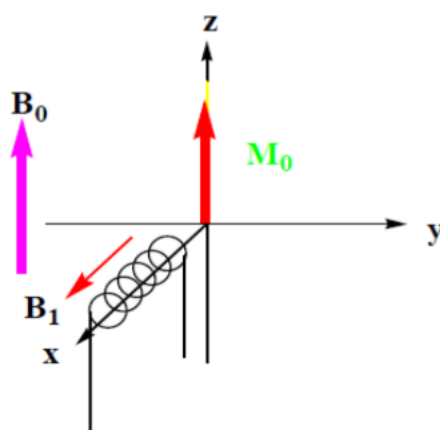
In addition to chromatographic methods such as High Performance Thin Layer Chromatography (HPTLC) [1], HPLC and GC [13, 15, 16], electrochemical methods such as cyclic voltametry, square wave voltametry, differential pulse voltametry and chronoamperometry [14, 32], have been also used to study the antioxidant activity of wines. The only spectroscopic method that has been used for the determination of the antioxidant capacity of wines is Electron Paramagnetic Resonance (EPR) spectroscopy. [33, 34]

EPR spectroscopy allows for the direct detection of paramagnetic species, such as the unpaired electrons of free radicals and the determination of the radical's identity is also possible. By the EPR spin trapping method, reactive free radicals are

trapped by a diamagnetic compound (called spin trap) via addition to a spin trap double bond to produce a more stable radical product (spin adduct), which has paramagnetic properties and can be detected by EPR. The spin traps that are usually used are α -(4-pyridyl-1-oxide)-*N*-*tert*-butylnitron (POBN) or α -phenyl-*N*-*tert*-butylnitron (PBN) and they scavenge free radical species via addition to a carbon located in an alpha position relative to the nitrogen. For the EPR method, Fenton conditions are used to measure the oxidation of wine's major constituents. More specifically, hydrogen peroxide in association with ferrous ions produce hydroxyl radicals, which in turn react with ethanol. Thus, the hydroxyl ethyl radical that is produced, can be trapped by spin trap molecules, such as POBN. ^[34-36]

1.4. NMR spectroscopy ^[37, 38]

Nuclear Magnetic Resonance spectroscopy utilizes a phenomenon that was discovered in 1946 by Bloch and Purcell and occurs when spin-active nuclei such as ^1H , ^{13}C , ^{31}P etc. are inserted in a homogeneous static magnetic field B_0 . Excited by a second magnetic field B_1 perpendicular to B_0 , spin-active nuclei emit electromagnetic radiation in the radio frequency region, which is detected as a frequency spectrum.



NMR spectroscopy is useful because the frequency of the emitted radiation depends on the chemical and electronic environment of NMR-active nuclei, providing us with useful information regarding the chemical structure of compounds. NMR spectroscopy can be applied to any sample containing molecules with a spin-active nuclei, the most common of which are ^1H and ^{13}C .

Depending on the type of analytical question, different NMR spectroscopy techniques involving 1D and 2D spectroscopy may be applied. Two-dimensional NMR spectra have two frequency axes F1 (vertical) and F2 (horizontal) which can be from the same (e.g. ^1H - ^1H) or different nuclei (^1H in F2 and ^{13}C in F1). The most commonly used 2D NMR experiments are COSY, HSQC and HMBC. COSY (correlation spectroscopy) is a homonuclear 2D experiment and it is useful for the assignment of complicated ^1H 1D spectra with overlapped signals. The HSQC (Heteronuclear Single Quantum Coherence) experiment allows the observation of the one-bond correlation between a ^1H nucleus which is directly bonded to a heteronucleus (usually ^{13}C or ^{15}N), while the HMBC (Heteronuclear Multiple Bond Coherence) experiment identifies the long-range heteronuclear shift correlation through two and three bond J coupling. Both of them are paramount for the spectral assignment and the structural characterization of organic compounds of interest.

NMR spectroscopy is widely used in organic chemistry for structure elucidation. NMR is also heavily used in analytical chemistry, as it permits not only the qualitative but also the quantitative analysis of complex organic mixtures, as the NMR signal area is proportional to the number of the nuclei that produce a certain peak. NMR spectroscopy is thus very important for the analysis of such complex samples as foods and beverages.

Wine is one of the first beverages that was analyzed by NMR spectroscopy. The first application of NMR in wine analysis was the determination of the amount of ethanol by quantifying the ethanol peaks in the ^1H NMR spectrum. Subsequent studies focused on the identification and detailed analysis of wine's organic components, authenticity issues, metabolomics analysis to classify wines in terms of their geographical origin, vintage and variety and most recently, to observe wine evolution during aging in barrels and bottles. ^[39-44]

1.5. LC-MS-QToF ^[45, 46]

Liquid chromatography-mass spectrometry (LC-MS) is an analytical tool that combines the physical separation and the mass analysis of complex organic mixtures. The most often employed interface is an electrospray ion source. LC-MS is widely used in many analytical applications, such as the identification of unknown compounds, the determination of the isotopic composition etc.

The basic principle of liquid chromatography is that the sample is carried by a liquid mobile phase at high pressure to a column that is packed with a stationary phase. There, the sample can physically be separated depending on factors such as size, charge, polarity etc. On the other hand, mass spectrometry (MS) is an analytical technique that measures the mass-to-charge ratio (m/z) of charged molecular species. More specifically, the mass spectrometer consists of three main parts. When a sample enters the mass spectrometer, first it vaporizes and then it is ionized by an ion source, forming charged particles. In the next step, a mass analyzer separates the different ions depending on their mass to charge ratio by applying a strong electromagnetic field. The third part of the mass spectrometer is the detector, which records the signal intensity as a function of the m/z value of the signals. (Fig. 4)

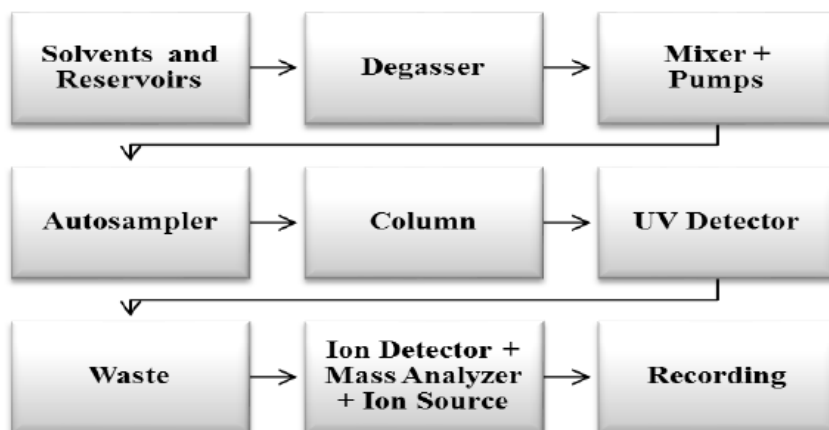


Fig .4: Schematic representation of an LC-MS system ^[45]

There are many different types of mass analyzers that can be used (e.g. single quadrupole, triple quadrupole, ion trap etc) in LC-MS spectroscopy, depending on the application. In the present study, the mass analyzer used was a quadrupole-time of flight (QToF) analyzer. (Fig. 5)

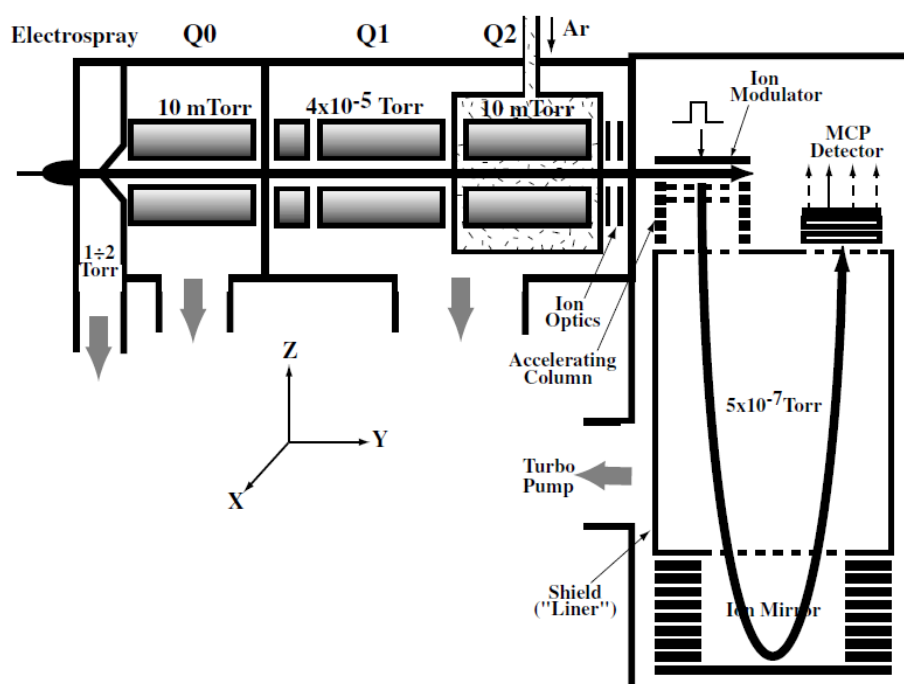


Fig. 5: Schematic representation of a mass spectrometer with a QToF mass analyzer ^[46]

1.6. Important SO₂ binders in wine

In the present dissertation, we chose to analyze in detail the following important compounds belonging to different categories of SO₂ binders: aldehydes, ketonic acids, vitamins, carbohydrates and peptides.

Acetaldehyde is the principal aldehyde present in wine and it is produced by yeast during alcoholic fermentation just before ethanol formation. Thus, the total amount of acetaldehyde produced during fermentation is almost the same with the molar amount of ethanol produced (~2M or 90 g/L). However, most acetaldehyde is immediately reduced to ethanol by yeast, and its final concentration reaches on average 25 mg/L in red and 40 mg/L in white wines, depending on the yeast strain and the initial SO₂ concentration, although it can range between 3-494 mg/L.^[47] After fermentation and during storage and aging, acetaldehyde is produced due to the oxidation of ethanol via the Fenton reaction.^[18]

Pyruvic acid is a ketonic acid produced by yeast metabolism and by the oxidation of lactic or malic acid. Also, glucose can be transformed to pyruvic acid due to catabolic reactions that take place during glycolysis. In *Saccharomyces cerevisiae* (the most important microorganism for the winemaking procedure), pyruvic acid is either decarboxylated to acetaldehyde or it can be used in the formation of acetyl-CoA. The quantity of pyruvic acid ranges in commercial wines between 11-460 mg/L, although the average is 14 mg/L in red wines and 25 mg/L in white wines.^[18, 47-49]

Ascorbic acid is a vitamin with strong antioxidant properties, naturally present in grapes (32 mg/kg), but it is rapidly consumed after crushing or during fermentation.

In white wines, ascorbic acid may be added as a preservative at several stages during winemaking, but usually just before bottling. The levels of added ascorbic acid range between 50 and 150 mg/L. [2, 9, 18, 50]

Glucose and fructose, are the two hexose reducing sugars preferred by yeast during glycolysis and alcoholic fermentation. In grapes, glucose and fructose have almost equal concentrations that range between 0.5-5 g/L. The ratio of glucose to fructose is reduced during fermentation from a starting value of 0.95 to 0.25 near to the end of fermentation. [50]

Cysteine is an amino acid and a useful nitrogen source for the yeast during fermentation. The formation of cysteine is briefly described below in Fig. 6. The concentration of cysteine is 6-8 mg/L in the must and rises up to 14mM in wine. [18, 50, 51]

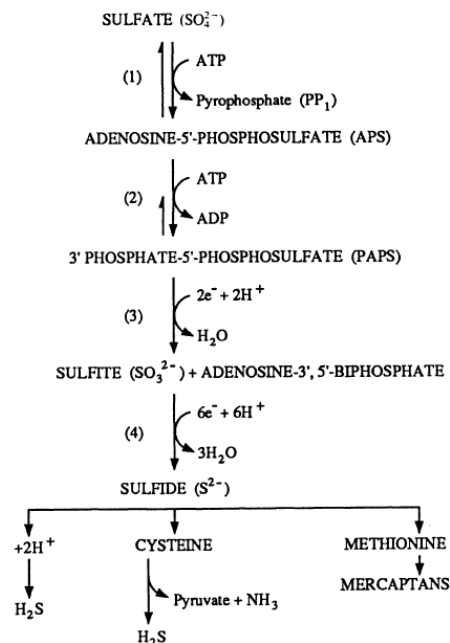


Fig. 6: The biosynthesis of cysteine [50]

Glutathione is a tripeptide consisting of glutamate, cysteine and glycine which is biosynthesized during fermentation. It takes part in many oxidation reactions as a reductant, providing protection against heavy metal toxicity, or the oxidation of lipids and polyphenols by ROS. Glutathione is also an important antioxidant as it can react as a nucleophile with reactive electrophiles, thus contributing to wine's chemical oxidative stability. Glutathione detected in wine is mostly in the reduced form, at levels between 56.3–371.8 μ mol/kg in grapes and 41.9–332.7mM in musts. The glutathione content of wine decreases during aging and reaches values between 0,1–5,1 mg/L. ^[18, 52, 53]

AIM OF THE PROJECT

In the present dissertation, we present an analytical study of the impact of sulfonation on the antioxidant and radical scavenging properties of wines. It is well known that bisulfite (HSO_3^-), which is the predominant form of sulfites at wine pH, reacts with different types of compounds typically present in wine to produce sulfonated adducts. The first objective of this study is the synthesis of a series of sulfonated adducts and their characterization by NMR spectroscopy and LC-MS-QToF. Our next objective is to study the ability of these model sulfonated compounds to scavenge free radicals by a series of analytical methods, such as the DPPH assay and EPR spectroscopy. The third and final part of this work deals with the analysis of a series of white wines by LC-MS-QToF to identify and quantify their content in various sulfonated adducts, and then to develop OPLS statistical models to explore correlations between the presence of some sulfonated compounds and the antioxidant capacity of the wines as studied by the DPPH assay and EPR spectrometry.

CHAPTER 2: EXPERIMENTAL

2.1. *Chemicals*

Acetaldehyde (**1**), pyruvic acid (**3**), ascorbic acid (**5**), glutathione (**7**), glucose (**9**), cysteine (**11**), 2,2-Diphenyl-1-picrylhydrazyl (DPPH), citric acid monohydrate, sodium phosphate dibasic, tartaric acid, Iron (II) sulfate, hydrogen peroxide, α -(4-Pyridyl N-oxide)-N-tert-butyl nitron (POBN), methanol, ethanol and deuterium oxide were purchased from Sigma – Aldrich. Sodium bisulfite and L-ascorbic acid 2-sulfate dipotassium salt (**6**) were purchased from Merck and ChemCruzBiochemicals respectively.

2.2. *Synthesis of sulfones*

For the synthesis of the sulfonated adducts, a model wine solution was prepared by adding 12% of ethanol and 5g/L of tartaric acid to 1L of ultrapure water. To control the pH value at 3.5, some drops of 10% w/v NaOH solution were used. The ultrapure water and the model wine that were used for the experiments were degassed using argon (Ar) gas for 2 min.

Acetaldehyde-sulfonate (Acet-SO₃H, **2**): 2.3 μ L of acetaldehyde were poured slowly into a sodium bisulfite solution (6 mg in 500 μ L of model wine) at room temperature. After the addition, the sample was stirred. The reaction was monitored for 2 days with ¹H-NMR control of free acetaldehyde consumption.

Pyruvic-sulfonate (Pyr-SO₃H, **4**): 5.6 μ L of pyruvic acid were poured slowly into a sodium bisulfite solution (6 mg in 500 μ L of model wine) at room temperature. After the addition, the sample was stirred. The reaction was monitored for 2 days with ¹H-NMR control of free pyruvic acid consumption.

Glucose-sulfonate (Gluc-SO₃H, **9**): 70mM of glucose (7.6 mg in 500 μ L of model wine) were dissolved into a sodium bisulfite solution (20 mg in 500 μ L of model

wine) at room temperature. After the addition, the sample was stirred. The reaction was monitored for 6 weeks with ^1H -NMR control of free glucose consumption.

Glutathione-sulfonate (GSH-SO₃H, 7): 70mM of glutathione (12.9 mg in 500 μL of model wine) were dissolved into a sodium bisulfite solution (20 mg in 500 μL of model wine) at room temperature. After the addition, the sample was stirred. The reaction was monitored for 6 weeks with ^1H -NMR control of free glutathione consumption.

Cysteine-sulfonate (Cys-SO₃H, 11): 70mM of cysteine (5.1 mg in 500 μL of model wine) were dissolved into a sodium bisulfite solution (20 mg in 500 μL of model wine) at room temperature. After the addition, the sample was stirred. The reaction was monitored for 6 weeks with ^1H -NMR control of free cysteine consumption.

The 500 μL of each solution and 100 μL of a solution containing 1.74mM 3-trimethylsilylpropanoic acid sodium salt (TSP) in D₂O were added in a 5 mm-o.d. Wilmad NMR tube for analysis. The signal from the TSP served as an internal standard (IS).

2.3. NMR characterization

NMR experiments were performed on a Bruker 600 MHz spectrometer at a constant temperature of 298K. For the ^1H NMR spectra, the WET multiple solvent suppression experiment was used since its use leads to the simultaneous suppression of all proton peaks of water and ethanol. The 2D acquisition parameters for the COSY experiment were as follows: The standard cosygpprqf Bruker pulse sequence was used, with a spectral width of 9014.4 Hz (F2) and 9003.4 Hz (F1), the acquisition time was 0.11 sec, 2K(t2) \times 256 (t1) data points, 32 scans and 16 dummy scans. Acquisition parameters for the ^1H - ^{13}C HSQC experiment were as follows: The hsqcedetgpcisp2.3 Bruker pulse sequence, which also incorporates DEPT editing of the signals based on

carbon multiplicity (methine, methylene, methyl) was used, with a spectral width of 9615.3 Hz in the F2 dimension and 24904.9 Hz in the F1 dimension. The acquisition time was 0.106 sec, 2K (t2) × 128 (t1) data points, 96 scans and 16 dummy scans. Acquisition parameters for the ^1H - ^{13}C HMBC experiment were as follows: The hmbcgp1pndqf Bruker pulse sequence was used, with a spectral width 7812.5Hz in the F2 dimension and 33207.4 Hz in the F1 dimension. Acquisition time was 0.262 sec, 4K (t2) × 128 (t1) data points, 96 scans and 16 dummy scans.

All NMR data were processed using Topspin 3.5 NMR (Bruker) software.

2.4. DPPH assay

DPPH assay was carried out based on the protocol proposed by Romanet et al. (2019) (Under review). 10 mL of DPPH (0.63mM in methanol) and 90 mL of citrate / phosphate buffer (12.5 mMNa₂HPO₄ and 14.6mM citric acid were dissolved in a H₂O: Methanol (4:5 v/v) solution) were added in a 100 mL amber volumetric flask and left to rest for one hour before use.

10⁻² M of each tested compound were prepared in 10 mL of ultrapure water and diluted to the model wine solution to achieve a final volume of 4mL. The ultrapure water and the model wine were degased for 2 minutes using argon (Ar) gas. Sulfonated samples were degased using CO₂ for 5 minutes to ensure the lack of residual free SO₂. To decide the quantity of the analyzed compound that was needed for the DPPH assay, 4 different concentrations of the compound (5x10⁻⁵M, 10⁻⁴M, 5x10⁻⁴M, 10⁻³M) were tested. To 100μL of each concentration, 3.9 mL of the DPPH solution were added. The procedure was done under anaerobic conditions and was repeated three times. After four hours, the reaction was completed and the samples were measured spectrophotometrically at 525nm. The appropriate concentration had to reach an absorbance of about 70-75% in order to correctly calculate the EC₂₀.

20, 40, 60, 80, 100 μL of the selected concentration were used and filled with ultrapure water until 100μL respectively. After that, 3.9mL of the final DPPH solution were added to each tube. Anaerobic conditions were also used and the whole procedure was repeated three times. After four hours, the samples were measured spectrophotometrically at 525nm using 10mm QS absorption cells.

To calculate the EC₂₀, a graph using the absorbance of each volume (20, 40, 60, 80 and 100 µL) and the molar ratio between the moles of the sample and the moles of the DPPH solution was prepared. The equation that was used to determine the EC₂₀ is the following:

$$EC_{20} = [(80 - b) / a] * 100\%$$

a and b are the coefficients of the linear equation of the graph ($y = ax + b$).

2.5. EPR spin trapping methodology

EPR analysis was carried out based on the protocol proposed by Nikolantonaki et al. (2019).^[54] 10⁻²M of the analyzed compound were prepared in ultrapure water. Different concentrations were tested by diluting the initial solution to the model wine to achieve a final volume of 4mL. The ultrapure water and the model wine were degassed for 2 minutes using argon (Ar) gas. Sulfonated samples were degassed using CO₂ for 5 minutes to ensure the lack of residual free SO₂.

For the EPR analysis, three different solutions were prepared in amber vials. FeSO₄·7H₂O (50µM) and H₂O₂ (954 µM) were used as a source of hydroxyl radicals and 30mM of POBN solution as a spin trap. Finally, each sample was added to achieve a final volume of 1mL. When the EPR conditions were fine, the whole sample were stirred and quickly transferred to an EPR capillary. EPR measurements were performed using an ER300 EPR spectrometer. The parameters used for the experiments were as follows: modulation frequency 100 kHz, modulation amplitude 0.9 G, time constant 10.24ms, conversion time 2.56ms, microwave power 10mW and receiver gain 104. Spectra were recorded at room temperature (298 K). Serial 2-min EPR acquisitions were performed. The intensity of the EPR signals was determined by the WINESR software program.

2.6. LC-MS-QToF

The analysis has been realized using an ultra-high-pressure liquid chromatography (Dionex Ultimate 3000, ThermoFischer) coupled to a MaXis plus MQ ESI-Q-TOF mass spectrometer (Bruker, Bremen, Germany). The column used was an Acquity

BEH C18 1.7 μ m, 100 x 2.1 mm by Waters (Guyancourt, France) in reverse phase to analyzed non-polar compounds. The mobile phase was (A) acidified water (0.1% v/v of formic acid) and (B) 95% (v/v) acidified acetonitrile (0.1% v/v of formic acid). The temperature of elution was 40°C using the gradient: 0-1.10 min 5% (v/v) of B and 95% (v/v) of B at 6.40 min. The flow was 400 μ L/min. The positive ionization takes place in electrospray (2 bars pressure for nebulizer and 10L/min for nitrogen dry gas flow). End plate offset (500V) and capillary voltage (4500V) permit the ions transfer. To recalibrate spectrum, 4 times diluted calibrant (ESI-L Low Concentration Tuning Mix (Agilent, Les Ulis, France)) is inject at the beginning of each run. Before each analysis batch, the mass spectrometer was calibrated using undiluted Tuning Mix in enhanced quadratic mode (errors <0.5ppm). The mass range was between 100 and 1500m/z in positive ionization mode. Quality control were analyzed before and throughout each batch, to verify the stability of the LC-MS system. All sample were analyzed randomly. Detection was carried out in negative ionization mode with the following parameters: Nebulizer pressure = 3.0 bar, dry gas flow = 10.0 l/min, dry gas temperature = 200 °C, capillary voltage = 3500 V, end plate off set= -500 V, mass range = 50–1500 m/z. For individual recalibration of each chromatogram a sodium formate solution (0.05% formic acid/1% NaOH (0.1 M) /Propanol: H₂O (1/1 v/v)), solution was injected via a six-port valve before each run between 0.1 and 0.3 min.

CHAPTER 3. RESULTS - DISCUSSION

This section will have three parts. The identification and structure elucidation of the sulfonated compounds of cysteine, glutathione, glucose, acetaldehyde, pyruvic acid and ascorbic acid will be described in the first part as performed by a series of 1D and 2D NMR experiments, as well as the quantification of the synthesized compounds. The experiments have been performed in model wine (12% ethanol, 5g/L tartaric acid, pH=3.5) at room temperature (RT) and TSP salt has been used as an internal standard to quantify the percentage of the sulfonated adduct produced. In the second part, the antioxidant capacity of acetaldehyde, pyruvic acid, ascorbic acid and their sulfonated products will be compared using the DPPH assay and an EPR spin trapping methodology. Finally, in the third part will be presented the research of the sulfonated products in wine samples using LC-MS-QToF.

3.1. NMR and LC-MS-QToF characterization of the sulfonated compounds

In the following discussion and figures, the ^1H NMR spectra of free and sulfonated adduct are presented in (a) and (b) respectively. In addition, NMR results (A) will be compared to those from LC-MS-QToF (B).

1A. NMR characterization of acetaldehyde sulfonate (2)

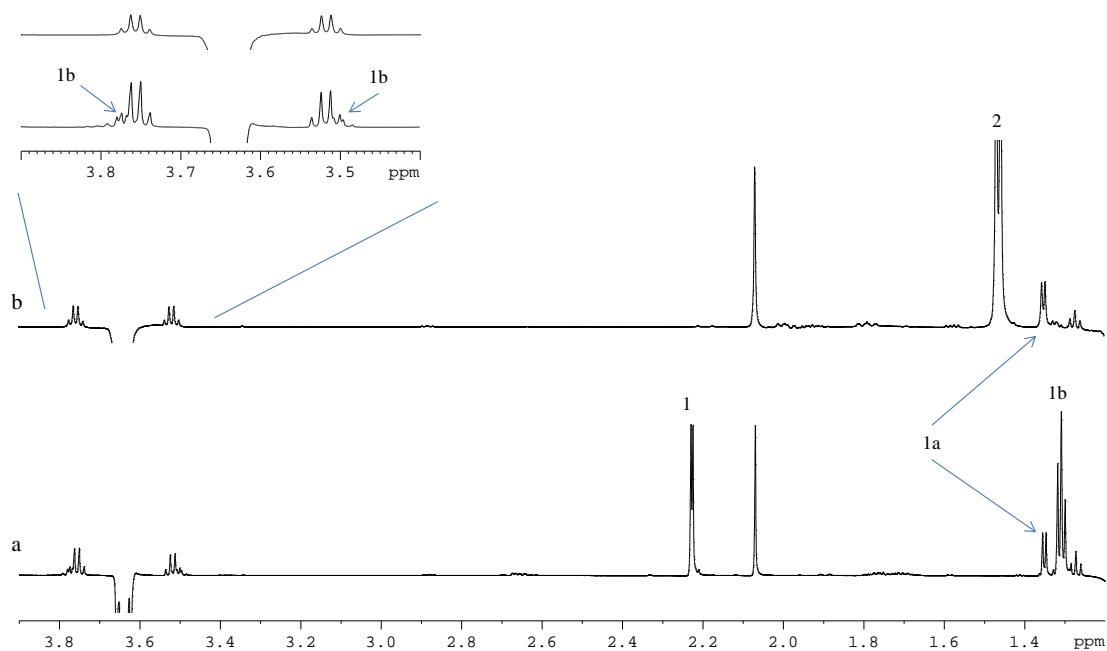


Fig.7: Aliphatic region of the ¹H NMR spectra of acetaldehyde (a) and acetaldehyde sulfonate (b) in model wine solution (12% ethanol, 5g/L tartaric acid, pH=3.5, RT) and D₂O-TSP (1: acetaldehyde, 1a: acetaldehyde hydrated, 1b: acetaldehyde ethyl hemiacetal, 2: acetaldehyde sulfonate)

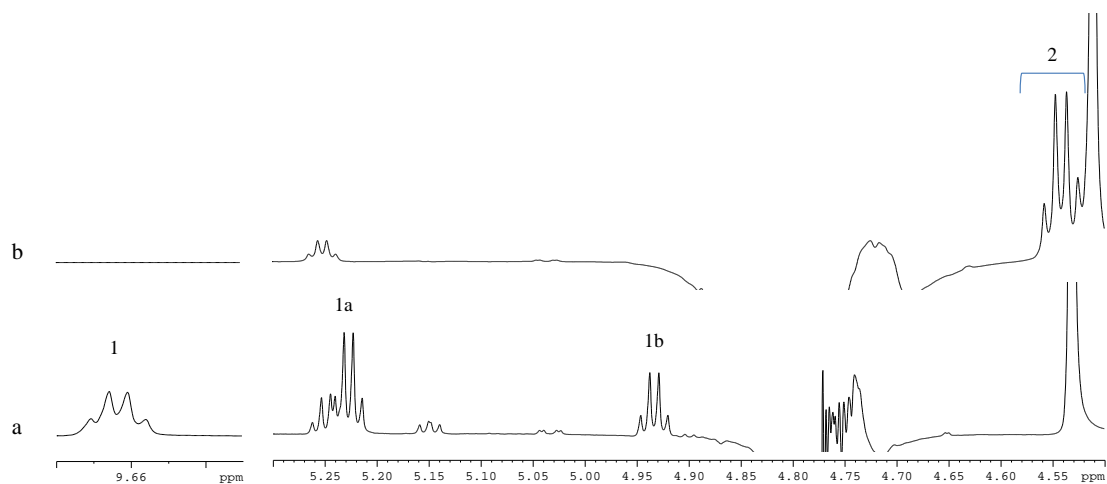
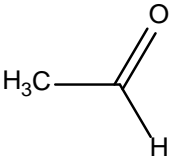
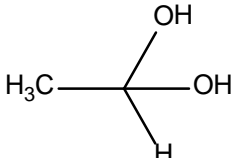
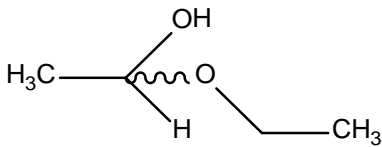
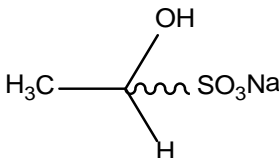


Fig.8: ¹H NMR spectra of acetaldehyde (a) and acetaldehyde sulfonate (b) in model wine solution (12% ethanol, 5g/L tartaric acid, pH=3.5, RT) and D₂O-TSP (1: acetaldehyde, 1a: acetaldehyde hydrated, 1b: acetaldehyde ethyl hemiacetal, 2: acetaldehyde sulfonate)

Chemical structure of the compounds in Figs.7-8:

Acetaldehyde 1	Acetaldehyde Hydrated 1a
	
Acetaldehyde Ethyl Hemiacetal 1b	Acetaldehyde sulfonate 2
	

In Figs. 7 and 8, the assignment of the free (a) and sulfonated (b) acetaldehyde is presented. When acetaldehyde is dissolved in model wine (spectra a), the hydrated and the ethyl hemiacetal forms are produced. After the addition of bisulfite, the quadruple from the $-\text{CH}$ group (9.66 ppm) and the doublet of the $-\text{CH}_3$ (2.23 ppm) group of free acetaldehyde are protected and shifted to a higher field region at 4.54 ppm and 1.46 ppm respectively. Also, the signals of the hydrated and ethyl hemiacetal forms have been disappeared. The results of this research are consistent with those from the literature.^[17] The sulfonated adduct is formed with a yield of 90% after one hour of reaction.

1B. LC-MS-QToF characterization of acetaldehyde sulfonate (**2**)

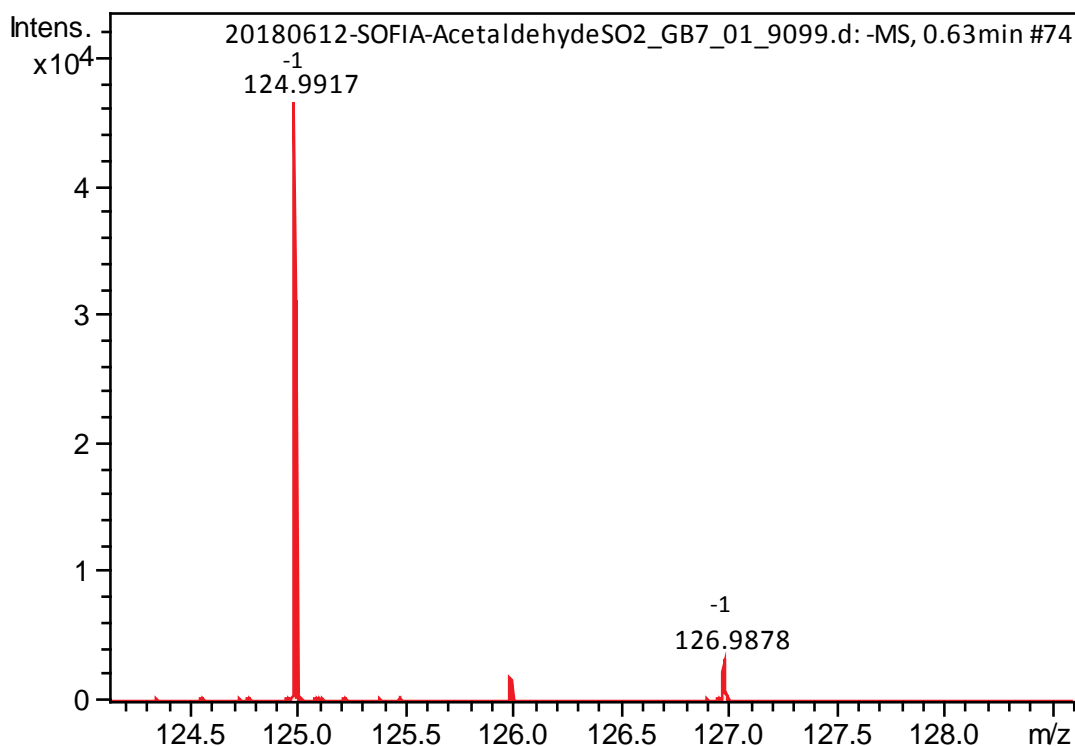


Fig. 9: MS [M-H]⁻ spectrum of the acetaldehyde sulfonate (10⁻³ M, model wine: 12% ethanol, 5g/L tartaric acid, pH=3.5, RT)

Table 2: Theoretical and experimental *m/z* values of the sulfonation product of acetaldehyde (**2**) in 0.63 min.

Compound	Detected Mass [M-H] ⁻	Theoretical Mass [M-H] ⁻	Error (ppm)	Formula
2	124.9917	124.9914	0.0003	C ₂ H ₆ O ₄ S
2 isotope a	-	125.9939	-	¹³ C ₂ H ₆ O ₄ S
2 isotope b	126.9878	126.9872	0.0006	C ₂ H ₆ O ₄ ³⁴ S

In Fig. 9, the mass spectrum of the sulfonated adduct of acetaldehyde is presented. As we can observe in Table 2, the theoretical and experimental *m/z* is quite the same. So, the chemical structure of acetaldehyde sulfonate can be confirmed using both of two methods.

2A. NMR characterization of pyruvic sulfonate (4)

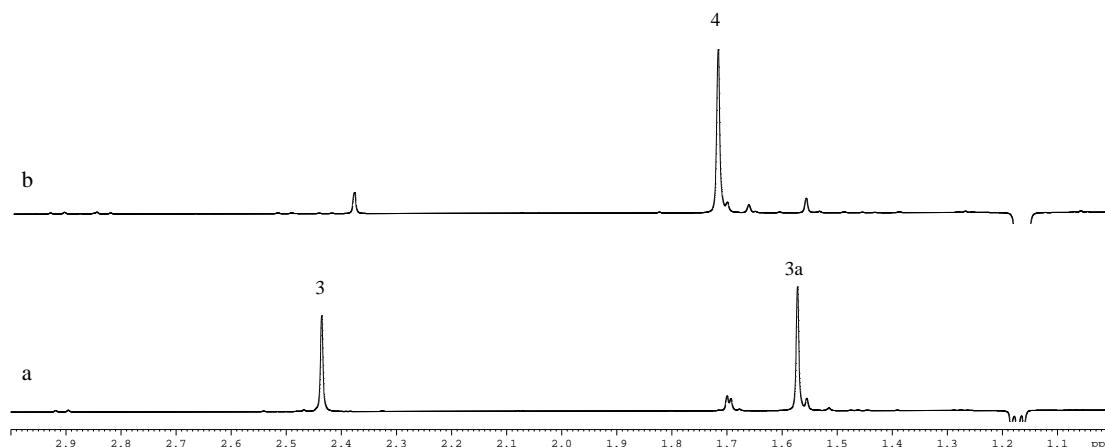


Fig. 10: ^1H NMR spectra of pyruvic acid (a) and pyruvic sulfonate (b) in model wine solution (12% ethanol, 5g/L tartaric acid, pH=3.5, RT) and D_2O -TSP. (3: pyruvic acid, 3a: pyruvic acid hydrated, 4: pyruvic sulfonate)

Chemical structure of the compounds in Fig. 10:

Pyruvic acid 3	Pyruvic Hydrated 3a	Pyruvic sulfonate 4

In Fig. 10, the ^1H NMR spectra of the free and sulfonated adduct of pyruvic acid are presented. The series of chemical reactions observed for acetaldehyde also takes place with pyruvic acid. When pyruvic acid is dissolved in model wine, the hydrated form is initially produced. After the addition of sulfonate, the single peak (2.44 ppm) from the $-\text{CH}_3$ group of the free compound, is protected and shifted to 1.57 ppm. The results of

this research are consistent with those from the literature. ^[17] The sulfonated adduct is formed with a yield of 97% after 1 hour of reaction.

2B. LC-MS-QToF characterization of pyruvic sulfonate (**4**)

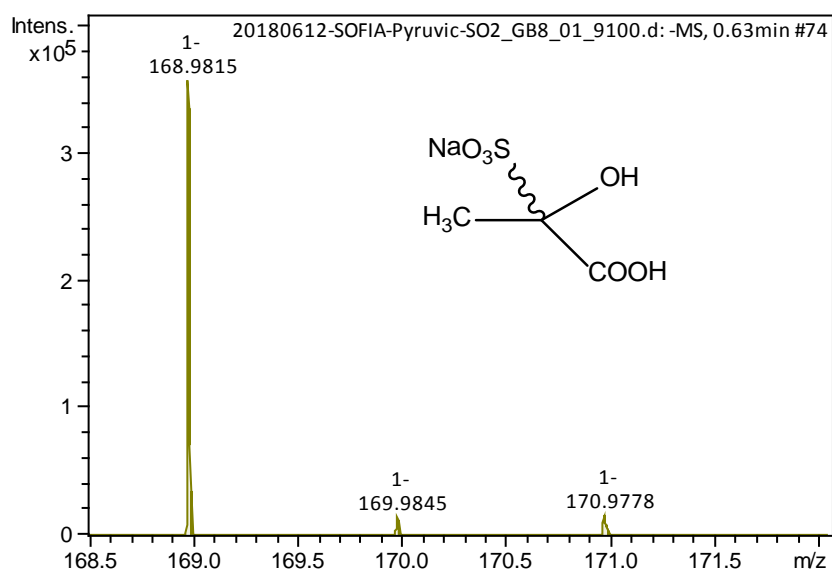


Fig. 11: MS $[M-H]^-$ spectrum of the pyruvic sulfonate (10^{-3} M, model wine: 12% ethanol, 5g/L tartaric acid, pH=3.5, RT)

Table 3: Theoretical and experimental m/z values of the sulfonation product of pyruvic acid (**4**) in 0.63 min.

Compound	Detected Mass $[M-H]^-$	Theoretical Mass $[M-H]^-$	Error (ppm)	Formula
4	168.9815	168.9812	0.0003	$C_3H_6O_6S$
4 isotope a	169.9845	169.9840	0.0005	$^{13}C_3H_6O_6$ S
4 isotope b	170.9778	170.9790	0.0012	$C_3H_6O_6^{34}$ S

In Fig. 11, the mass spectrum of pyruvic sulfonate is presented. We can observe in Table 3 that the theoretical and experimental m/z is quite the same. So, the chemical structure of pyruvic sulfonate can be confirmed by using both NMR spectroscopy and LC-MS-QToF.

3A. NMR characterization of the ascorbic sulfonate (**6**)

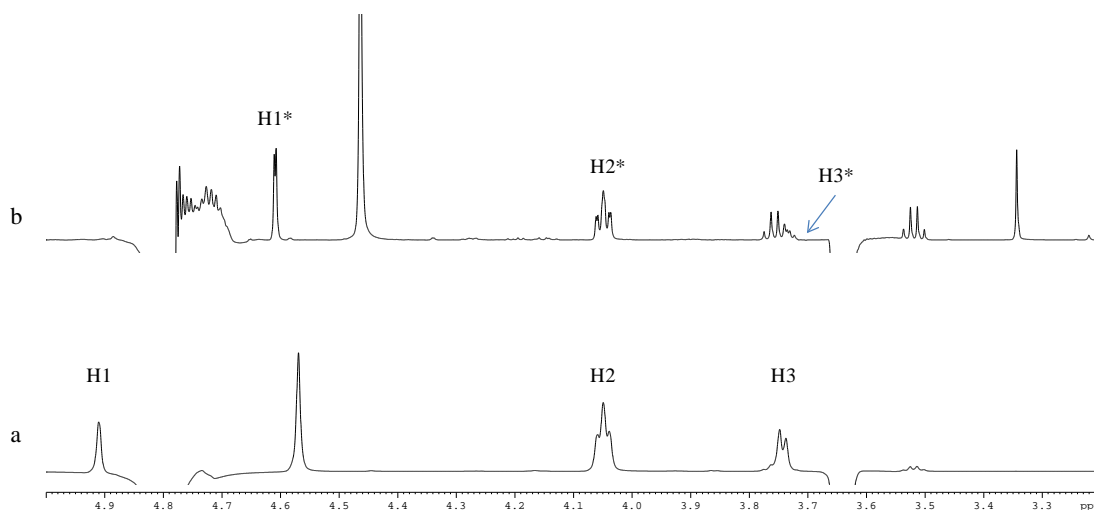
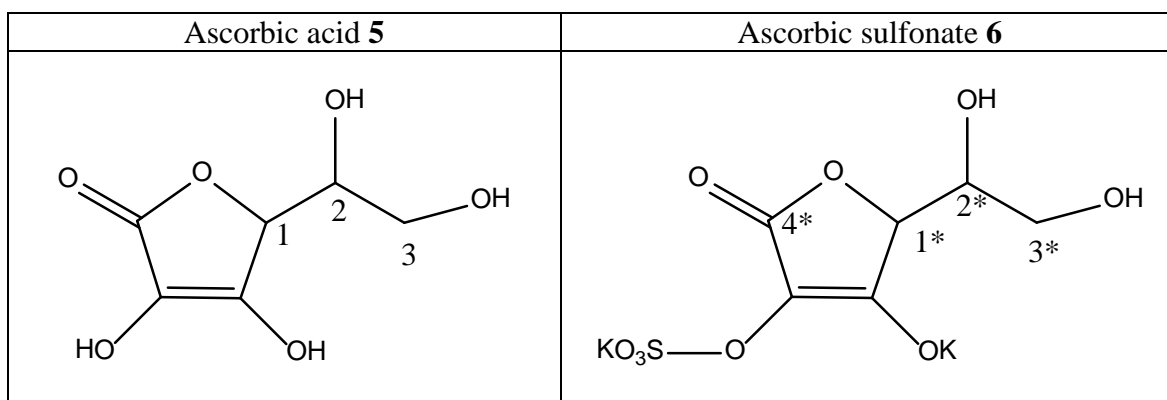


Fig. 12: ^1H NMR spectra of ascorbic acid (H1, H2, H3) (a) and ascorbic sulfonate (H1*, H2*, H3*) (b) in model wine solution (12% ethanol, 5g/L tartaric acid, pH=3.5, RT) and D_2O -TSP.

Chemical structure of the compounds in Fig. 12:



The assignment of the protons of ascorbic acid and ascorbic sulfonate is shown in Fig. 12. In spectra a, H1 and H3 protons have two doublets (d) at 4.91 ppm and 3.74 ppm

respectively instead of H2 proton which give a dt peak at 4.05 ppm. The assignment for the sulfonation adduct has been verified by the integration of the respective peaks and by 2D experiments since literature NMR data for this sulfonated compound aren't available.

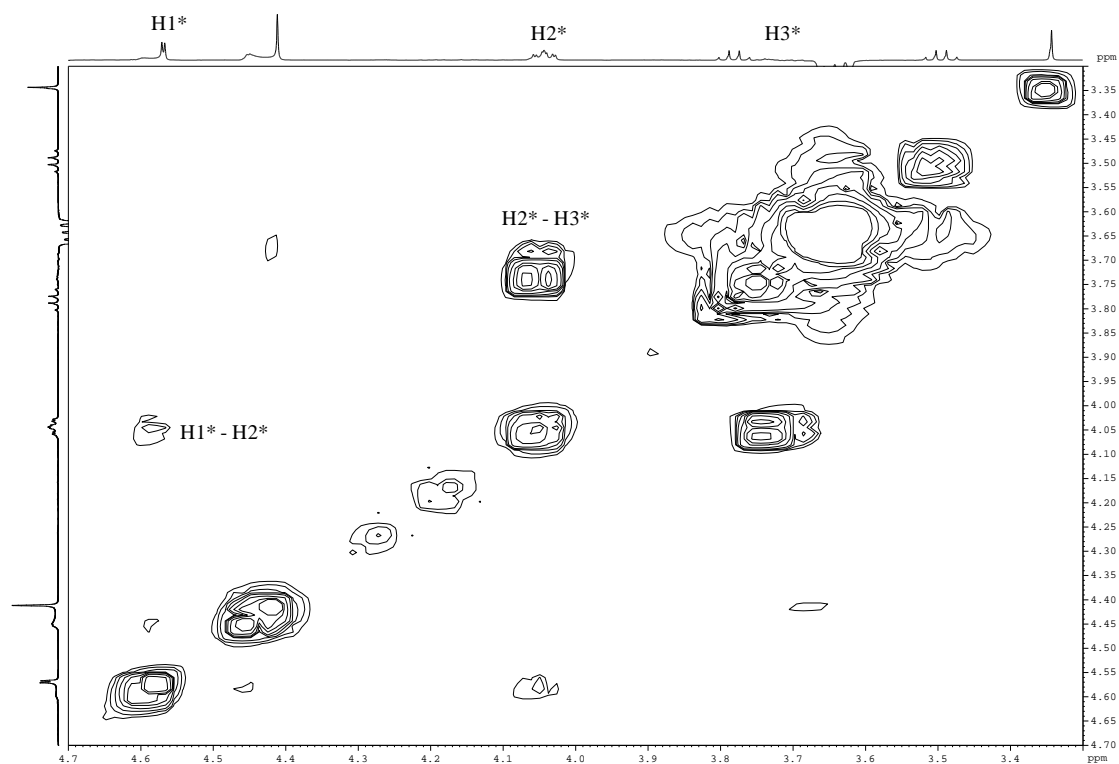


Fig. 13: Homonuclear correlation ^1H - ^1H gCOSY 2D NMR spectrum of ascorbic sulfonate

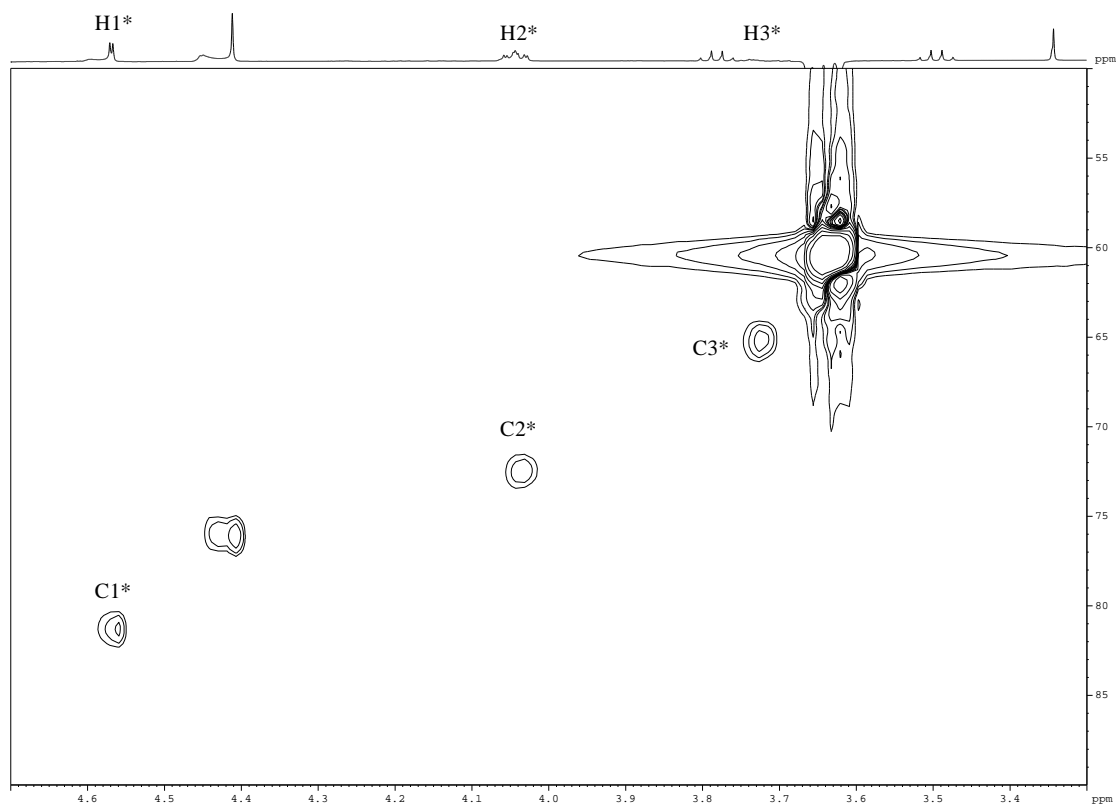


Fig. 14: ^1H - ^{13}C gHSQC 2D NMR spectra of ascorbic sulfonate

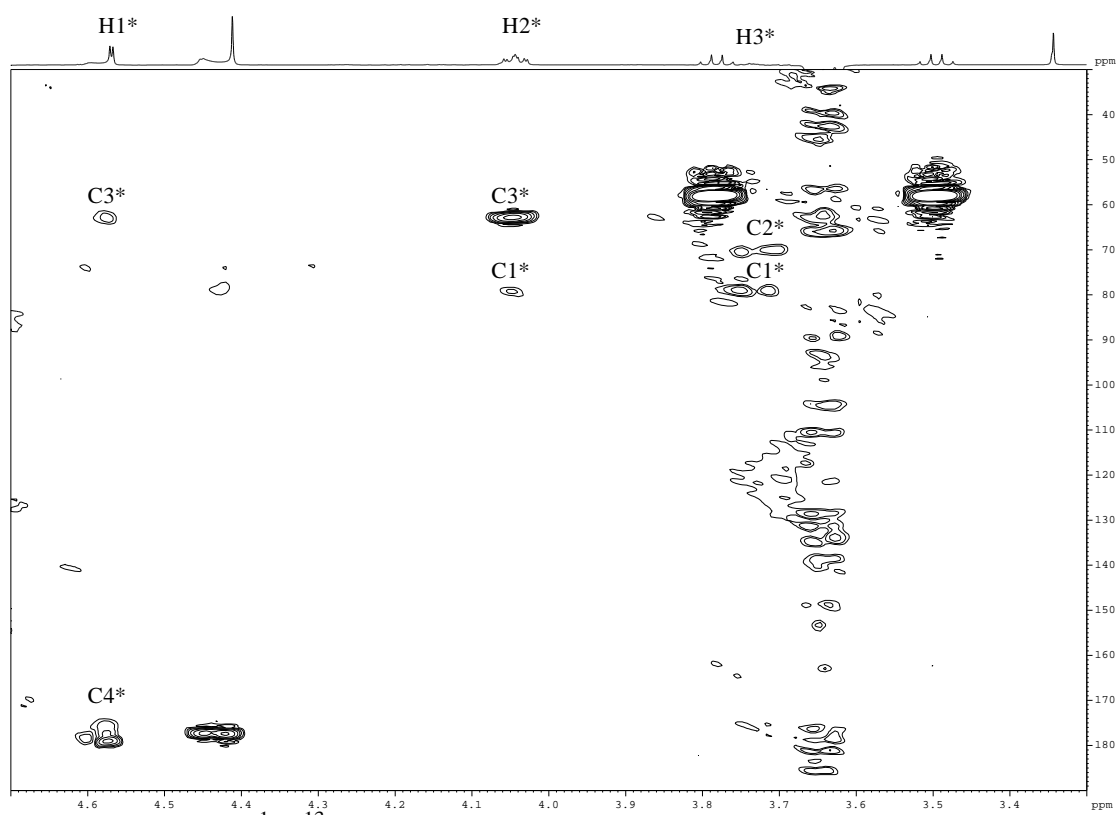


Fig. 15: ^1H - ^{13}C gHMBC 2D NMR spectra of ascorbic sulfonate

After the sulfonation, H2* and H3* are almost in the same region with H2 and H3 (4.04 ppm and 3.72 ppm respectively). The only proton which has a shift at a lower ppm region is H1* and it appears at 4.57 ppm, indicating that after the sulfonation, H1* is more protected. In Table 4, the assignment of ascorbic acid (**5**) and ascorbic sulfonate (**6**) is presented.

Table 4: Assignment of ascorbic acid (**5**) and ascorbic sulfonate (**6**)

Compound	¹ H ppm	¹³ C ppm
Ascorbic acid 5	4.91 (H1)	77.03
	4.05 (H2)	69.76
	3.74 (H3)	62.93
Ascorbic sulfonate 6	4.57 (H1*)	81.35
	4.04 (H2*)	72.58
	3.72 (H3*)	65.28

3B. LC-MS-QtoF characterization of ascorbic acid (**5**) and ascorbic sulfonate (**6**)

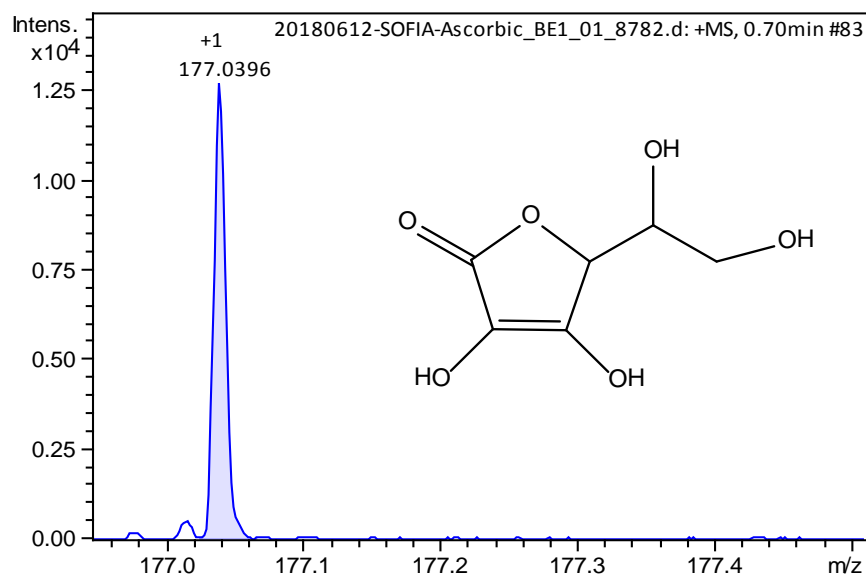


Fig. 16: MS [M+H]⁺ spectrum of ascorbic acid (10⁻⁴M, model wine: 12% ethanol, 5g/L tartaric acid, pH=3.5, RT)

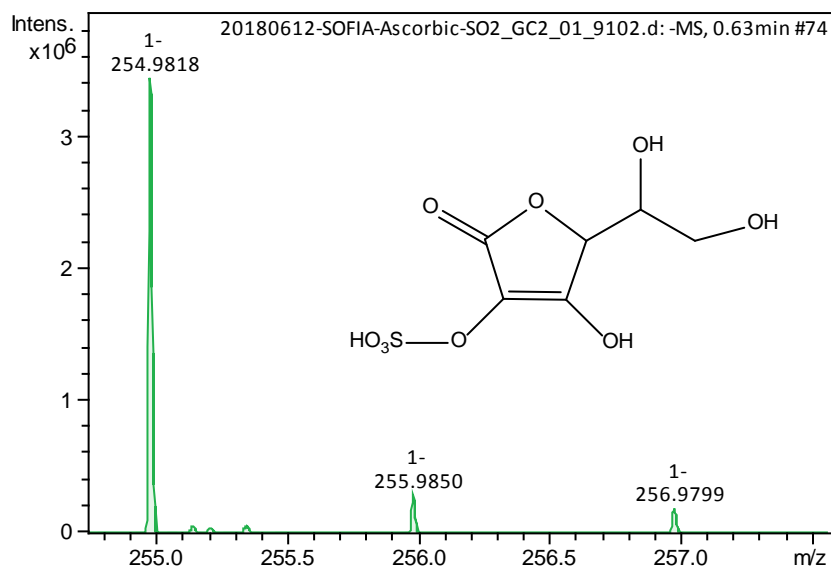


Fig. 17: MS $[M-H]^-$ spectrum of ascorbic sulfonate (10^{-3} M, model wine: 12% ethanol, 5g/L tartaric acid, pH=3.5, RT)

Table 5: Theoretical and experimental m/z values of ascorbic acid (**5**) at 0.70 min

Compound	Detected Mass $[M+H]^+$	Theoretical $[M+H]^+$	Mass Error (ppm)	Formula
5	177.0396	177.0394	0.0002	$C_6H_8O_6$

Table 6: Theoretical and experimental m/z values of ascorbic sulfonate (**6**) at 0.63 min

Compound	Detected Mass $[M-H]^-$	Theoretical Mass $[M-H]^-$	Error (ppm)	Formula
6	254.9818	254.9816	0.0002	$C_6H_8O_9S$
6 isotope a	255.9850	255.9846	0.0004	$^{13}C_6H_8O_9S$
6 isotope b	256.9799	256.9802	0.0003	$C_6H_8O_9^{34}S$

In Figs. 16 and 17, the mass spectra of ascorbic acid and its sulfonated adduct are presented. The theoretical and experimental values for both of these compounds are similar (Table 5 and 6).

Finally, the chemical structure of ascorbic sulfonate has been confirmed by NMR and LC-MS.

4A. NMR characterization of glucose sulfonate (**10**)

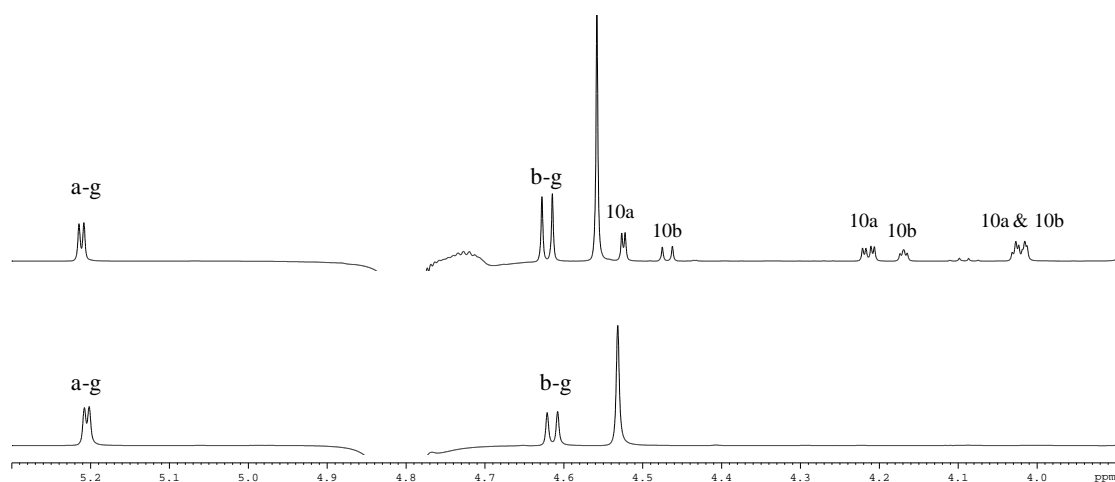


Fig. 18: ^1H NMR spectra of glucose (a) and glucose sulfonate (b) in model wine solution (12% ethanol, 5g/L tartaric acid, pH=3.5, RT) and D_2O -TSP. (α -g: α -glucose, β -g: β -glucose, 10a, 10b: 2 different forms of the glucose sulfonate)

Chemical structure of the compounds in Fig. 18:

D-glucose 9	Glucose sulfonate 10a	Glucose sulfonate 10b
$ \begin{array}{c} 1^* \text{ or } 1' \\ \text{CHO} \\ \\ 2^* \text{ or } 2' \text{ H} - \text{C} - \text{OH} \\ \\ \text{HO} - \text{C} - \text{H} \quad 3^* \text{ or } 3' \\ \\ 4^* \text{ or } 4' \text{ H} - \text{C} - \text{OH} \\ \\ 5^* \text{ or } 5' \text{ H} - \text{C} - \text{OH} \\ \\ \text{CH}_2\text{OH} \\ 6^* \text{ or } 6' \end{array} $	$ \begin{array}{c} \text{NaO}_3\text{S} \quad \text{H} \quad 1 \quad \text{OH} \\ \quad \quad \quad \diagdown \quad \diagup \\ \quad \quad \quad \text{C} \\ \\ 2 \quad \text{H} - \text{C} - \text{OH} \\ \\ \text{HO} - \text{C} - \text{H} \quad 3 \\ \\ 4 \quad \text{H} - \text{C} - \text{OH} \\ \\ 5 \quad \text{H} - \text{C} - \text{OH} \\ \\ \text{CH}_2\text{OH} \\ 6 \end{array} $	$ \begin{array}{c} \text{HO} \quad \text{H} \quad 1 \quad \text{SO}_3\text{Na} \\ \quad \quad \quad \diagdown \quad \diagup \\ \quad \quad \quad \text{C} \\ \\ 2 \quad \text{H} - \text{C} - \text{OH} \\ \\ \text{HO} - \text{C} - \text{H} \quad 3 \\ \\ 4 \quad \text{H} - \text{C} - \text{OH} \\ \\ 5 \quad \text{H} - \text{C} - \text{OH} \\ \\ \text{CH}_2\text{OH} \\ 6 \end{array} $

The chemical structure of glucose sulfonate has been reported in previous study^[55], where it was found by X-ray crystallography that two different forms of this adduct are formed in a ratio 10a : 10b = 1.9:1. The basic peaks of α and β -glucose are also present in the (b) spectrum of the sulfonation reaction, indicating sulfonation is not 100%. The confirmation of the chemical structure has been done using 2D NMR experiments too.

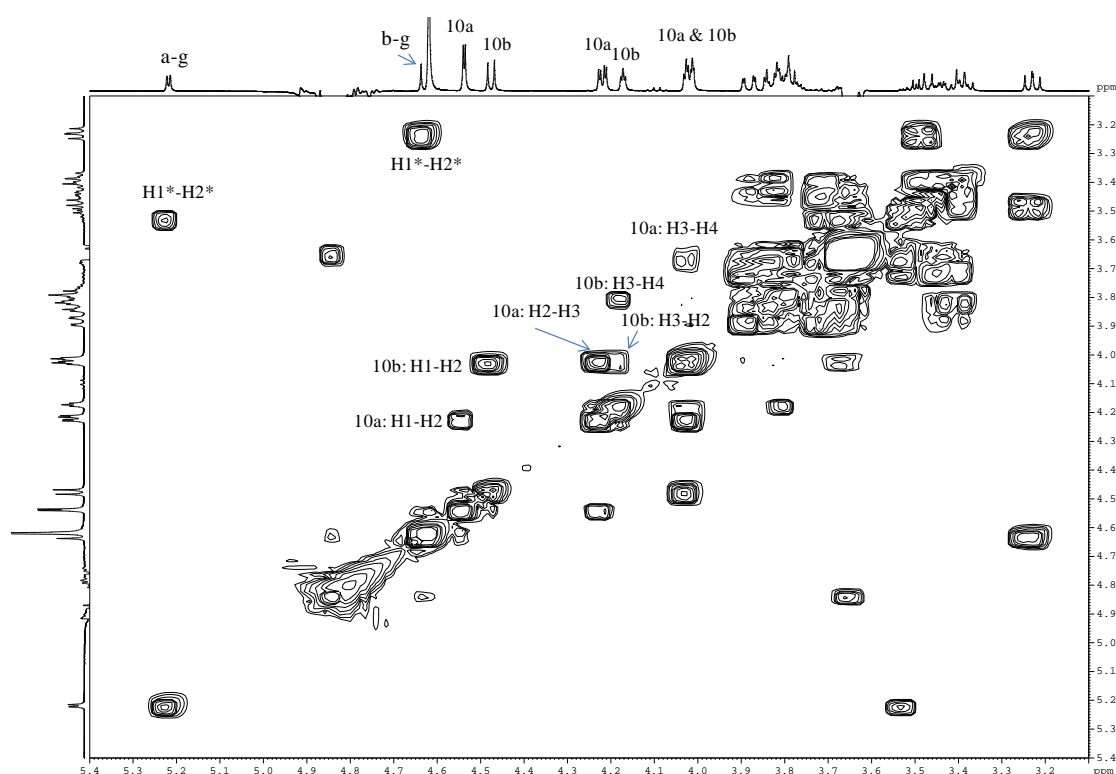


Fig. 19: Homonuclear correlation ^1H - ^1H gCOSY 2D NMR spectrum of glucose sulfonate

In Fig. 19, COSY 2D experiment is presented. We can clearly observe the correlation between the protons of glucose sulfonate **10a** and **10b**, as the signals of the protons H1, H2, H3 and H4 of the compounds are intense. Also, the correlation between H1-H4 and their carbons is presented in HSQC (Fig. 20) but to confirm the chemical structure, HMBC experiment was performed and is presented in Fig. 21.

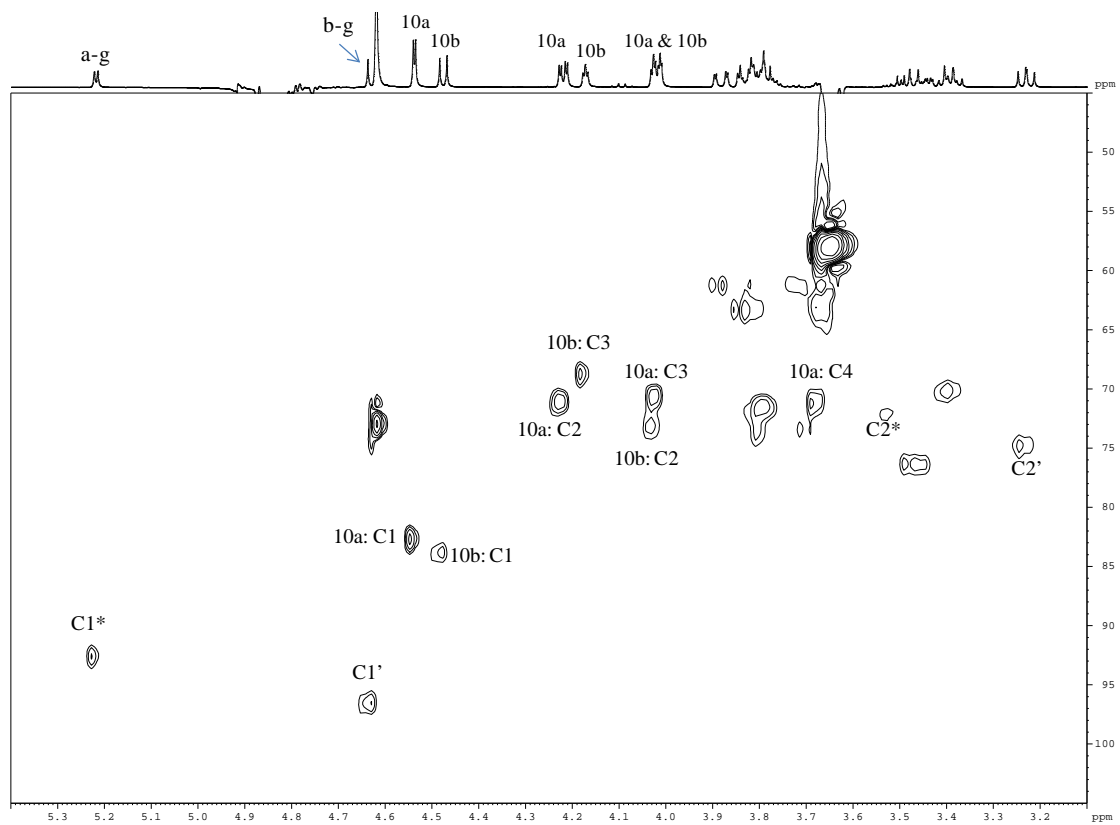


Fig. 20: ^1H - ^{13}C gHSQC 2D NMR spectra of glucose sulfonate

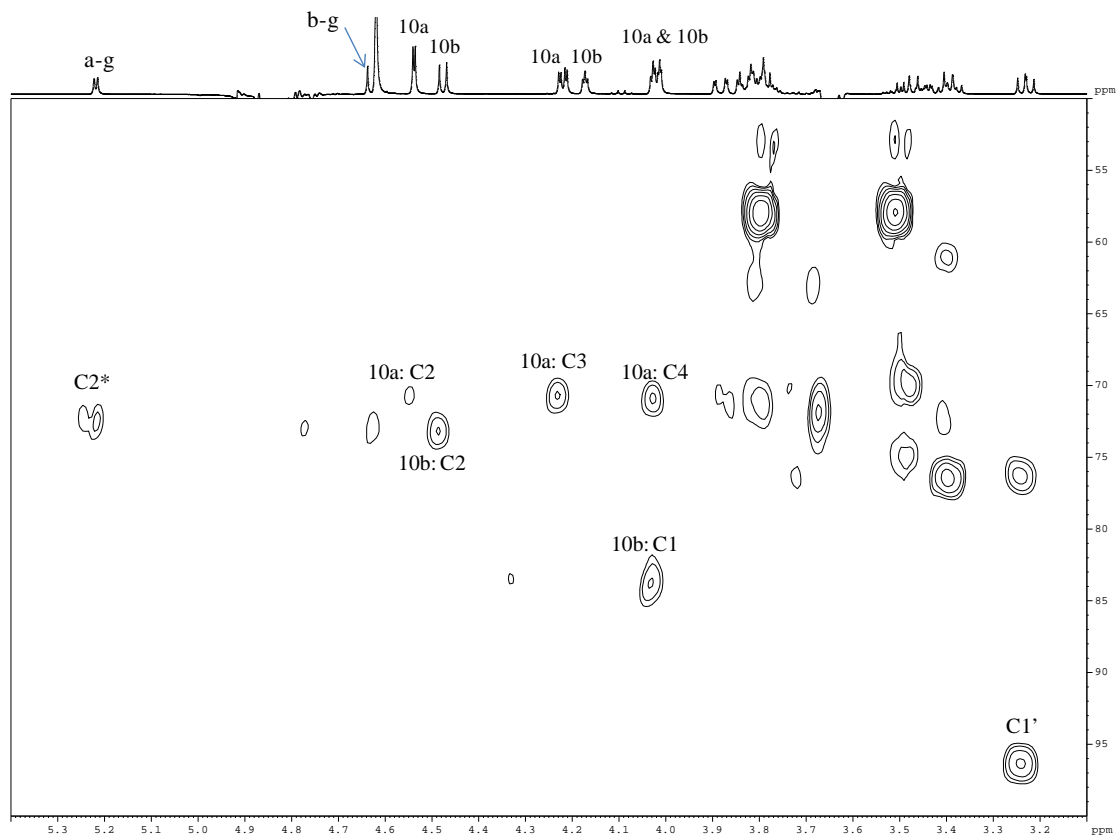


Fig. 21: ^1H - ^{13}C gHMBC 2D NMR spectra of glucose sulfonate

In HMBC we observe correlations between protons and carbons in four different compounds. For the compound **10a**, we observe the correlation between H1 and C2, H2 and C3, H3 and C4 while for the compound 10b we observe the correlation between H1 and C2 and H2 and C1. Our results are in agreement with the literature.^[55] In Table 7, the assignment for both forms of glucose sulfonate (10a and 10b) is presented.

Table 7: Assignment of glucose and glucose sulfonate **10a** and **10b** (as they are presented in Fig. 18 in spectrum b)

Compound	¹ H ppm	¹³ C ppm
a-glucose	5.22 (H1*)	92.66
	3.53 (H2*)	72.23
b-glucose	4.64 (H1')	96.58
	3.24 (H2')	74.86
Glucose sulfonate 10a	4.55 (H1)	82.80
	4.22 (H2)	71.10
	4.02 (H3)	70.76
	3.67 (H4)	71.18
Glucose sulfonate 10b	4.48 (H1)	83.87
	4.03 (H2)	73.17
	4.18 (H3)	68.77
	3.81 (H4)	-

Finally, it should be noted that the reaction yield was measured at about 30% for **10a** and 16% for **10b**, a result that agrees with the product ratio reported in the literature.

^[55] This reaction had not yet reached full conversion after 6 weeks.

4B. LC-MS-QToF characterization of glucose (**9**) and glucose-SO₃Na (**10a** & **10b**)

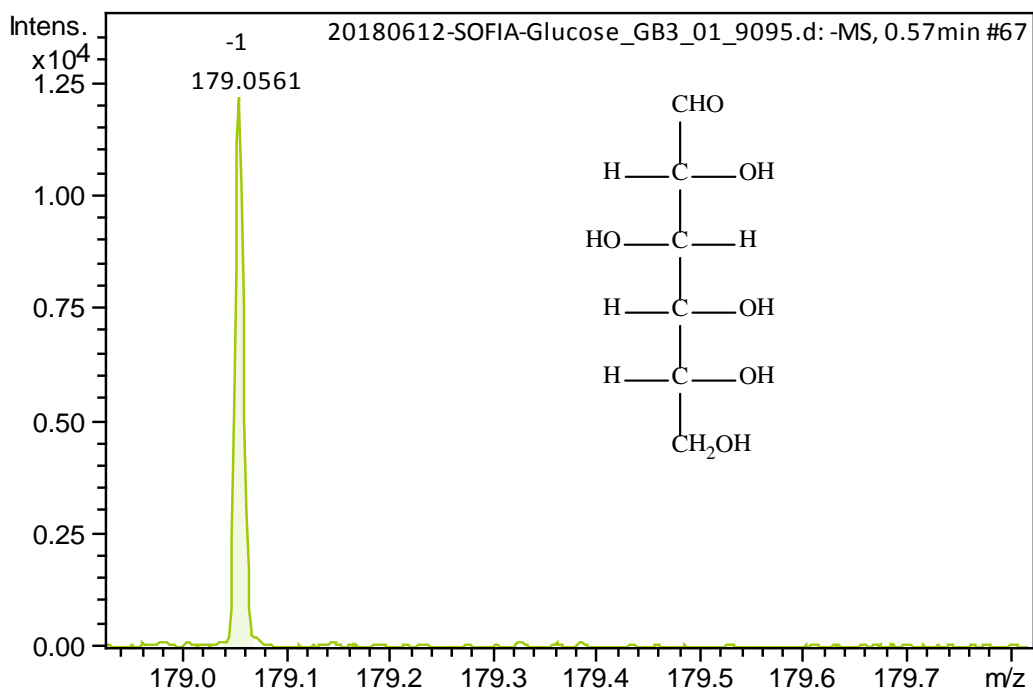


Fig. 22: MS [M-H]⁻ spectrum of glucose (10⁻⁴ M, model wine: 12% ethanol, 5g/L tartaric acid, pH=3.5, RT)

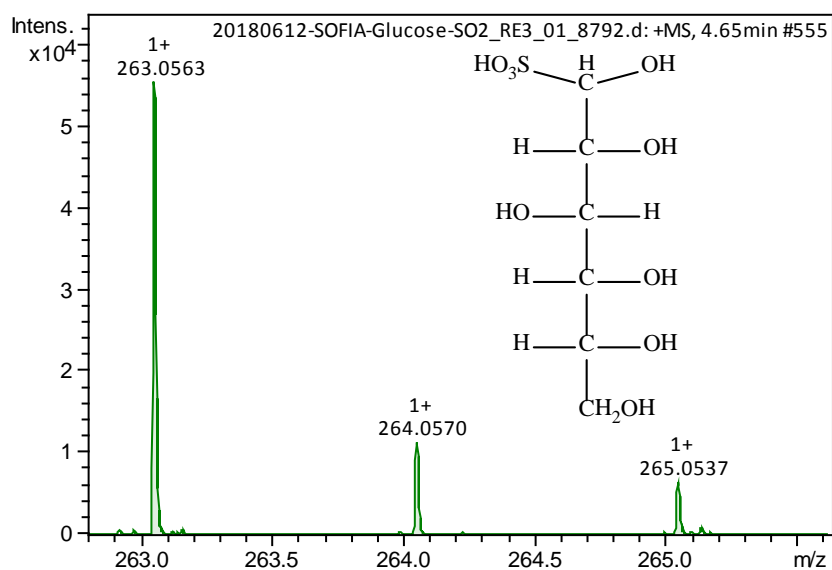


Fig. 23: MS [M+H]⁺ spectrum of glucose sulfonate (10⁻³ M, model wine: 12% ethanol, 5g/L tartaric acid, pH=3.5, RT)

Table 8: Theoretical and experimental *m/z* values of glucose (**9**) at 0.57 min.

Compound	Detected Mass [M-H] ⁻	Theoretical Mass [M-H] ⁻	Mass[M-H]	Error (ppm)	Formula
9	179.0561	179.0561		-	C ₆ H ₁₂ O ₆

Table 9: Theoretical and experimental m/z values of glucose sulfonate (**10a & 10b**) at 4.65 min.

Compound	Detected [M+H] ⁺	Mass Theoretical [M+H] ⁺	Mass Error (ppm)	Formula
10 (a & b)	263.0563	263.0431	0.0132	C ₆ H ₁₄ O ₉ S
10 isotope a	264.0570	264.0462	0.0108	¹³ C ₆ H ₁₄ O ₉ S
10 isotope b	265.0537	265.0417	0.0120	C ₆ H ₁₄ O ₉ ³⁴ S

In Figs. 22 and 23, the mass spectra of glucose and glucose sulfonate are presented. As it is shown in Table 8, the theoretical and the experimental value of m/z for glucose was exactly the same. In Table 9, it is shown that there is an important error between the theoretical and experimental value of m/z for glucose sulfonate. That leads to the conclusion that the experimental conditions used is not the most appropriate for the ionization of this adduct, and needs to be optimized.

Nevertheless, both methods used can confirm the proposed structure of the sulfonated adduct of glucose.

5A. NMR characterization of cysteine sulfonate (**12**)

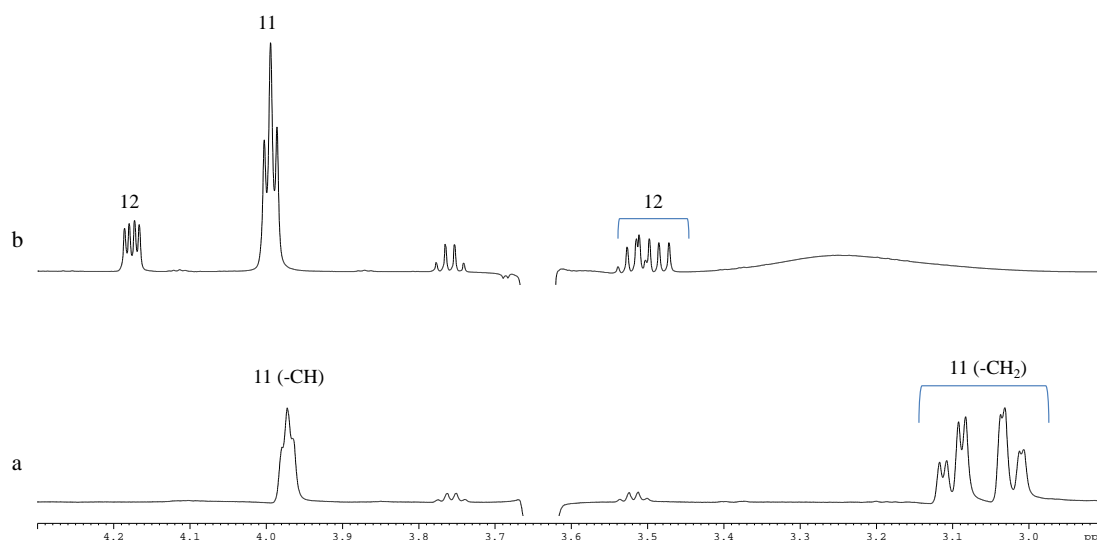
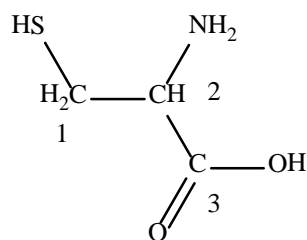


Fig. 24: ¹H NMR spectra of cysteine (a) and cysteine sulfonate (b) in model wine solution (12% ethanol, 5g/L tartaric acid, pH=3.5, RT) and D₂O-TSP. (11: cysteine, 12: cysteine sulfonate)

Chemical structure and numbering of cysteine (11) (Fig.24):



The assignment of the cysteine sulfonate is complicated since the $-\text{SO}_3\text{Na}$ group can bind to three different positions ($-\text{SH}$, $-\text{NH}_2$ or $\text{C}=\text{O}$), even if the $-\text{SH}$ side is the most probable. At the bottom (a) NMR spectrum of free cysteine in Fig.18, there are 2 doublet of doublets (dd) peaks at 3.06 and 3.1 ppm from the protons of the cysteine CH_2 group (H1) and a dd at 3.97 ppm from the methine proton (H2). At the top (b) NMR spectrum which belongs to the sulfonated adduct, 2 dd at 3.49 and 4.18 ppm were observed. To further elucidate the chemical structure of cysteine sulfonate, 2D NMR experiments were performed.

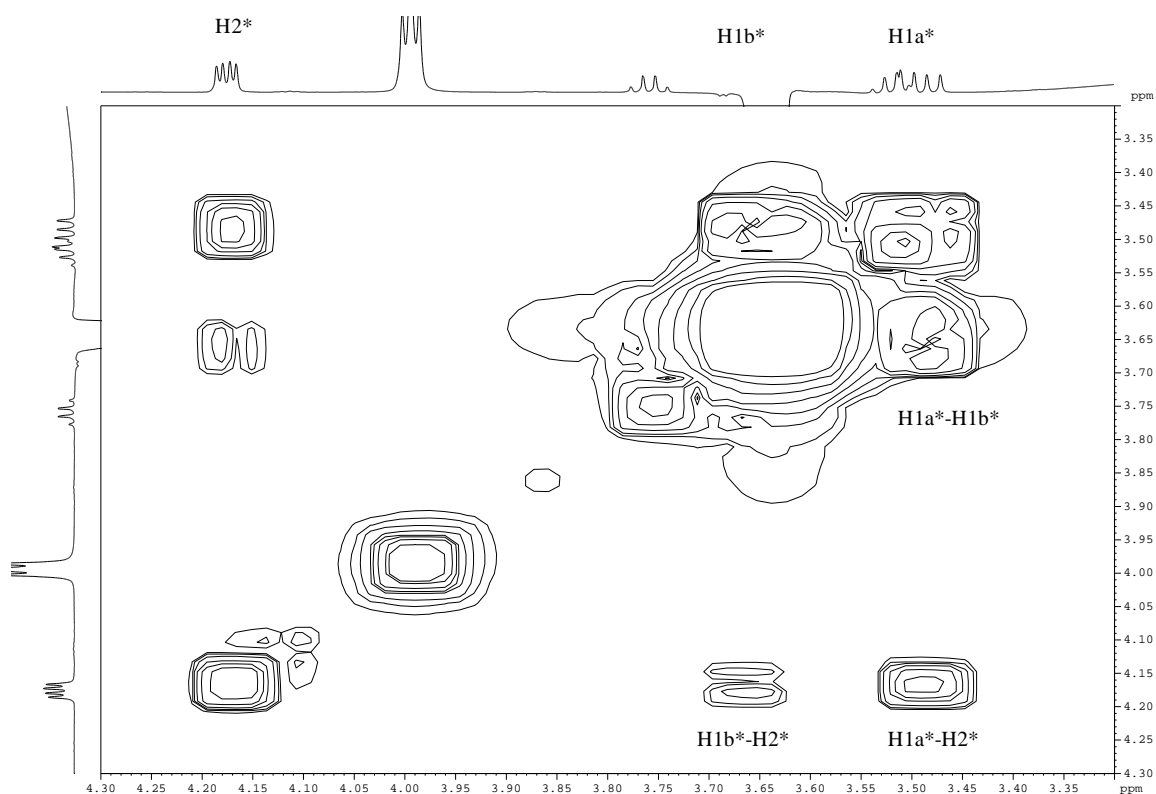


Fig. 25: Homonuclear correlation ^1H - ^1H gCOSY2D NMR spectrum of cysteine sulfonate

In this 2D NMR spectrum of Fig. 25, a correlation crosspeak between a proton (dd) at 3.49 ppm and a proton at 3.66 ppm is observed (this proton is not visible in the 1D proton spectrum due to the ethanol peak). Also, these two protons are correlated with a dd at 4.18 ppm, leading to the conclusion that H1a and H1b can be assigned to the two protons of the CH₂ group of cysteine sulfonate, while H2 is assigned to the proton of the CH group of the same compound. To confirm this assignment, 2D HSQC and HMBC NMR experiments were performed.

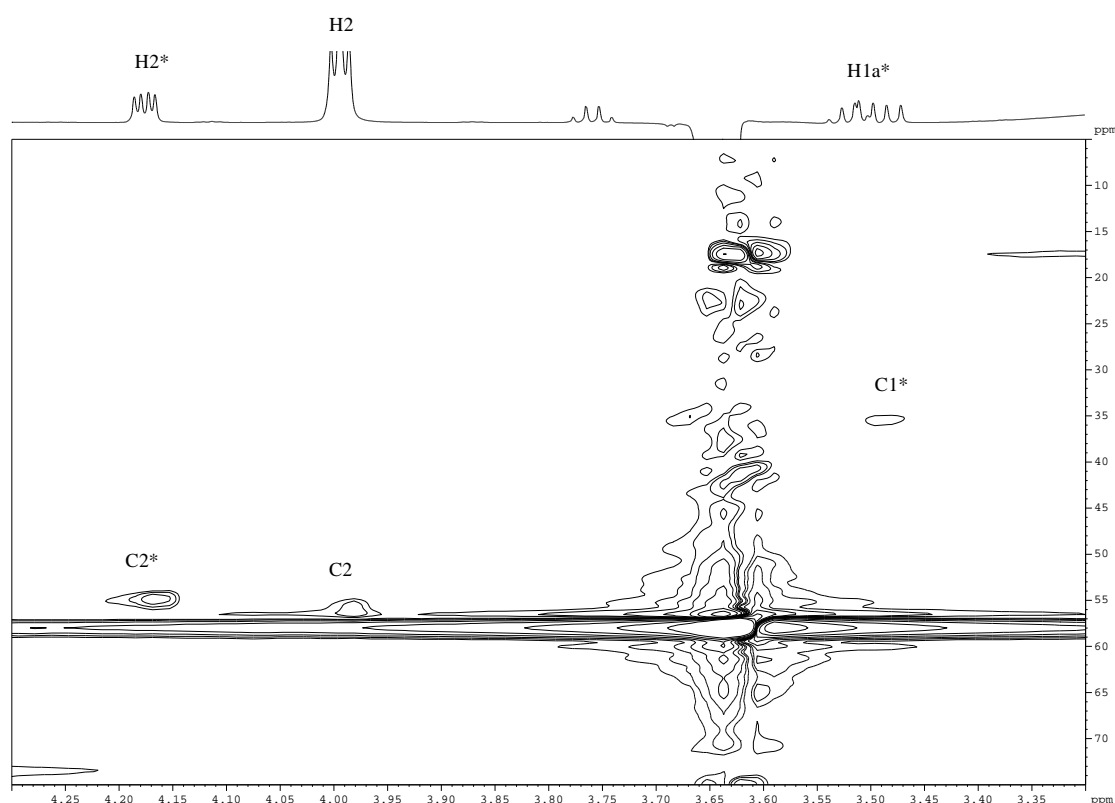


Fig. 26: ¹H-¹³C gHSQC 2D NMR spectra of cysteine sulfonate

In the HSQC spectrum of Fig. 26 we observe a correlation peak between proton H1a* at 3.49 ppm and its attached carbon C1, at 35.55 ppm, a spectral region characteristic of carbons that chemically bound to sulfur. Additionally it is observed that proton H2* at 4.18 ppm is correlated with a carbon at 55.01 ppm, a spectral region characteristic of C-N carbons bound to a nitrogen. So, we conclude that the sulfonation takes place at the -SH side and not to the -NH₂.

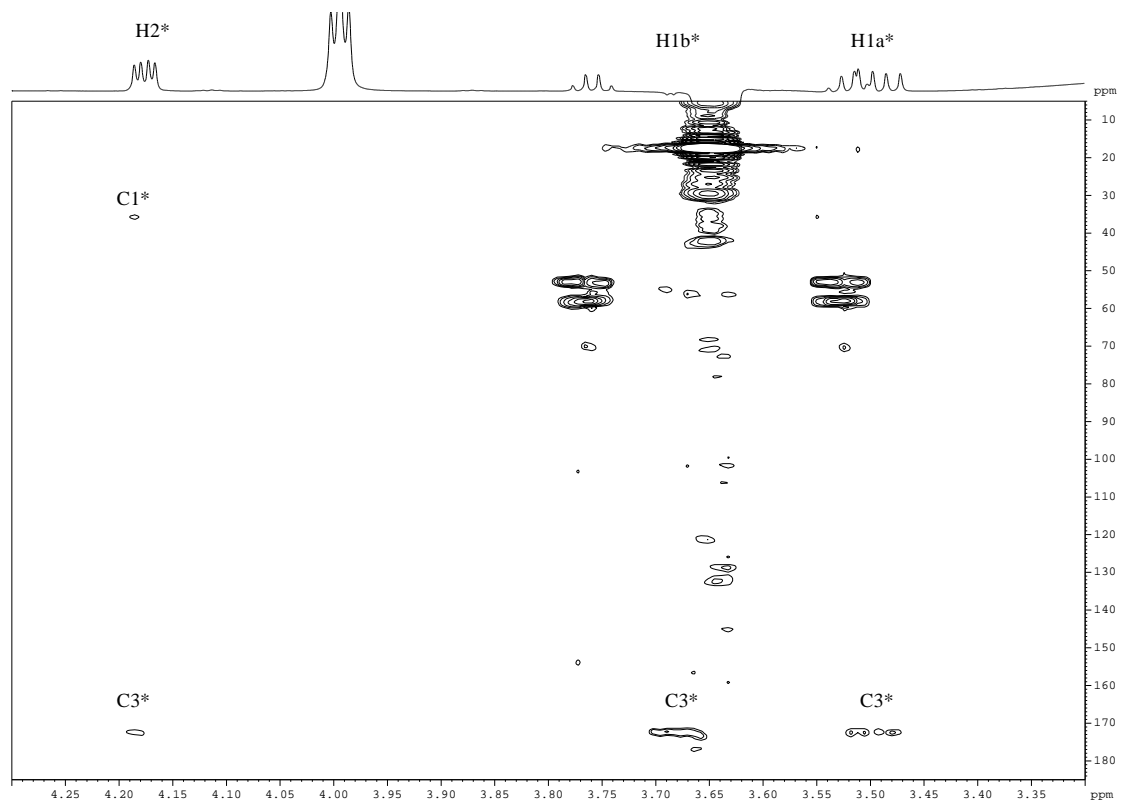
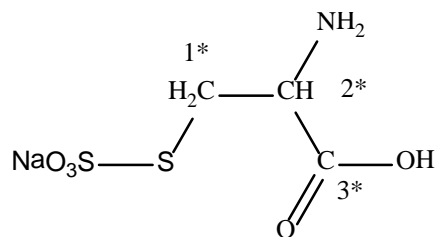


Fig. 27: ^1H - ^{13}C gHMBC 2D NMR spectra of cysteine sulfonate

The HMBC spectrum reported in Fig. 27 shows that all these three protons (H1a*, H1b* and H2*) have a long range H-C correlation with the carboxyl carbon C3, verifying that sulfonation does not happen at the $-\text{COOH}$ group.

Finally, it is reported that after 6 weeks of reaction, the yield is only at 36%.

Chemical structure of cysteine sulfonate (12) in Figs. 24-27:



5B. LC-MS-QToF characterization of the cysteine (11) and cysteine sulfonate (12)

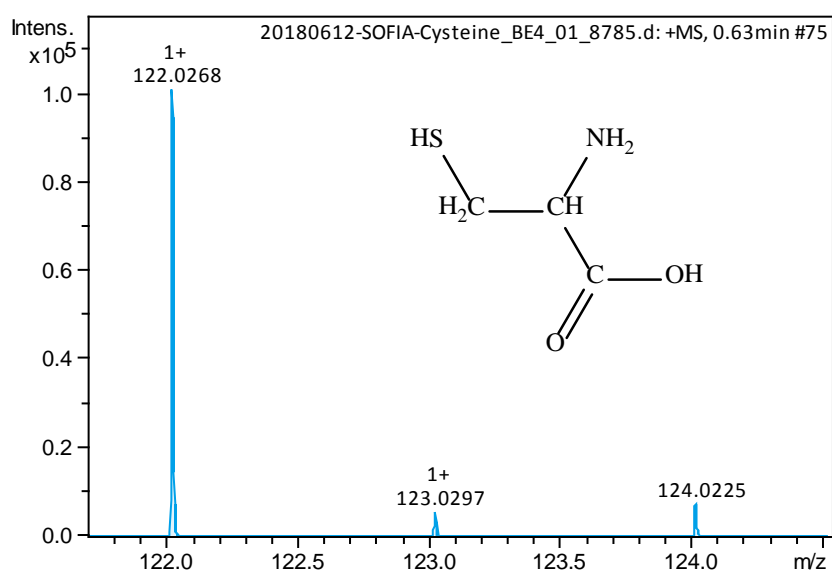


Fig. 28: MS [M+H]⁺ spectrum of cysteine (10⁻⁴ M, model wine: 12% ethanol, 5g/L tartaric acid, pH=3.5, RT)

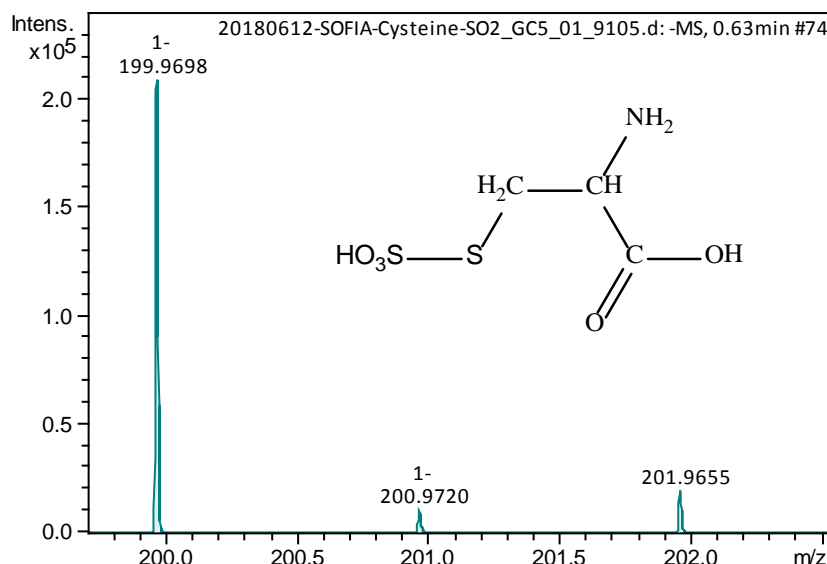


Fig. 29: MS $[M-H]^-$ spectrum of cysteine sulfonate (10^{-3} M, model wine: 12% ethanol, 5g/L tartaric acid, pH=3.5, RT)

Table 10: Theoretical and experimental m/z values of cysteine (**11**) at 0.63 min.

Compound	Detected Mass $[M+H]^+$	Theoretical Mass $[M+H]^+$	Error (ppm)	Formula
11	122.0268	122.0270	0.0002	$C_3H_7O_2NS$
11 isotope a	123.0297	123.0293	0.0004	$^{13}C_3H_7O_2NS$
11 isotope b	124.0225	124.0228	0.0003	$C_3H_7O_2N^{34}S$

Table 11: Theoretical and experimental m/z values of cysteine sulfonate (**12**) at 0.63 min.

Compound	Detected Mass $[M-H]^-$	Theoretical Mass $[M-H]^-$	Error (ppm)	Formula
12	199.9698	199.9693	0.0005	$C_3H_7O_5NS_2$
12 isotope a	200.9720	200.9711	0.0009	$^{13}C_3H_7O_5NS$
12 isotope b	201.9655	201.9660	0.0005	$C_3H_7O_5N^{34}S$

In Figs. 28 and 29, the mass spectra of cysteine and cysteine sulfonate are presented. Their theoretical and experimental values of m/z are shown in Table 10 and 11 and it is obvious that they are similar. These values have been also reported in previous study.^[6]

Using the information from 1D and 2D NMR experiments as well as the mass spectra, we can confirm the chemical structure of the sulfonated adduct of cysteine.

6A. NMR characterization of glutathione sulfonate (**8**)

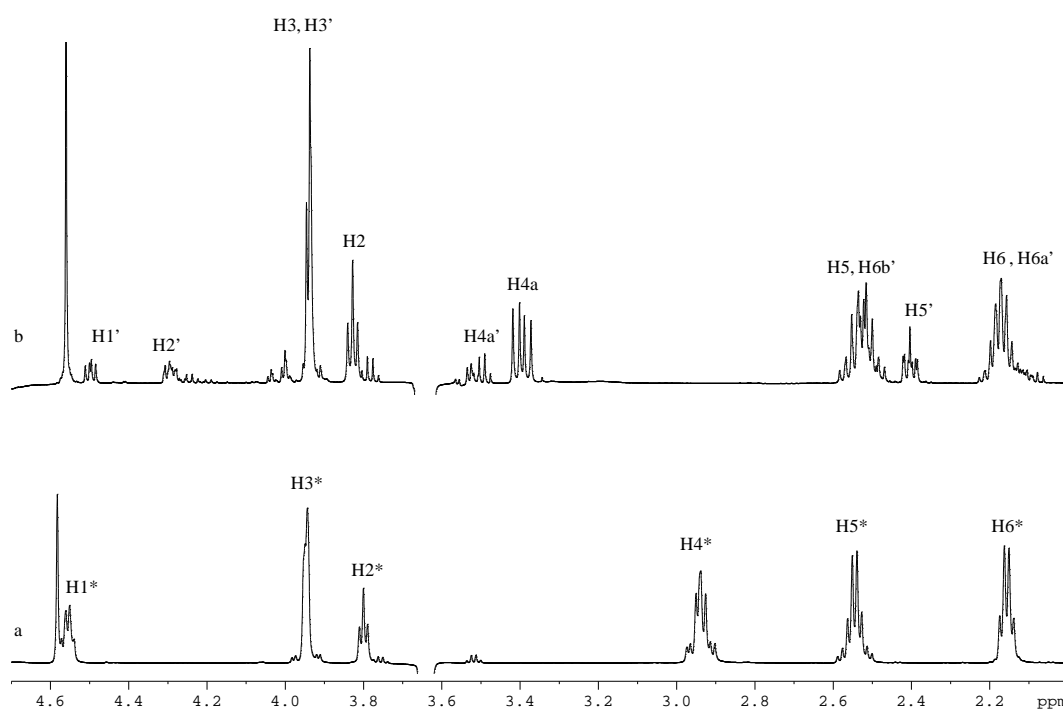
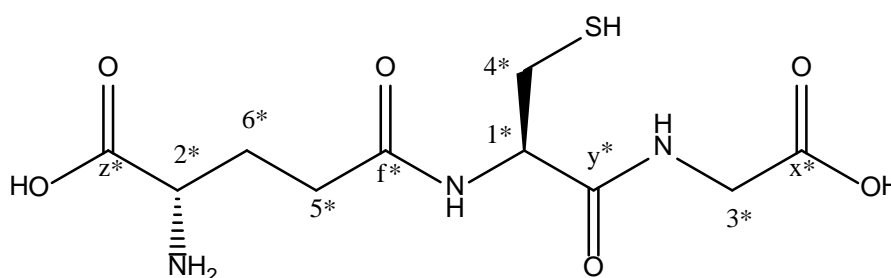
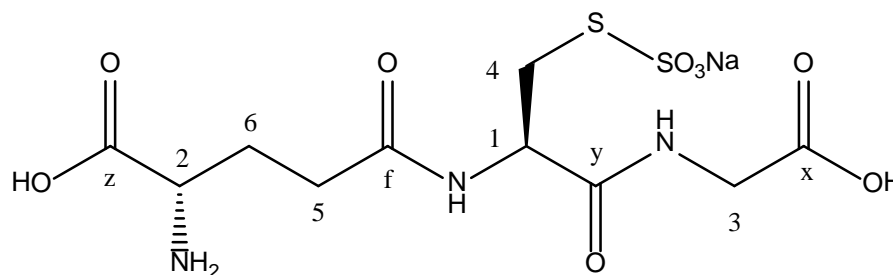


Fig. 30: ^1H NMR spectra of glutathione **7** (a) and glutathione sulfonate **8** (b) in model wine solution (12% ethanol, 5g/L tartaric acid, pH=3.5, RT) and D_2O -TSP

Chemical structure and numbering of glutathione (**7**) (Fig. 30):



Chemical structure of glutathione sulfonate (8) in Figs. 30-33:



As it is referred previously, glutathione is a tripeptide composed of glutamate, cysteine and glycine. In the case of glutathione sulfonate, the direct assignment of the peaks in ^1H NMR spectrum is not possible due to its complexity. Thus, 2D NMR experiments like COSY, HSQC and HMBC, were necessary.

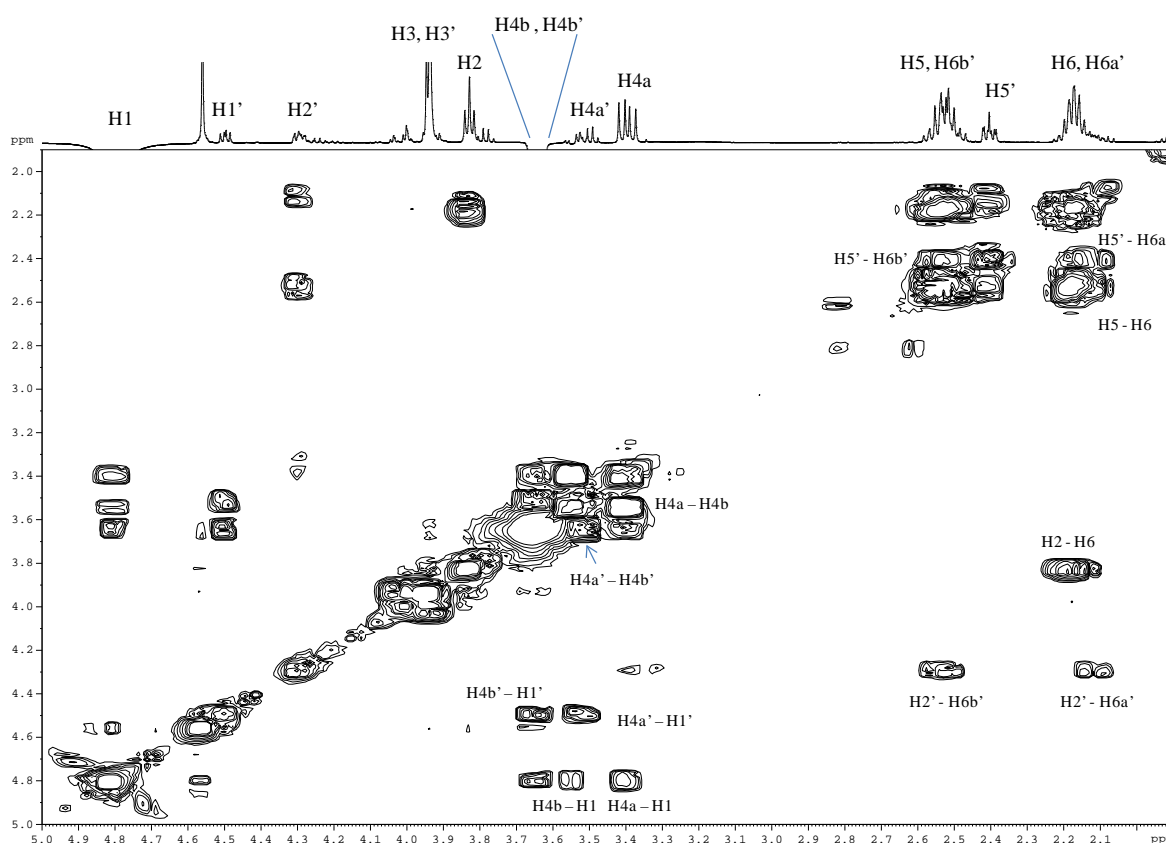


Fig. 31: Homonuclear correlation ^1H - ^1H gCOSY 2D NMR spectrum of glutathione sulfonate

H1-H6 are the protons from glutathione sulfonate. In COSY we can observe the correlation between the protons H5-H6, H2-H6, 2 H4 and H4-H1. Also, there are other peaks with assignment from H1' to H6' but it isn't clear yet if they belong to one or two different compounds and they will be analyzed later. The HSQC spectrum is also presented in Fig. 32 where we observe the correlation between a proton and its carbon but to confirm the recommended structure, HMBC 2D experiment is necessary (Fig. 33). In HMBC, the correlation between proton H3 and the carboxyl carbon (Cx), proton H2 and the carbonyl carbon (Cz) and proton H5 and the carbonyl carbon (Cf) are observed. Thus, we can clearly confirm the chemical structure of glutathione sulfonate. The assignment of free and sulfonated glutathione is presented in Table 12. Also, it is reported that after 6 weeks of reaction, the yield reaches 82%.

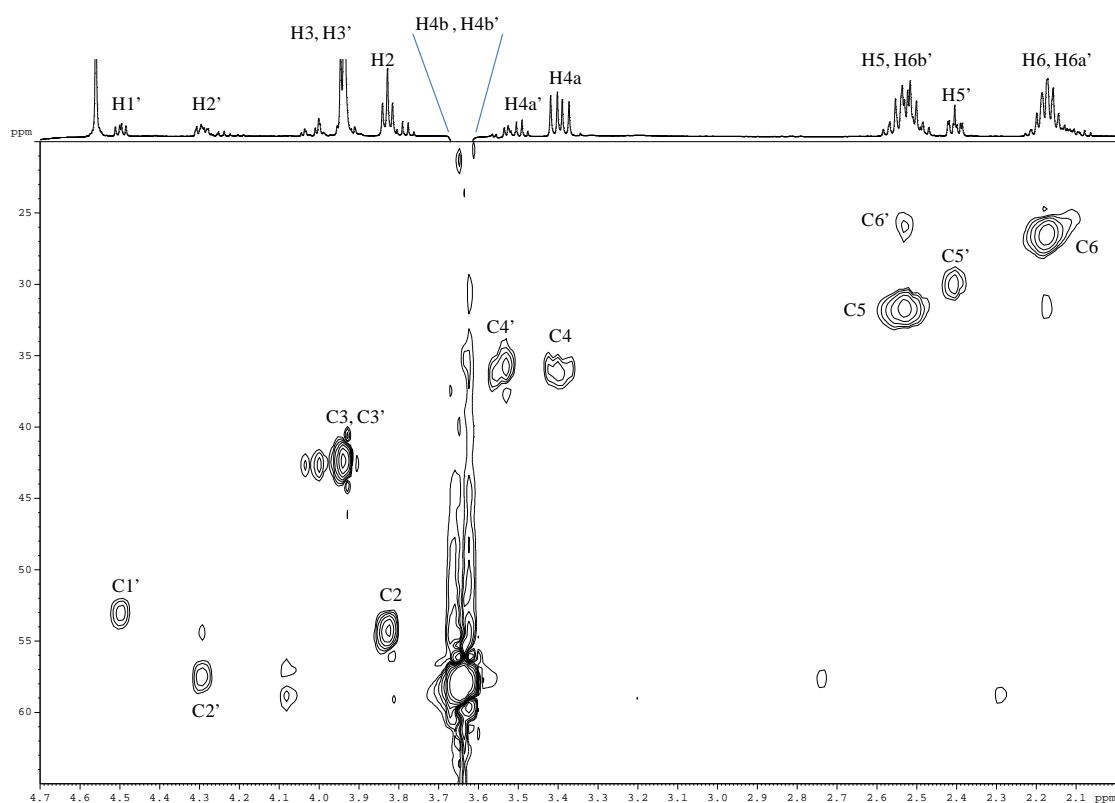


Fig. 32: ^1H - ^{13}C gHSQC 2D NMR spectra of glutathione sulfonate

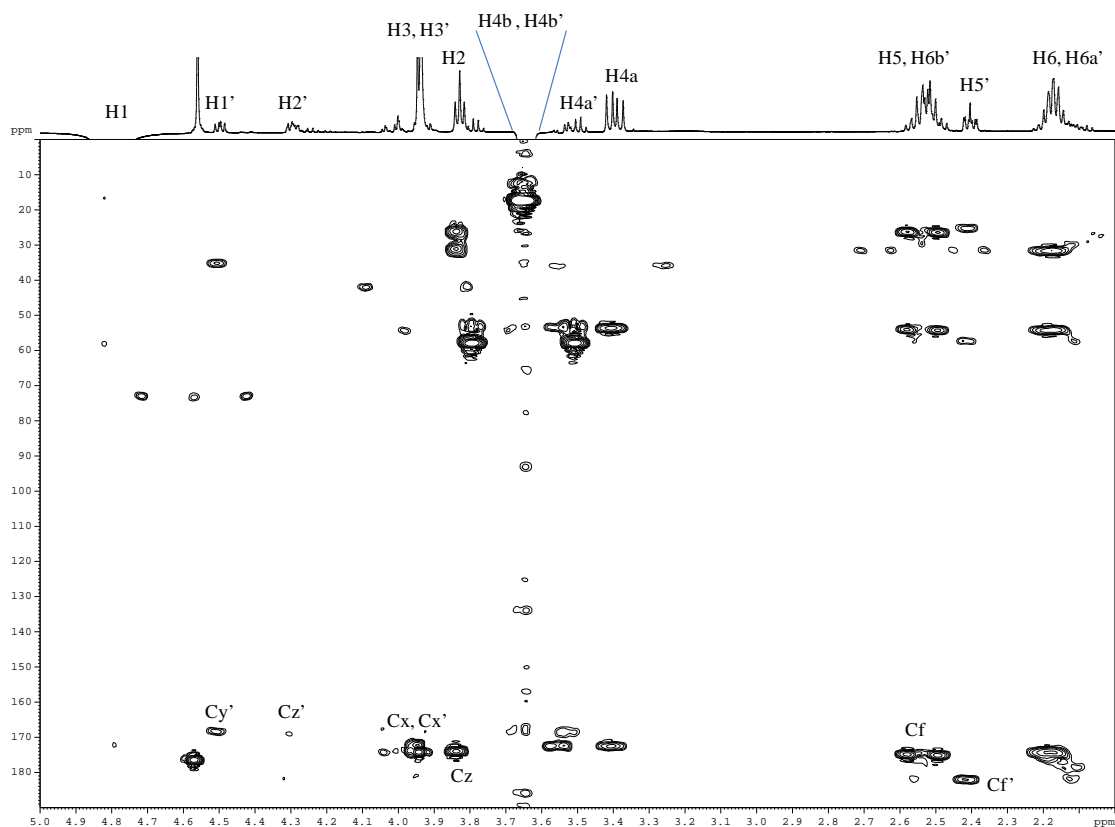


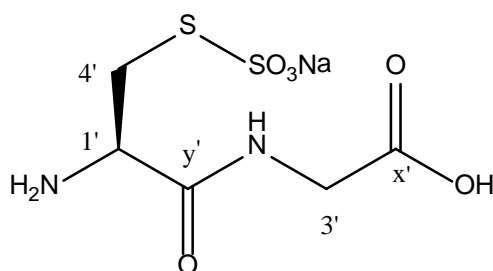
Fig. 33: ^1H - ^{13}C gHMBC 2D NMR spectra of glutathione sulfonate

Table 12: Assignment of glutathione and glutathione sulfonate

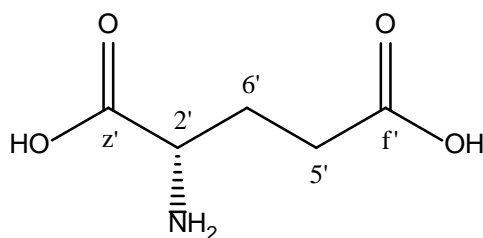
Compound	^1H ppm	^{13}C ppm
Glutathione	2.16 (H6*)	29.06
	2.55 (H5*)	34.05
	2.94 (H4*)	28.32
	3.80 (H2*)	57.17
	3.94 (H3*)	46.35
	4.56 (H1*)	58.55
	-	179.10 (Cx*)
	-	174.51 (Cy*)
	-	177.72 (Cf*)
-	176.83 (Cz*)	
Glutathione sulfonate	2.179 (H6)	26.64
	2.540 (H5)	31.81
	3.405 (H4a)	36.17
	3.558 (H4b)	36.17
	3.835 (H2)	54.44
	3.946 (H3)	42.48
	4.804 (H1)	53.75
	-	174.34 (Cx)
	-	172.66 (Cy)
	-	174.98 (Cf)
	-	174.08 (Cz)

Except from the peaks of glutathione sulfonate, we observed some other peaks that are labeled in the NMR spectra as H' (for proton) and C' (for carbon). The hypothesis that we did is that the bond between the glutamate and cysteine breaks, and two different compounds are produced. The first is glutamate (**8b**) and the second one is a dipeptide composed of the sulfonated cysteine and glycine (**8a**).

Chemical structure of $C_5H_{10}O_6N_2S_2$ (**8a**) in Fig. 30-33:



Chemical structure of glutamate (**8b**) in Fig. 30-33:



In the COSY spectrum of Fig. 31, we observe the correlation between the two H4' protons and their correlation with H1'. On the other hand there is also a correlation between H5' and the two H6' that appear at 2.145 ppm and 2.536 ppm respectively, due to stereochemical reasons. In HSQC we observe the correlation between the protons of glutamate and their carbon and this assignment is almost consistent with the literature. ^[5] The error between the theoretical and experimental values are normal since in bibliography the pH of the solution is 7.4 instead of ours which is at 3.5. Also, in HSQC we observe the protons and their carbons of the dipeptide **8a**. Their assignment is consistent with the respective assignment of glutathione sulfonate. Of

course there are small deviations since it is another compound. Finally, in the HMBC spectrum of Fig. 33, the correlation between proton H2' and the carboxyl carbon (Cz') and proton H5' and the carboxyl carbon (Cf') for glutathione is depicted. Also, the correlation between proton H1' and the carbonyl carbon (Cy') as well as proton H3' and the carboxyl carbon (Cx'), are observed. In conclusion, the assignment of the NMR spectra of these two compounds (8a and 8b) is presented in Table 13.

Table 13: Assignment of glutamate (**8b**) and dipeptide C₅H₁₀O₆N₂S₂ (**8a**):

Compound	¹ H ppm	¹³ C ppm
Glutamate	4.299 (H2')	57.57
	2.411 (H5')	30.05
	2.145 / 2.536 (H6')	25.98
	-	182.04 (Cf')
	-	169.14 (Cz')
Dipeptide C ₅ H ₁₀ O ₆ N ₂ S ₂	4.505 (H1')	53.13
	3.946 (H3')	42.48
	3.546 / 3.651 (H4')	35.88
	-	172.33 (Cx')
	-	168.41 (Cy')

6B. LC-MS-QToF characterization of glutathione (**7**), glutathione sulfonate (**8**) and dipeptide C₅H₁₀O₆N₂S₂ (**8a**)

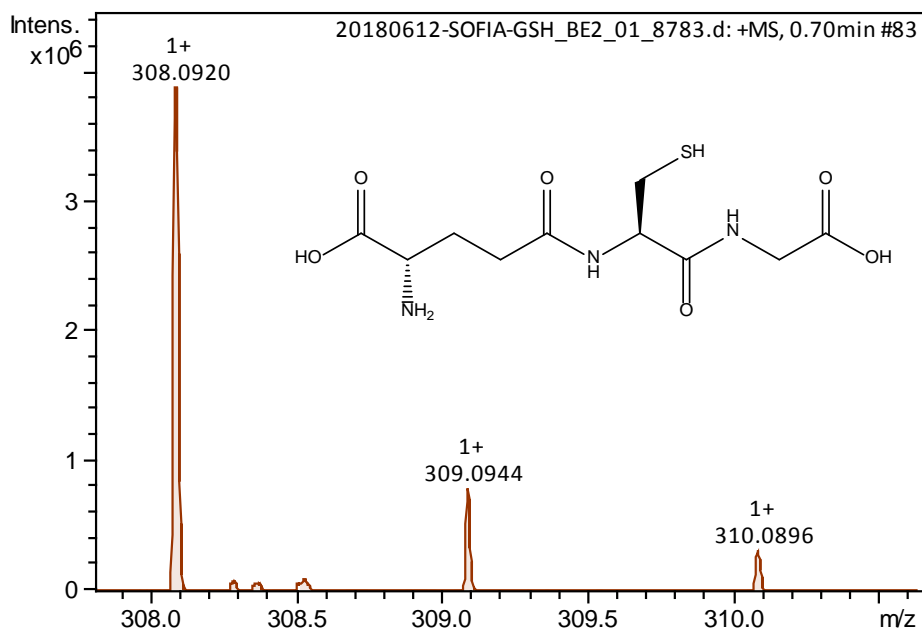


Fig. 34: MS [M+H]⁺ spectrum of glutathione (10⁻⁴ M, model wine: 12% ethanol, 5g/L tartaric acid, pH=3.5, RT)

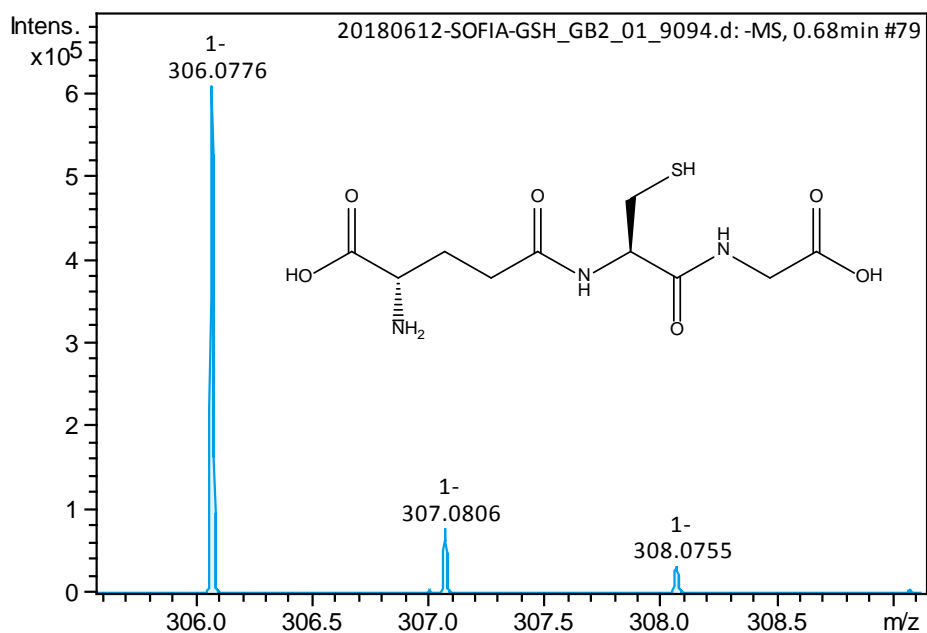


Fig. 35: MS $[M-H]^-$ spectrum of glutathione (10^{-4} M, model wine: 12% ethanol, 5g/L tartaric acid, pH=3.5, RT)

In Figs. 34 and 35, the MS spectra of glutathione are presented in both positive and negative ionization, with the results in the positive mode being better. Additionally, the mass spectrum of glutathione sulfonate is presented in Fig. 36.

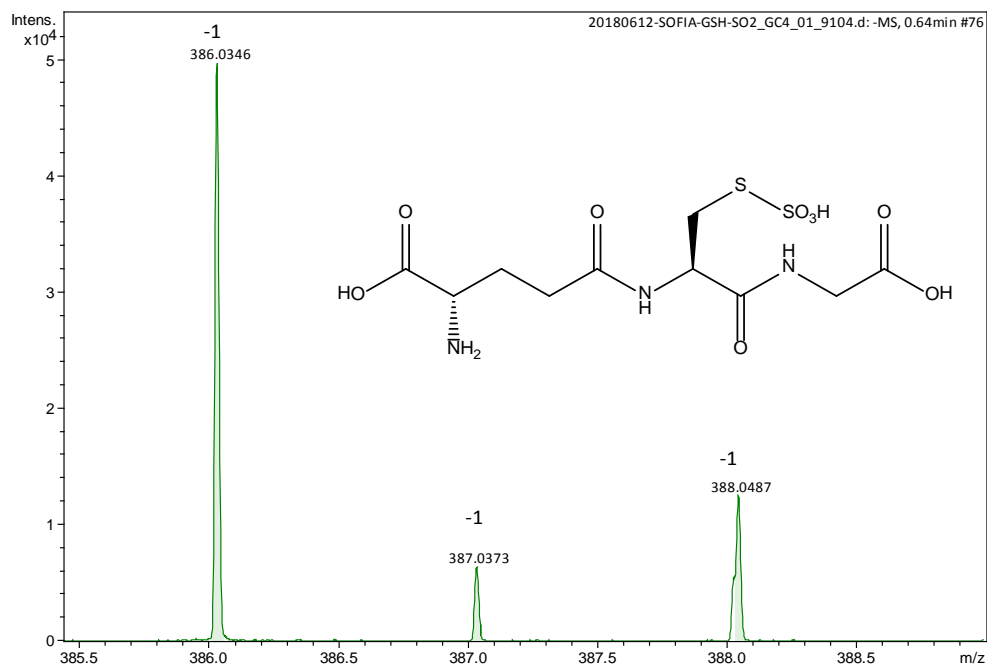


Fig. 36: MS $[M-H]^-$ spectrum of glutathione sulfonate (10^{-3} M, model wine: 12% ethanol, 5g/L tartaric acid, pH=3.5, RT)

Table 14: Theoretical and experimental m/z values of glutathione (**7**) (positive form) at 0.70 min.

Compound	Detected Mass [M+H] ⁺	Theoretical Mass [M+H] ⁺	Error (ppm)	Formula
7	308.0920	308.0911	0.0009	C ₁₀ H ₁₇ O ₆ N ₃ S
7 isotope a	309.0944	309.0937	0.0007	¹³ C ₁₀ H ₁₇ O ₆ N ₃ S
7 isotope b	310.0896	310.0896	-	C ₁₀ H ₁₇ O ₆ N ₃ ³⁴ S

Table 15: Theoretical and experimental m/z values of glutathione (**7**) (negative form) at 0.68 min.

Compound	Detected Mass [M-H] ⁻	Theoretical Mass [M-H] ⁻	Error (ppm)	Formula
7	306.0776	306.0765	0.0011	C ₁₀ H ₁₇ O ₆ N ₃ S
7 isotope a	307.0806	307.0792	0.0014	¹³ C ₁₀ H ₁₇ O ₆ N ₃ S
7 isotope b	308.0755	308.0751	0.0004	C ₁₀ H ₁₇ O ₆ N ₃ ³⁴ S

Table 16: Theoretical and experimental m/z values of glutathione sulfonate (**8**) at 0.64 min.

Compound	Detected Mass [M-H] ⁻	Theoretical Mass [M-H] ⁻	Error (ppm)	Formula
8	386.0346	386.0333	0.0013	C ₁₀ H ₁₇ O ₉ N ₃ S ₂
8 isotope a	387.0373	387.0358	0.0015	¹³ C ₁₀ H ₁₇ O ₉ N ₃ S
8 isotope b	388.0487	388.0312	0.0175	C ₁₀ H ₁₇ O ₉ N ₃ ³⁴ S ₂

We can clearly observe in Tables 14-16 that the theoretical values are close to the experimental values for both free and sulfonated glutathione. Also, these values have been reported in previous study. ^[56] Thus, we confirm the chemical structure of glutathione sulfonate that we recommended previously using the NMR spectroscopy.

Additionally, the dipeptide **8a** has been detected in negative form and is presented in Fig. 37. Its theoretical and experimental values are also presented in Table 17.

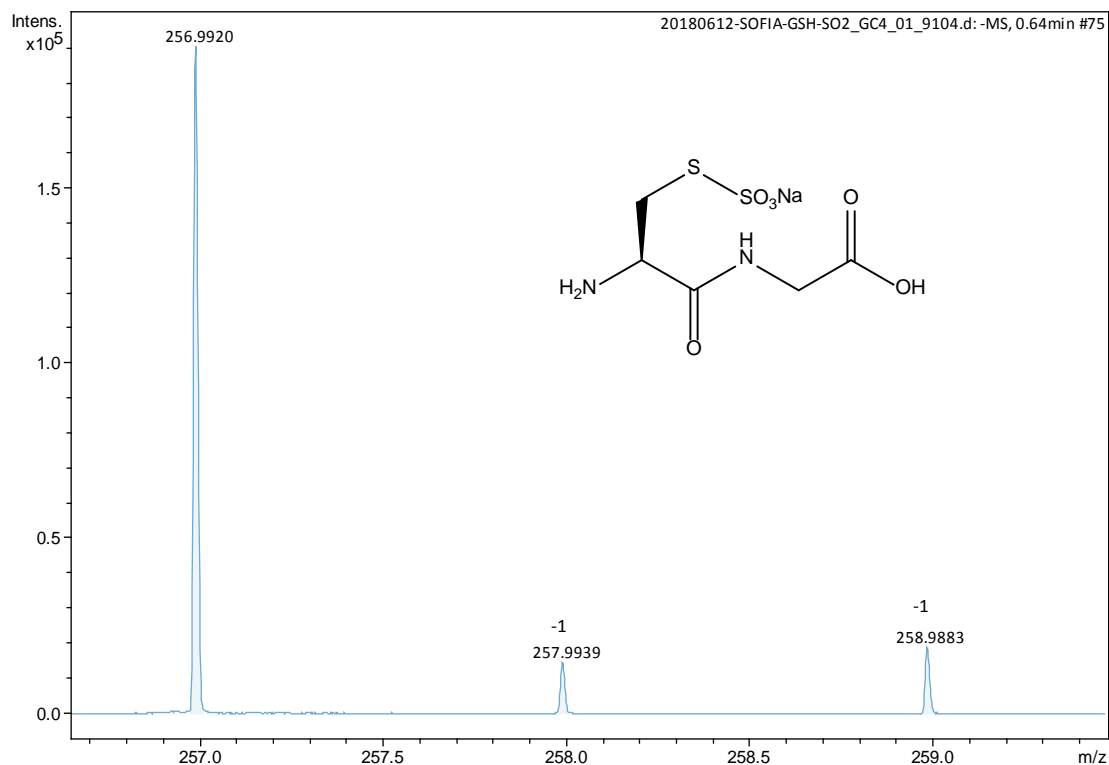


Fig. 37: MS $[M-H]^-$ spectrum of $C_5H_{10}O_6N_2S_2$ (**8a**) (10^{-3} M, model wine: 12% ethanol, 5g/L tartaric acid, pH=3.5, RT)

Table 17: Theoretical and experimental m/z values of $C_5H_{10}O_3N_2S$ (**8a**) at 0.64 min.

Compound	Detected Mass $[M-H]^-$	Theoretical Mass $[M-H]^-$	Error (ppm)	Formula
8a	256.9920	256.9908	0.0012	$C_5H_{10}O_3N_2S$
8a isotope a	257.9939	257.9928	0.0011	$^{13}C_5H_{10}O_3N_2S$
8a isotope b	258.9883	258.9878	0.0005	$C_5H_{10}O_3N_2^{34}S$

Unfortunately, the detection of glutamate couldn't be done since the MS conditions for its ionization is not appropriate. Nevertheless, by the detection of the dipeptide **8a**, we confirmed the results obtained by the 2D NMR experiments.

7. Assignment of the proton and carbon NMR chemical shifts of all the characterized compounds.

In this section we present the results of the assignment of the proton and carbon NMR chemical shifts of the compounds that were analyzed. To obtain a better understanding of the sulfonation reaction and verify the structure of its products, 2D NMR experiments (COSY, HSQC, HMBC) and several public NMR databases were used. [57-59]

Table 18: Assignment of free and sulfonated compounds

Compound	¹ H (ppm)	¹³ C (ppm)
Acetaldehyde	9.66 (1H, q)	207.19 ^b
	2.23 (3H, d)	30.75 ^b
Acetaldehyde hydrated	5.23 (1H, q)	88.80 ^b
	1.35 (3H, d)	23.84 ^b
Acetaldehyde Ethyl Hemiacetal	3.76 (1H, dt)	63.31 ^b
	3.52 (1H, dt)	63.31 ^b
	1.32 (3H, d)	22.62 ^b
Acetaldehyde sulfonate	4.54 (1H, q)	80.99 ^b
	1.46 (3H, d)	17.56 ^b
Pyruvic acid	2.44 (3H, s)	26.56 ^b
Pyruvic acid hydrated	1.57 (3H, s)	25.77 ^b
Pyruvic sulfonate	1.72 (3H, s)	21.37 ^b
α-glucose	5.22 (H1*, d)	92.66
	3.53 (H2*, dd)	72.23
β-glucose	4.64 (H1', d)	96.58
	3.24 (H2', dd)	74.86
Glucose sulfonate 10a	4.55 (H1,d)	82.80
	4.22 (H2, dd)	71.10
	4.02 (H3, dd)	76.76
	3.67 (H4)	71.18
Glucose sulfonate 10b	4.48 (H1,d)	83.87
	4.03 (H2, dd)	73.17
	4.18 (H3, dd)	68.77
Ascorbic acid	4.91 (H1, d)	77.03 ^b
	4.05 (H2, dt)	69.76 ^b
	3.74 (H3, d)	62.93 ^b
Ascorbic sulfonate	4.57 (H1*, d)	81.35
	4.04 (H2*, dt)	72.58
	3.72 (H3*, d)	65.28
Cysteine	3.06 (H1, dd)	27.79 ^b
	3.97 (H2, dd)	58.88 ^b
	-	173.07 (C3) ^b
Cysteine sulfonate	3.49 (H1a*, dd)	35.54
	3.66 (H1b*)	35.54
	4.18 (H2*, dd)	55.05
	-	172.42 (C3*)
Glutathione	2.16 (H6*)	29.06
	2.55 (H5*)	34.05
	2.94 (H4*)	28.32
	3.80 (H2*)	57.17
	3.94 (H3*)	46.35
	4.56 (H1*)	58.55
	-	179.10 (Cx*)
	-	174.51 (Cy*)

	-	177.72 (Cf*)
	-	176.83 (Cz*)
Glutathione sulfonate	2.179 (H6)	26.64
	2.540 (H5)	31.81
	3.405 (H4a)	36.17
	3.558 (H4b)	36.17
	3.835 (H2)	54.44
	3.946 (H3)	42.48
	4.804 (H1)	53.75
	-	174.34 (Cx)
	-	172.66 (Cy)
	-	174.98 (Cf)
	-	174.08 (Cz)

^b: from bibliography 3-5

Table 19: Results of LC-MS-QToF of all the analyzed compounds (theoretical m/z, experimental m/z and the retention time)

Compound	Theoretical m/z	Experimental m/z	Retention time
Acetaldehyde sulfonate (M-H)	124.991403	124.9917	0.63
	125.993862	-	
	126.987199	126.9878	
Pyruvic sulfonate (M-H)	168.981232	168.9815	0.63
	169.983947	169.9845	
	170.978952	170.9778	
Ascorbic acid (M+H)	177.039364	177.0396	0.70
Ascorbic sulfonate (M-H)	254.981626	254.9818	0.63
	255.984643	255.9850	
	256.980198	256.9799	
Glucose (M-H)	179.056112	179.0561	0.57
Glucose sulfonate (M+H)	263.043129	263.0563	4.65
	264.046185	264.0570	
	265.041713	265.0537	
Cysteine (M+H)	122.027026	122.0268	0.63
	123.029263	123.0297	
	124.022822	124.0225	
Cysteine sulfonate (M-H)	199.969288	199.9698	0.63
	200.971136	200.9720	
	201.966039	201.9655	
Glutathione (M+H)	308.091083	308.0920	0.70
	309.093733	309.0944	
	310.089641	310.0896	
Glutathione (M-H)	306.076530	306.0776	0.68
	307.079174	307.0806	
	308.075084	308.0755	

Glutathione sulfonate (M-H)	386.033345	386.0346	0.64
	387.035818	387.0373	
	388.031187	388.0487	

3.2. Evaluation of the antioxidant capacity of acetaldehyde sulfonate, pyruvic sulfonate and ascorbic sulfonate

3.2.1. DPPH assay

In this section, we present the results obtained from the analysis of the antioxidant capacity of initial and sulfonated compounds via the DPPH method. To evaluate the antioxidant capacity of acetaldehyde, pyruvic acid, ascorbic acid and their sulfonated adducts, it is necessary to calculate the EC₂₀ which is the concentration of a substance that is needed to bind 20% of the DPPH radicals.

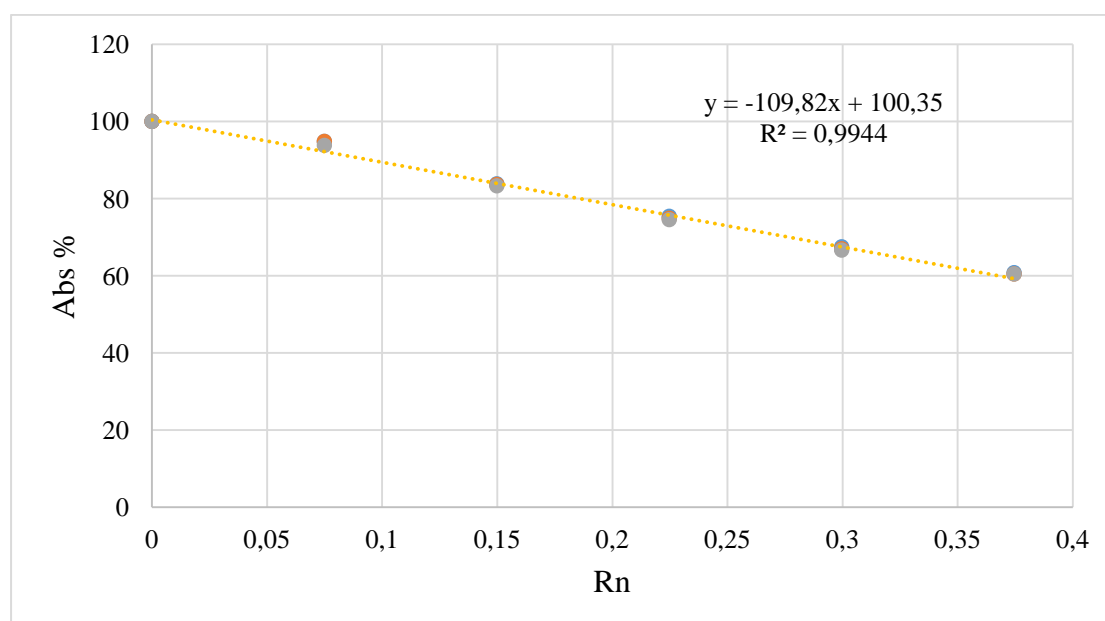


Fig. 38: Example of a graph that is created to measure the EC₂₀ of SO₂ (10⁻³ M)

Fig. 38 presents a graph of the molar ratio (Rn) of a compound in relation to the % percentage of absorbance. To calculate Rn and EC₂₀ we used the equations that are presented below:

$$Rn = n_{\text{sample}} / n_{\text{DPPH}}$$

$$y = ax + b$$

$$EC_{20} = [(80 - b) / a] * 100\%$$

Table 20: EC₂₀ values of tested model compounds that were analyzed and the concentration that was used

Compound	Concentration	EC ₂₀
SO ₂	10 ⁻³ M	0,18 ±0,0012
Ascorbic acid	5*10 ⁻⁴ M	0,09 ±0,0019
Ascorbic sulfonate	5*10 ⁻⁴ M	0,16±0,0021
Pyruvic acid	5*10 ⁻⁴ M	NR
Pyruvic sulfonate	5*10 ⁻⁴ M	0,12 ±0,0022
Acetaldehyde	5*10 ⁻⁴ M	NR
Acetaldehyde sulfonate	10 ⁻³ M	0,20±0,0033

NR: Not Reacting

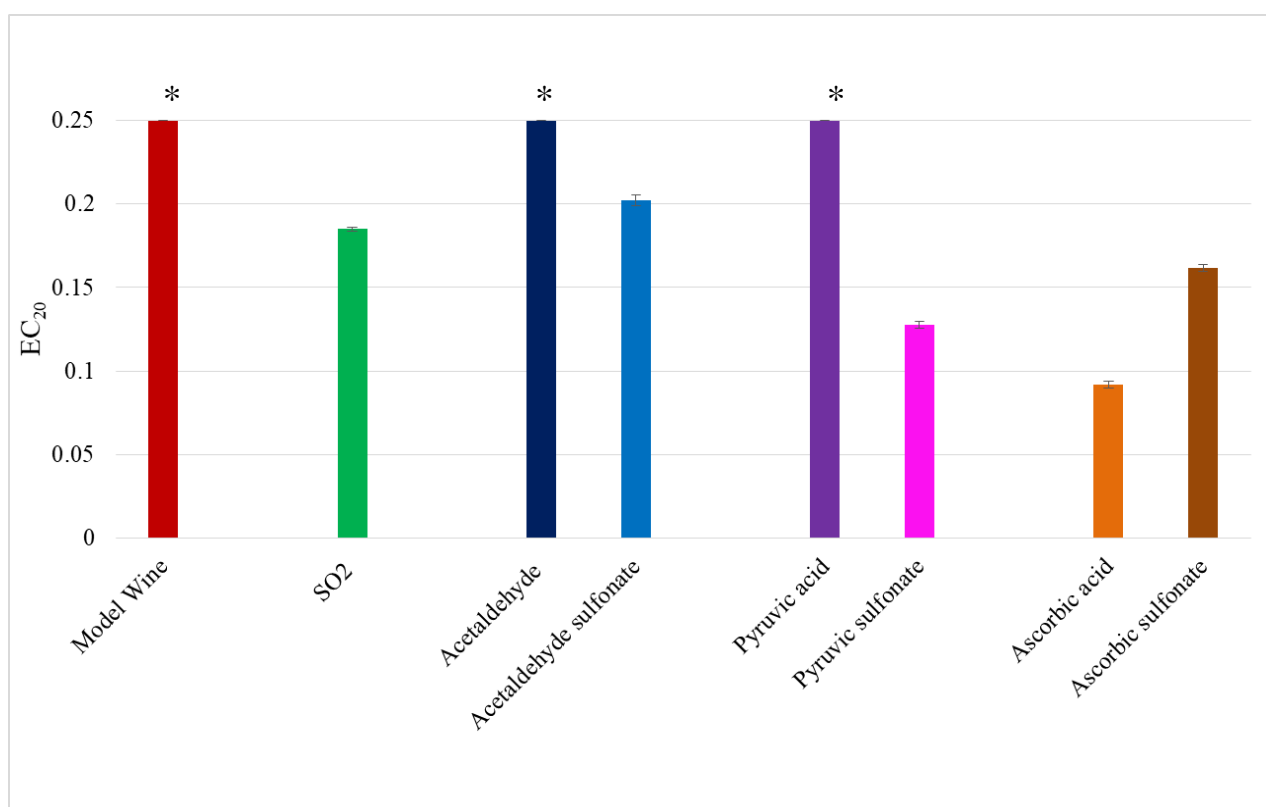


Fig. 39: Antioxidant capacity of specific compounds using the DPPH method (*:No Reaction)

SO₂ alone has an antioxidant activity and this is one of the reasons that is widely used to the wine industry. Compared to SO₂ antiradical activity, we show for the first time that sulfonated products had a greater antioxidant activity. These compounds are the

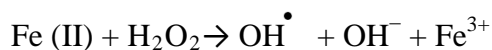
sulfonated adducts of pyruvic acid and acetaldehyde. Also, this research shows that even if some compounds like acetaldehyde and pyruvic acid have no antioxidant capacity, their sulfonated adducts are really good antioxidants.

In the case of ascorbic acid and ascorbic sulfonate, we can observe that the bisulfite that reacts with the ascorbic acid can lead to the oxidative stability of ascorbic acid and wine.

3.2.2. EPR method

In this section, the results of the EPR analysis are presented. For this method, the Fenton conditions were used. More specifically, hydrogen peroxide in association with ferrous ions produce hydroxyl radicals, which in turn react with ethanol. Thus, hydroxyl ethyl radical that is produced, can be trapped by the spin trap POBN.

Mechanism of the Fenton reaction:



After this reaction, there are two types of results:

- The compound is an antioxidant (Fig. 40)
- The compound is a prooxidant (Fig. 41)

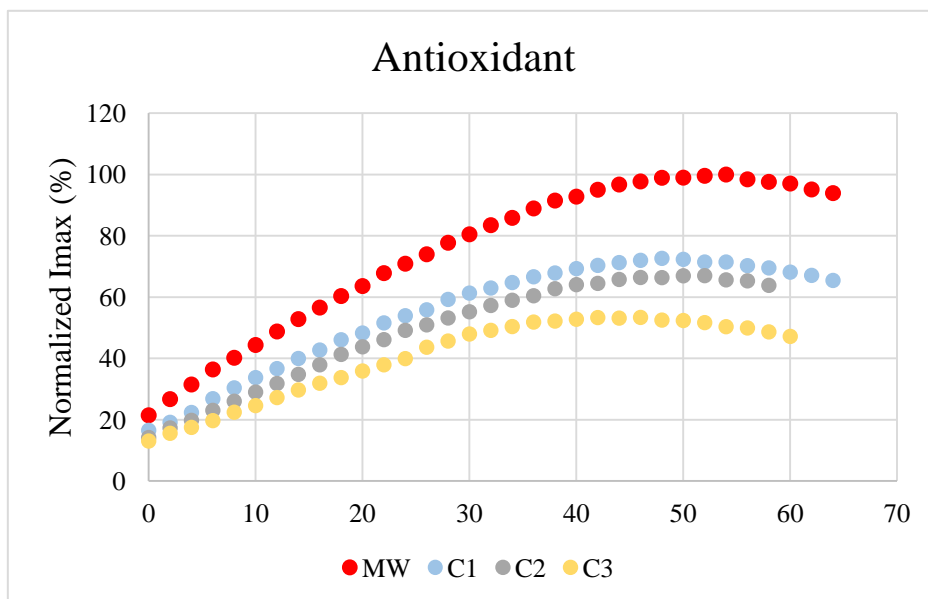


Fig. 40: Curves of the kinetics of the reaction of hydroxyl-ethyl radical with POBN when a compound is an antioxidant. ($C1 < C2 < C3$)

In Fig. 40, the red curve comes from the reaction of hydroxyl-ethyl radical with POBN in the model wine (blank). When an antioxidant compound is added to the model wine solution, the curve of the reaction will have lower maximum intensity and lower slope. As it is shown in Fig. 40, as the concentration of the compound increases, the antioxidant capacity increases too.

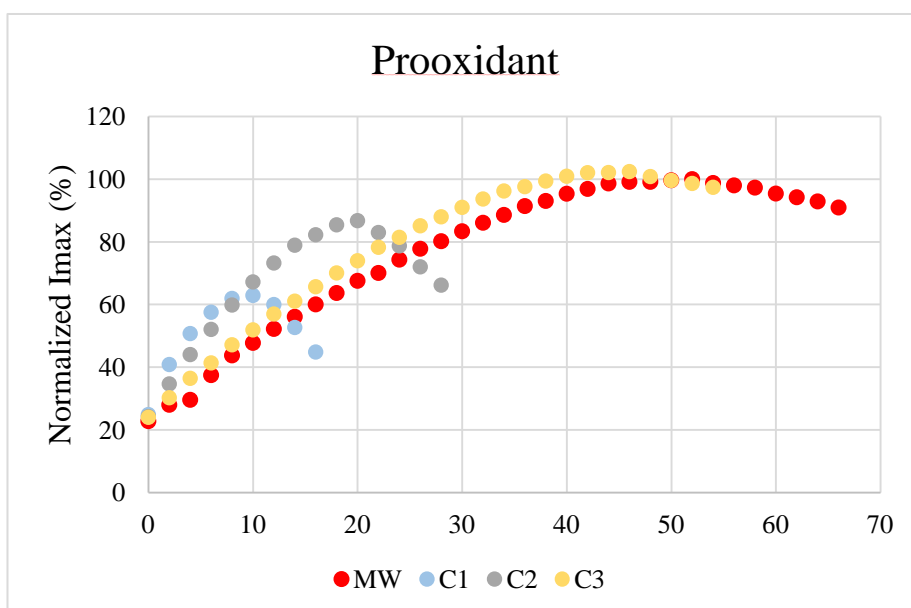


Fig. 41: Curves of the kinetics of the reaction of hydroxyl-ethyl radical with POBN when a compound is a prooxidant. ($C1 > C2 > C3$)

In Fig. 41, the red curve comes from the reaction of hydroxyl-ethyl radical with POBN in the model wine (blank). When a prooxidant compound is added to the model wine solution, the curve of the reaction will have a steeper slope.

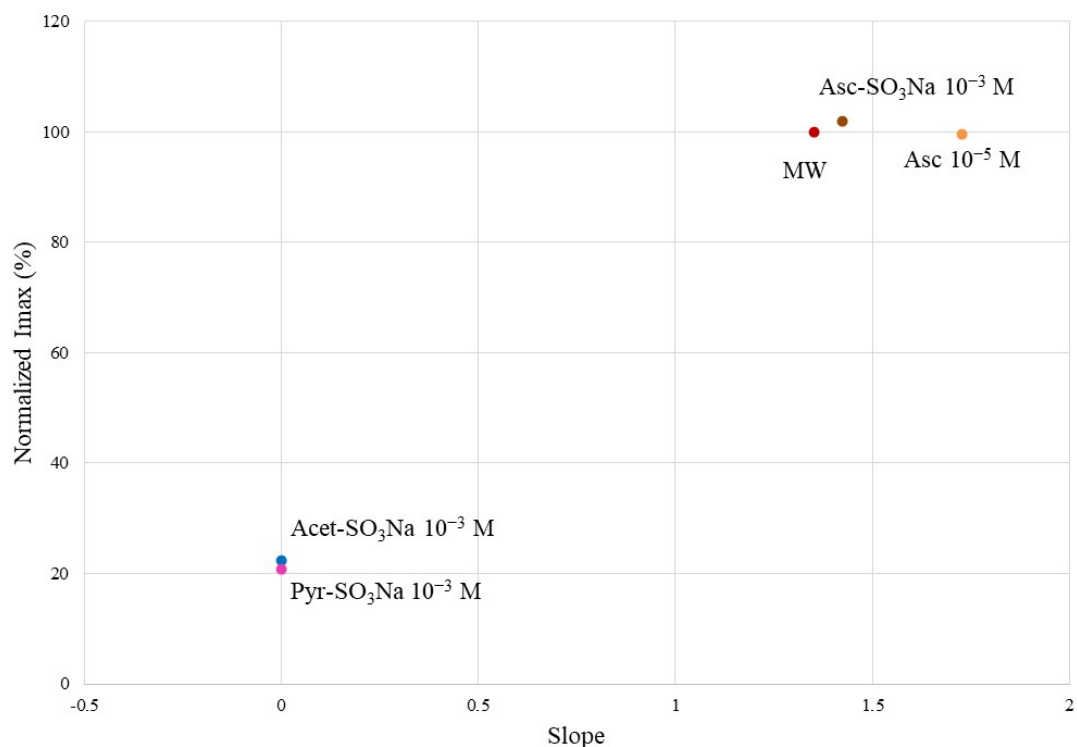


Fig. 42: Plot of the slope vs the % normalized I_{max} from the EPR kinetics diagrams for the sulfonated compounds. (Pyr-SO₃Na: pyruvic sulfonate, Acet-SO₃Na: acetaldehyde sulfonate, Asc: ascorbic acid, Asc-SO₃Na: ascorbic sulfonate, MW: model wine)

In Fig. 42, the kinetics for ascorbic acid and the sulfonated adducts of acetaldehyde, ascorbic acid and pyruvic acid are presented. In all samples and concentrations, the first point is almost at 20% but the I_{max} (maximum point) and the T_{max} (time to reach the maximum) depend on the compound studied. As it is mentioned above, compounds that have lower slope and lower maximum point than the model wine, are antioxidants. In Fig. 42, pyruvic sulfonate has a lower I_{max} than acetaldehyde sulfonate but both of them have zero slope. So, we can conclude that pyruvic sulfonate is a better antioxidant than acetaldehyde sulfonate. This result is consistent with the DPPH results, where it was found that pyruvic sulfonate has a lower EC₂₀ than acetaldehyde sulfonate.

On the other hand, the EPR study of ascorbic acid showed that it displays an irregular behavior, since at concentrations higher than 10^{-5} M, it acts as a prooxidant (Table 21).

Table 21: First and maximum point of the curves of the kinetics for different concentrations of ascorbic acid

Ascorbic acid	%FP	%Imax
10^{-3} M	46.85	46.85
10^{-4} M	39.52	112.68
$5 \cdot 10^{-5}$ M	32.04	103.6
10^{-5} M	23.24	99.57
Model Wine	21.53	100

As in the literature ^[2], ascorbic acid has scavenging properties, but most importantly for our work it can scavenge hydrogen peroxide. This means that it is oxidized and it generates radicals that finally form dehydroascorbate (Fig.43). As a result, the concentration of the hydroxyl radicals and hydroxy-ethyl radicals increases. Thus, the reaction of hydroxy-ethyl radicals with the spin trap POBN is faster. This behavior seems to be the reason why in the DPPH method ascorbic acid acts as a good antioxidant, but when studied with the EPR method it is found to act as a prooxidant. Finally, in Fig. 42 we can observe that ascorbic sulfonate is a prooxidant since it has a steeper slope than the model wine. The explanation for this result follows along the same lines as with that for ascorbic acid.

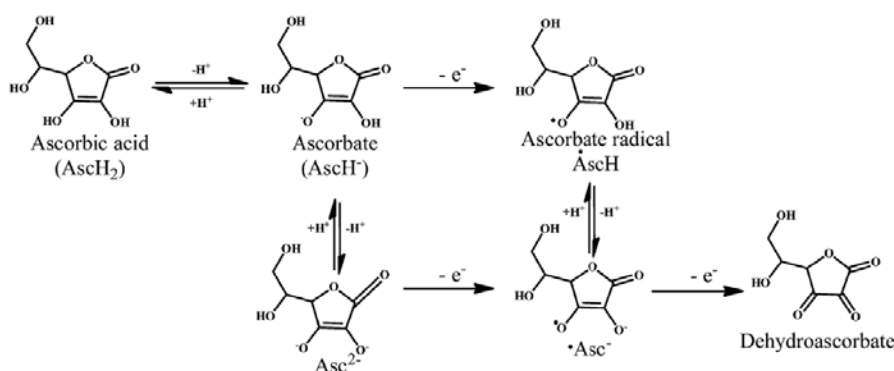


Fig. 43: Mechanism of radical scavenging activity of ascorbic acid ^[60]

3.3. Analysis of the sulfonated compounds in white wine samples by LC-MS-QToF

In this section, the identification of the studied sulfonated compounds in white wine samples has been attempted by LC-MS-QToF. Additionally, we tried to also identify other sulfonated compounds that have been already reported as present in wines in the literature. ^[17, 55-59] Table 22 provides details of the white wine samples of varied vintage and different appellations and have been profiled by LC-MS-QToF. Samples 1-8 had different aging conditions, while samples 9 and 10 were vintage wines. The sulfonated adducts that were identified in the wine samples were acetaldehyde sulfonate, pyruvic sulfonate, glucose sulfonate, cysteine sulfonate and glutathione sulfonate, and the full results of the MS analysis are presented in Table 25 in the Appendix. It is worth noting that, in some wines we also identified some of the sulfonated compounds that have been reported in the literature, namely α -ketoglutaric acid bisulfite (**13**) and indole lactic acid hexoside sulfonate (**14**). The characteristic m/z values of these two sulfonated compounds are reported in Tables 23 and 24.

Table 22: List of the white wine samples

	<u>Code name</u>	<u>Appellation</u>	<u>Year of production</u>
1	R-17-71	Batard Montrachet	2016
2	R-17-72	Pulligny Village	2016
3	R-17-73	Chevalier Montrachet	2016
4	R-17-74	Meursault dos d'âne	2016
5	R-17-75	Pulligny Pucelle	2016
6	R-17-76	Clavoillon	2016
7	DNO-17 (98-105)	Clavoillon	2017
8	DNO-18 (58-65)	Clavoillon	2018
9	161005 GSH (549-556)	Côte de Beaune	2008
10	161005 GSH (557-572)	Côte de Beaune	2009

Table 23: Theoretical and experimental m/z values of a-ketoglutaric acid bisulfite (**13**) at 0.15 min.

Compound	Detected Mass [M-H] ⁻	Theoretical Mass [M-H] ⁻	Error (ppm)	Formula
13	226.9784	226.9867	0.0083	C ₅ H ₈ O ₈ S
13 isotope a	227.9815	227.9897	0.0082	¹³ C ₅ H ₈ O ₈ S
13 isotope b	228.9832	228.9850	0.0018	C ₅ H ₈ O ₈ ³⁴ S

Table 24: Theoretical and experimental m/z values of indole lactic acid hexoside sulfonate (**14**) at 7.41 min.

Compound	Detected Mass [M-H] ⁻	Theoretical Mass [M-H] ⁻	Error (ppm)	Formula
14	446.0763	446.0762	0.0001	C ₁₇ H ₂₁ O ₁₁ NS
14 isotope a	447.0793	447.0794	0.0001	¹³ C ₁₇ H ₂₁ O ₁₁ N S
14 isotope b	448.0773	448.0766	0.0007	C ₁₇ H ₂₁ O ₁₁ N ³⁴ S

Figs. 44 and 45, plot the intensity of the MS peaks of some sulfonated adducts in the MS spectra of the two vintage wine samples from 2008 and 2009 respectively, is presented. These wines have been analyzed after 9 and 8 years respectively and the average intensity of each compound is presented. It is also worth noting that in these samples, the sulfonated adduct of indole lactic acid hexoside, previously reported in the literature, ^[56] was detected.

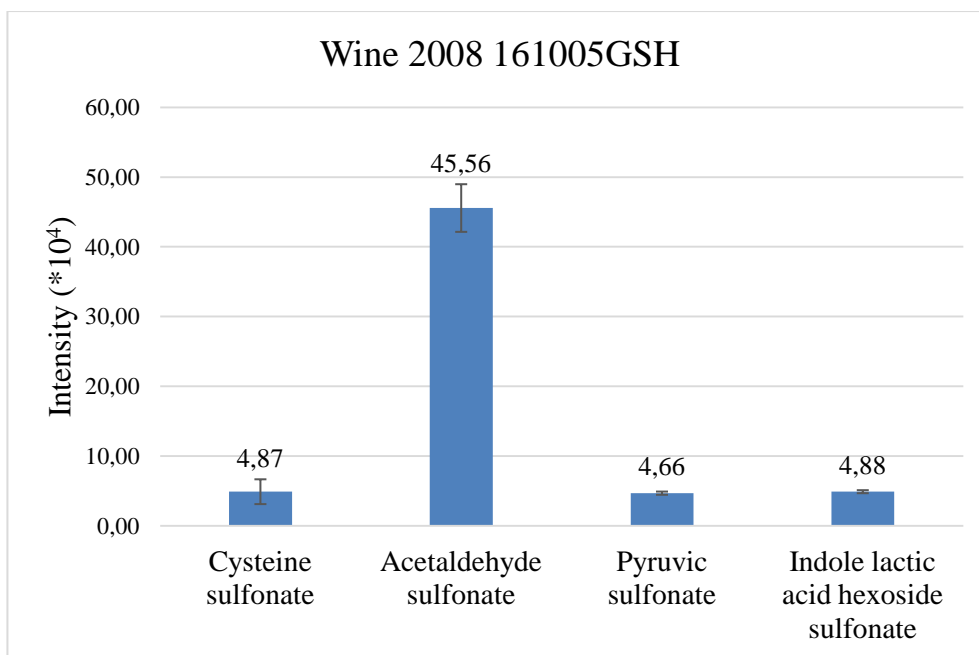


Fig. 44: Intensity of four sulfonated compounds in a wine sample from 2008

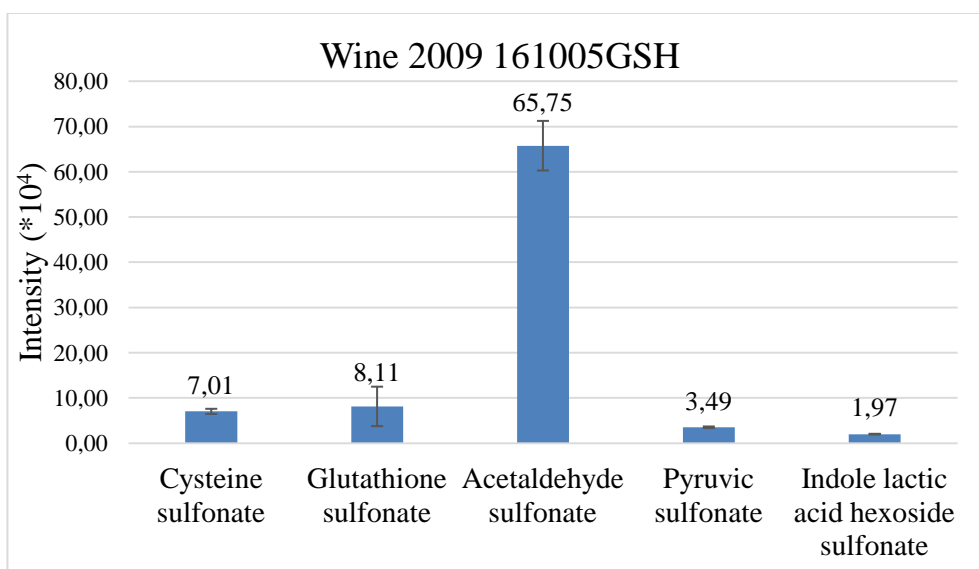


Fig. 45: Intensity of five sulfonated compounds in a wine sample from 2009

The wine samples 1-8 constitute an extensive experimental data set (n=26) for which mass spectrometry data and DPPH measurements are available, while EPR data are also available for 13 of the 26 samples. This prompted us to use multivariate statistical analysis models to explore possible correlations between the mass spectrometry peak intensity data of sulfonated products and the antioxidant activity of wines as expressed by the DPPH methodology, EC20, and the EPR measurements (Tmax, Imax, Slope).

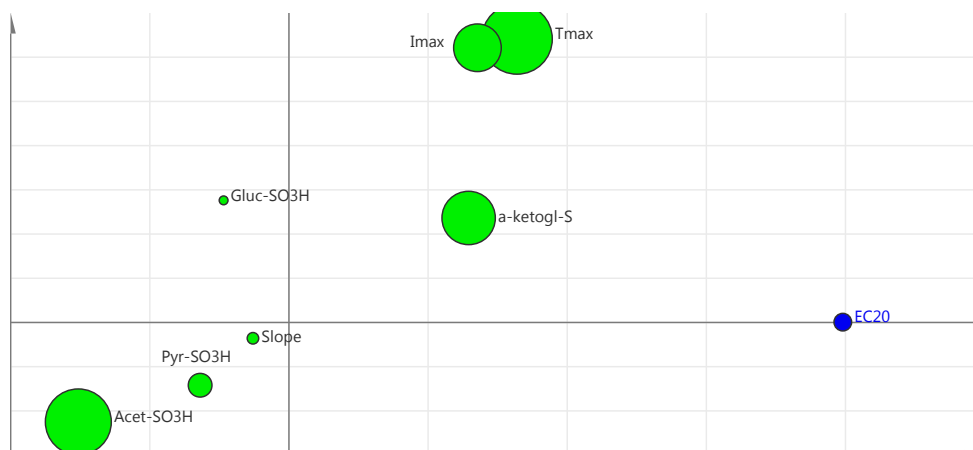


Fig. 46: Variable contribution plot of an OPLS model using LC-MS and EPR data (X variables) to predict the antioxidant capacity of wines based on DPPH (Y variable). The size of the points is a measure of the importance (VIP parameter) of the X variables.

Fig. 46 presents the OPLS statistical model using all the data from the three analytical methods (EPR, DPPH and LC-MS-QToF) for 26 samples. As it is shown, Tmax, Imax (or Max) and a-ketoglutaric bisulfite (less important) have a positive correlation with EC_{20} . This means that EC_{20} decreases while Tmax and Imax decrease too. On the other hand, the sulfonated adducts of acetaldehyde and pyruvic acid have a negative correlation with EC_{20} , which means that EC_{20} decreases while the intensity of acetaldehyde sulfonate increases.

For this, we developed an Orthogonal Projection to Latent Structures (OPLS) model that examined whether MS and EPR data were capable of simulating the antioxidant activity of wines based on their DPPH values (EC_{20}). Fig. 46 presents the variable contribution plot of this OPLS statistical model, where variables that have a positive correlation with DPPH are closer to the right hand side of the plot (where the EC_{20} point is), while variables with a negative correlation are situated to the left hand side. The size of the points in this diagram represents the Variable Importance Parameter (VIP), so the bigger the size the larger the contributions of the variable to the OPLS model showsn, that the EPR parameters Tmax, Imax (or Max) and the MS intensity of a-ketoglutaric bisulfite have an important and positive correlation with EC_{20} . While on the other hand, the sulfonated adducts of acetaldehyde and pyruvic acid have a negative correlation with EC_{20} , with the acetaldehyde adduct being more important for the model.

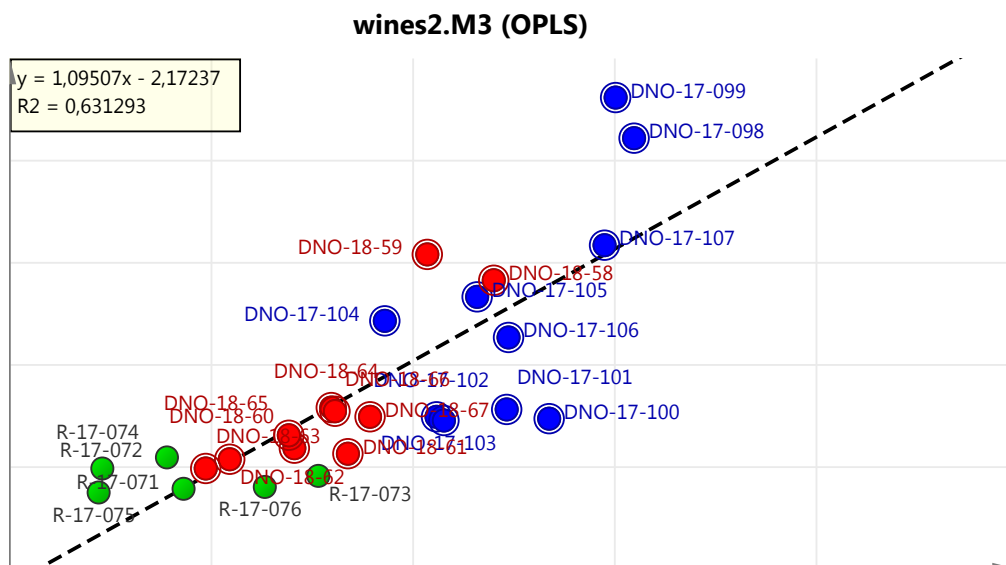


Fig. 47: Comparison of actual (y axis) and predicted (x axis) EC_{20} values of wines based on an OPLS model that used LC-MS-QToF and EPR data.

Fig. 47 compares the experimental and predicted EC_{20} values of the wines by an OPLS model built from the MS intensities of sulfonated compounds and the EPR results of the wines. The R^2 value of 0.63 shows that there is very good correlation between the three analytical methodologies, MS, EPR and DPPH, and good prediction of EC_{20} based on the EPR and LC-MS-QToF data.

A similar OPLS model was also developed, but this time using only the LC-MS results to predict the antioxidant activity of the 26 samples based on the EC_{20} from the DPPH method (leaving out the EPR results). Fig. 48 presents the experimental and predicted EC_{20} values of the wines based on only LC-MS data. Although the correlation coefficient R^2 is now slightly smaller at 0.58, there is still excellent correlation of the LC-MS data with DPPH, indicating that the LC-MS data alone contain important information regarding the antioxidant activity of wines.

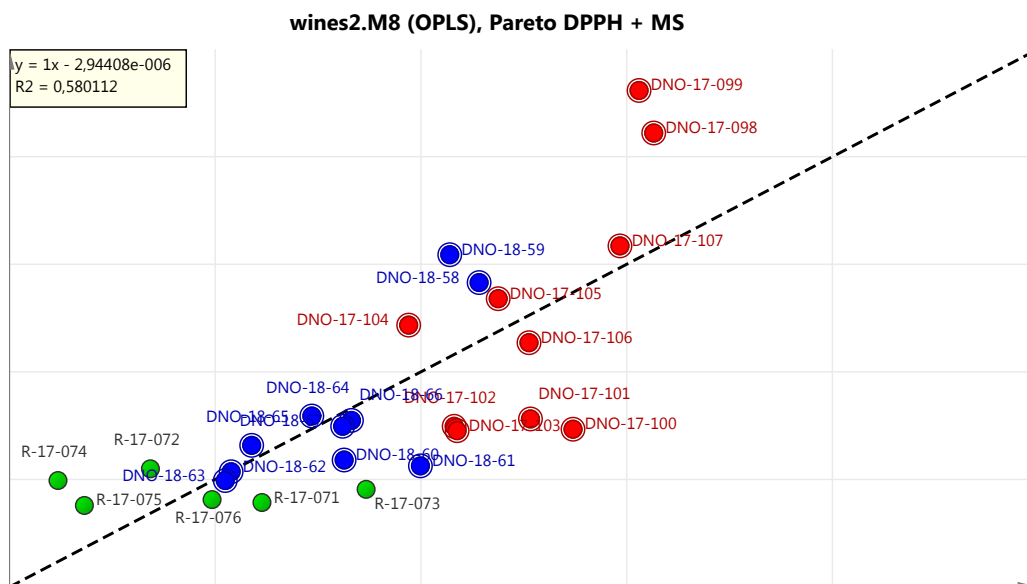


Fig. 48: Comparison of actual (y axis) and predicted (x axis) EC_{20} values of wines based on an OPLS model that uses only LC-MS-QToF data.

Comparing all the samples, we observe that acetaldehyde sulfonate and pyruvic sulfonate are present in wine samples from the first months whereas in some samples we observe the sulfonated adduct of glucose. In addition, cysteine sulfonate and glutathione sulfonate appear in aged wines.

CHAPTER 4: CONCLUSIONS

The aim of this dissertation was to study the impact of sulfonation on the antioxidant properties of wines and the ability of various sulfonated adducts to scavenge free radicals. The synthesis and characterization of the sulfonated adducts of acetaldehyde, pyruvic acid, glucose, cysteine and glutathione has been successfully accomplished. Both NMR spectroscopy (1D and 2D) and liquid mass spectrometry coupled with a mass spectrometer were used to characterize these compounds. Using both one-dimensional ^1H NMR spectra and two-dimensional COSY, HSQC and HMBC NMR spectra it was possible to identify all the sulfonated compounds and verify their chemical their structure. The information provided by LC-MS spectrometry regarding the exact mass of the compounds was equally valuable, as it allowed us to confirm independently the structure of the synthesized compounds.

In order to evaluate the antioxidant capacity of the sulfonated compounds synthesized two different analytical approaches were used, the DPPH assay and EPR spectroscopy. DPPH results showed that compared to SO_2 , the sulfonated products of pyruvic acid had a greater antioxidant/radical scavenging activity. Also, the present research showed that although some compounds such as acetaldehyde and pyruvic acid do not possess any antioxidant capacity, their sulfonated adducts can act as really strong antioxidants. In the case of ascorbic acid and ascorbic sulfonate, we observed that the reaction of bisulfite with ascorbic acid could enhance the oxidative stability of both ascorbic acid and the wine itself.

On the other hand, EPR results showed that pyruvic sulfonate has a lower I_{max} that acetaldehyde sulfonate, while both of them have zero slope, leading to the conclusion that pyruvic sulfonate is a better antioxidant that acetaldehyde sulfonate, a result also consistent with our DPPH results. Also, it is worth mentioning that during the EPR experimental procedure, ascorbic acid can scavenge both the hydroxyl radical and hydrogen peroxide, resulting in the generation of radicals that react with POBN and compete with the hydroxyl ethyl radical. Thus, ascorbic acid and its sulfonated product act as prooxidants during EPR analysis.

Finally, the analysis and identification of sulfonated compounds in commercial white wine samples by LC-MS-QToF provided interesting results when

compared with DPPH and EPR results for their antioxidant properties. Acetaldehyde sulfonate, pyruvic sulfonate, glucose sulfonate and α -ketoglutaric acid bisulfite were found to be present in fresh wine samples by LC-MS, while on the contrary cysteine sulfonate, glutathione sulfonate and indole lactic acid hexoside sulfonate were identified in aged wine samples. Furthermore, multivariate statistical analysis combining the antioxidant capacity analyses of the wines by DPPH and EPR and the LC-MS intensities of the sulfonated adducts of acetaldehyde, pyruvic acid, α -ketoglutaric acid and glucose from LC-MS, was performed. This analysis showed for the first time that there is a significant correlation between the presence of specific sulfonated compounds, namely acetaldehyde sulfonate and α -ketoglutaric acid bisulfite, and the antioxidant capacity of wines.

The fuller understanding of the chemistry of wine and the mechanisms that are involved in their aging are some of the more general questions that need to be answered. This dissertation showed that some sulfonated compounds can play an important role contributing to better wine preservation. The next step is to analyze more sulfonated products that may be produced by the reaction of bisulfite with chemical compounds present in wine, and evaluate their antioxidant and radical scavenging properties. With this approach, it is hoped that it might be possible to discover novel alternatives for the preservation of wine during aging and result in the reduction of the use of sulfites in wine production, which are suspected as the cause of serious health problems.

BIBLIOGRAPHY

1. Di Lorenzo, C., et al., *Antioxidant activity of wine assessed by different in vitro methods*. BIO Web Conf., 2017. **9**: p. 04008.
2. Carocho, M. and I.C.F.R. Ferreira, *A review on antioxidants, prooxidants and related controversy: Natural and synthetic compounds, screening and analysis methodologies and future perspectives*. Food and Chemical Toxicology, 2013. **51**: p. 15-25.
3. Garaguso, I. and M. Nardini, *Polyphenols content, phenolics profile and antioxidant activity of organic red wines produced without sulfur dioxide/sulfites addition in comparison to conventional red wines*. Food Chemistry, 2015. **179**: p. 336-342.
4. Carmona-Jiménez, Y., et al., *Simplification of the DPPH assay for estimating the antioxidant activity of wine and wine by-products*. Food Chemistry, 2014. **165**: p. 198-204.
5. Fernández-Pachón, M.S., et al., *Antioxidant activity of wines and relation with their polyphenolic composition*. Analytica Chimica Acta, 2004. **513**(1): p. 113-118.
6. Oliveira, C.M., et al., *Oxidation mechanisms occurring in wines*. Food Research International, 2011. **44**(5): p. 1115-1126.
7. Coetzee, C. and W.J. du Toit, *Sauvignon blanc wine: Contribution of ageing and oxygen on aromatic and non-aromatic compounds and sensory composition - A review*. South African Journal of Enology and Viticulture, 2015. **36**: p. 347-365.
8. Kilmartin, P.A., H. Zou, and A.L. Waterhouse, *A Cyclic Voltammetry Method Suitable for Characterizing Antioxidant Properties of Wine and Wine Phenolics*. Journal of Agricultural and Food Chemistry, 2001. **49**(4): p. 1957-1965.
9. Skouroumounis, G.K., et al., *The influence of ascorbic acid on the composition, colour and flavour properties of a Riesling and a wooded Chardonnay wine during five years' storage*. Australian Journal of Grape and Wine Research, 2005. **11**(3): p. 355-368.
10. Carrascon, V., et al., *Gas chromatography-mass spectrometry strategies for the accurate and sensitive speciation of sulfur dioxide in wine*. Journal of Chromatography A, 2017. **1504**: p. 27-34.
11. Roullier-Gall, C., et al., *Sulfites and the wine metabolome*. Food Chemistry, 2017. **237**: p. 106-113.
12. Skovgaard, N., *Evaluation of certain food additives*. . Vol. 149. 2011: WHO Technical Report Series.
13. Aberl, A. and M. Coelhan, *Determination of sulfur dioxide in wine using headspace gas chromatography and electron capture detection*. Food Additives & Contaminants: Part A, 2013. **30**(2): p. 226-233.
14. Gonçalves, L.M., et al., *Determination of free and total sulfites in wine using an automatic flow injection analysis system with voltammetric detection*. Food Additives & Contaminants: Part A, 2010. **27**(2): p. 175-180.
15. Peterson, A.L., A. Gambuti, and A.L. Waterhouse, *Rapid analysis of heterocyclic acetals in wine by stable isotope dilution gas chromatography-mass spectrometry*. Tetrahedron, 2015. **71**(20): p. 3032-3038.
16. Han, G., et al., *A rapid, one step preparation for measuring selected free plus SO₂-bound wine carbonyls by HPLC-DAD/MS*. Talanta, 2015. **134**: p. 596-602.
17. Nikolantonaki, M., P. Magiatis, and A.L. Waterhouse, *Direct Analysis of Free and Sulfite-Bound Carbonyl Compounds in Wine by Two-Dimensional Quantitative Proton and Carbon Nuclear Magnetic Resonance Spectroscopy*. Analytical Chemistry, 2015. **87**(21): p. 10799-10806.

18. Waterhouse, A., G. Sacks, and D. Jeffery, *Understanding Wine Chemistry*. 2016: John Wiley & Sons.
19. Peterson, A.L. and A.L. Waterhouse, *¹H NMR: A Novel Approach To Determining the Thermodynamic Properties of Acetaldehyde Condensation Reactions with Glycerol, (+)-Catechin, and Glutathione in Model Wine*. *Journal of Agricultural and Food Chemistry*, 2016. **64**(36): p. 6869-6878.
20. Arapitsas, P., et al., *The influence of storage on the “chemical age” of red wines*. *Metabolomics*, 2014. **10**(5): p. 816-832.
21. Arapitsas, P., G. Guella, and F. Mattivi, *The impact of SO₂ on wine flavanols and indoles in relation to wine style and age*. *Scientific Reports*, 2018. **8**: p. 858.
22. Dinkova-Kostova, A.T. and P. Talalay, *Direct and indirect antioxidant properties of inducers of cytoprotective proteins*. *Molecular Nutrition & Food Research*, 2008. **52**(S1): p. S128-S138.
23. Joko, S., et al., *Comparison of chemical structures and cytoprotection abilities between direct and indirect antioxidants*. *Journal of Functional Foods*, 2017. **35**: p. 245-255.
24. Roginsky, V. and E.A. Lissi, *Review of methods to determine chain-breaking antioxidant activity in food*. *Food Chemistry*, 2005. **92**(2): p. 235-254.
25. Kaneda, H., et al., *Contribution of carbonyl-bisulfite adducts to beer stability*. *Journal of Agricultural and Food Chemistry*, 1994. **42**(11): p. 2428-2432.
26. Nardini, M. and I. Garaguso, *Effect of Sulfites on Antioxidant Activity, Total Polyphenols, and Flavonoid Measurements in White Wine*. *Foods*, 2018. **7**(3): p. 35.
27. Sánchez-Moreno, C., *Review: Methods Used to Evaluate the Free Radical Scavenging Activity in Foods and Biological Systems*. *Food Science and Technology International*, 2002. **8**(3): p. 121-137.
28. D. de Beer, et al., *Changes in the Phenolic Composition and Antioxidant Activity of Pinotage, Cabernet Sauvignon, Chardonnay and Chenin blanc Wines During Bottle Ageing*. *South African Journal for Enology and Viticulture*, 2005. **26**(1): p. 10.
29. Fogliano, V., et al., *Method for Measuring Antioxidant Activity and Its Application to Monitoring the Antioxidant Capacity of Wines*. *Journal of Agricultural and Food Chemistry*, 1999. **47**(3): p. 1035-1040.
30. Kedare, S.B. and R.P. Singh, *Genesis and development of DPPH method of antioxidant assay*. *Journal of food science and technology*, 2011. **48**(4): p. 412-422.
31. Molyneux, P., *The use of the stable radical Diphenylpicrylhydrazyl (DPPH) for estimating antioxidant activity*. *Songklanakarin J. Sci. Technol*, 2003. **26**.
32. Hoyos-Arbeláez, J., M. Vázquez, and J. Contreras-Calderón, *Electrochemical methods as a tool for determining the antioxidant capacity of food and beverages: A review*. *Food Chemistry*, 2017. **221**: p. 1371-1381.
33. Zhang, Q.-A., et al., *Free radical generation induced by ultrasound in red wine and model wine: An EPR spin-trapping study*. *Ultrasonics Sonochemistry*, 2015. **27**: p. 96-101.
34. Danilewicz, J.C., *Review of Reaction Mechanisms of Oxygen and Proposed Intermediate Reduction Products in Wine: Central Role of Iron and Copper*. *American Journal of Enology and Viticulture*, 2003. **54**(2): p. 73-85.
35. Polovka, M., *EPR spectroscopy: A tool to characterize stability and antioxidant properties of foods*. *Journal of food and nutrition research* 2006. **45**: p. 1-11.
36. John M. Carney, R.A.F., *PBN, DMPO, and POBN Compositions and Method of Use Thereof for Inhibition of Age-Associated Oxidation*. US Patent no 5,405,874, 1995.
37. A. Spyros, P.D., *NMR spectroscopy in food analysis*, ed. R.F. Analysis. 2013: Springer.
38. Macomber, R.S., *A Complete Introduction to Modern NMR Spectroscopy*. *Journal of Chemical Education*. Vol. 76. 1998: American Chemical Society. 473.
39. Godelmann, R., et al., *Quantitation of Compounds in Wine Using ¹H NMR Spectroscopy: Description of the Method and Collaborative Study*. *Journal of AOAC International*, 2016. **99**(5): p. 1295-1304.

40. Saurina, J., *Characterization of wines using compositional profiles and chemometrics*. TrAC Trends in Analytical Chemistry, 2010. **29**(3): p. 234-245.
41. Amargianitaki, M. and A. Spyros, *NMR-based metabolomics in wine quality control and authentication*. Chemical and Biological Technologies in Agriculture, 2017. **4**(1): p. 9.
42. Lee, J.-E., et al., *Evidence of vintage effects on grape wines using 1H NMR-based metabolomic study*. Analytica Chimica Acta, 2009. **648**(1): p. 71-76.
43. Son, H.-S., et al., *Metabolomic Studies on Geographical Grapes and Their Wines Using 1H NMR Analysis Coupled with Multivariate Statistics*. Journal of Agricultural and Food Chemistry, 2009. **57**(4): p. 1481-1490.
44. Cassino, C., et al., *Wine evolution during bottle aging, studied by 1H NMR spectroscopy and multivariate statistical analysis*. Food Research International, 2018.
45. Babu, A.V.S., *HPLC and LCMS – A review and a recent update*. Int. J. of Pharmacy and Analytical Research, 2017. **6**(3): p. 555-567.
46. Chernushevich, I.V., A.V. Loboda, and B.A. Thomson, *An introduction to quadrupole–time-of-flight mass spectrometry*. Journal of Mass Spectrometry, 2001. **36**(8): p. 849-865.
47. Elias, R.J., et al., *Analysis of selected carbonyl oxidation products in wine by liquid chromatography with diode array detection*. Analytica Chimica Acta, 2008. **626**(1): p. 104-110.
48. Morata, A., et al., *Pyruvic Acid and Acetaldehyde Production by Different Strains of Saccharomyces cerevisiae: Relationship with Vitisin A and B Formation in Red Wines*. Journal of Agricultural and Food Chemistry, 2003. **51**(25): p. 7402-7409.
49. Rankine, B.C., *Factors influencing the pyruvic acid content of wines*. Journal of the Science of Food and Agriculture, 1965. **16**(7): p. 394-398.
50. Zoecklein, B., et al., *Wine Analysis and Production*. 1995: Springer.
51. Hernández-Orte, P., et al., *Amino Acid Determination in Grape Juices and Wines by HPLC Using a Modification of the 6-Aminoquinolyl-N-Hydroxysuccinimidyl Carbamate (AQC) Method*. Chromatographia, 2003. **58**(1): p. 29-35.
52. Moreno-Arribas, M.V. and M.C. Polo, *Wine Chemistry and Biochemistry*. 2009: Springer Science+Business Media. 1-735.
53. Nikolantonaki, M., et al., *Impact of Glutathione on Wines Oxidative Stability: A Combined Sensory and Metabolomic Study*. Frontiers in chemistry, 2018. **6**: p. 182-182.
54. Nikolantonaki, M., et al., *Measurement of white wines resistance against oxidation by Electron Paramagnetic Resonance spectroscopy*. Food Chemistry, 2019. **270**: p. 156-161.
55. Cole, E.R., et al., *Structure and solution equilibria of d-glucose and d-mannose sulfite adducts*. Carbohydrate Research, 2001. **335**(1): p. 1-10.
56. Arapitsas, P., et al., *Wine metabolomics reveals new sulfonated products in bottled white wines, promoted by small amounts of oxygen*. Journal of Chromatography A, 2016. **1429**: p. 155-165.
57. <http://www.bmrbl.wisc.edu/>.
58. <http://www.hmdb.ca/>.
59. https://sdbs.db.aist.go.jp/sdbs/cgi-bin/direct_frame_top.cgi.
60. Nimse, S.B. and D. Pal, *Free radicals, natural antioxidants, and their reaction mechanisms*. RSC Advances, 2015. **5**(35): p. 27986-28006.

APPENDIX

Table 25: Intensity of each compound ($\times 10^4$) in 26 white wine samples and the available results of DPPH and EPR

Wine code	Acetaldehyde sulfonate	Pyruvic sulfonate	Glucose sulfonate	a-ketoglutaric bisulfite	Available results
R-17-71	7.5	3.8	0	0	DPPH + EPR
R-17-72	7.4	1.7	0	0	DPPH + EPR
R-17-73	5	0.46	0	0	DPPH + EPR
R-17-74	8	1.35	0	0	DPPH + EPR
R-17-75	8	1.8	0	0	DPPH + EPR
R-17-76	6.5	0.9	0	0	DPPH + EPR
DNO-17 (98-105)	1.69 ± 0.73	0.18 ± 0.12	0.29 ± 0.11	6.01 ± 0.16	DPPH
DNO-18 (58-65)	1.56 ± 0.77	0	4.11 ± 0.53	6.32 ± 0.29	DPPH + EPR (for 7/10 samples)